GEOLOGICAL SURVEY OF CANADA
BULLETIN 462

THE ILGACHUZ RANGE AND ADJACENT PARTS OF THE INTERIOR PLATEAU, BRITISH COLUMBIA

J.G. Souther and M.E.K. Souther

1994

Natural Resources Canada Ressources naturelles Canada

Canada

GEOLOGICAL SURVEY OF CANADA
BULLETIN 462

THE ILGACHUZ RANGE AND ADJACENT PARTS OF THE INTERIOR PLATEAU, BRITISH COLUMBIA

J.G. Souther and M.E.K. Souther

1994

Available in Canada through authorized
bookstore agents and other bookstores

or by mail from

Canada Communication Group – Publishing
Ottawa, Canada K1A 0S9

and from

Geological Survey of Canada offices:

601 Booth Street
Ottawa, Canada K1A 0E8

3303-33rd Street N.W.,
Calgary, Alberta T2L 2A7

100 West Pender Street
Vancouver, B.C. V6B 1R8

A deposit copy of this publication is also available for reference
in public libraries across Canada

Cat. No. M42-462E
ISBN 0-660-15500-1

Price subject to change without notice

Cover description

View looking southeast from Calliope Mountain at a thick succession of intracaldera rocks on Pipe Organ Mountain in the central Ilgachuz Range.

Critical reader

M.B. Lambert

Authors' addresses

J.G. Souther
Geological Survey of Canada
100 West Pender Street
Vancouver, B.C.
V6B 1R8

M.E.K. Souther
4352 Arundel Rd.
North Vancouver, B.C.
V7R 3T2

Original manuscript received: June 1992
Final version approved for publication: March 1993

CONTENTS

Illustrations

Tables

THE ILGACHUZ RANGE AND ADJACENT PARTS OF THE INTERIOR PLATEAU, BRITISH COLUMBIA

Abstract

Christensen Creek (93C/11) and Carnlick Creek (93C/14) map areas encompass the Ilgachuz Range, a highly dissected late Tertiary shield volcano that rises 1200 m above the general level of the Interior Plateau of central British Columbia.

The drift-covered plateau surface adjacent to the Ilgachuz Range contains isolated exposures of Mesozoic volcanic and sedimentary rocks, early Tertiary felsic volcanic and subvolcanic rocks, and mylonitic orthogneiss of the Eocene Tatla Lake Metamorphic Core Complex. Undeformed late Tertiary volcanic rocks rest unconformably on all of the older strata. They include Chilcotin Group basalt flows and lgachuz Group alkaline volcanic and subvolcanic rocks which form the Ilgachuz Range shield volcano.

The Ilgachuz Range is a composite volcanic shield comprising a thick lower section of highly alkaline to peralkaline felsic flows, domes, and hypabyssal intrusions, overlain by a relatively thin veneer of alkaline basalt. A small central caldera is filled with pyroclastic deposits, lacustrine beds, and ponded lava. K-Ar dates indicate that the entire volcanic edifice was built between 6 Ma and 4 Ma.

The Ilgachuz Range is one of three large shield volcanoes in the central part of the east-trending Anahim Volcanic Belt. Volcanoes along this belt become progressively younger from west to east and are believed to have formed on the American continental plate as it moved westward over a mantle hotspot. The chemistry and stratigraphy of the Ilgachuz Group rocks suggest that they are the product of crustal melting and crystal fractionation, accompanied by underplating with mantle-derived basaltic magma.

Résumé

Les régions cartographiques du ruisseau Christensen (93C/11) et du ruisseau Carnlick (93C/14) renferment le chaînon Ilgachuz, volcan-bouclier du Tertiaire tardif qui est fortement disséqué et qui s'élève à 1 200 m au-dessus du niveau général du Plateau intérieur dans le centre de la Colombie-Britannique.

À proximité du chaînon Ilgachuz, la surface du plateau est recouverte de débris glaciaires et présente des affleurements isolés de roches volcaniques et sédimentaires du Mésozoïque, de roches volcaniques et subvolcaniques du Tertiaire précoce et d'orthogneiss mylonitiques du Complexe métamorphique interne de Tatla Lake de l'Éocène. Des roches volcaniques non déformées du Tertiaire tardif reposent en discordance sur toutes les strates plus anciennes. Elles comprennent les coulées basaltiques du Groupe de Chilcotin et les roches volcaniques et subvolcaniques alcalines du Groupe d'Ilgachuz qui constituent le volcan-bouclier du chaînon Ilgachuz.

Le chaînon Ilgachuz est un volcan-bouclier composite qui comporte une épaisse tranche inférieure de coulées, de dômes et d'intrusions hypabyssales felsiques, fortement alcalins à hyperalcalins, que recouvre un placage de basalte alcalin. Une petite caldeira centrale est remplie de dépôts pyroclastiques, de couches lacustres et de laves endiguées. La datation au K-Ar indique que l'édifice volcanique tout entier s'est formé il y a entre 4 et 6 Ma.

Le chaînon Ilgachuz est un de trois grands volcans-boucliers dans le centre de la Zone volcanique d'Anahim, à direction est. Les volcans qui se rencontrent dans cette zone sont de plus en plus jeunes d'ouest en est et se sont vraisemblablement édifiés sur la plaque continentale américaine au fur et à mesure qu'elle se déplaçait vers l'ouest au-dessus d'un point chaud mantellique. La chimie et la stratigraphie des roches du Groupe d'Ilgachuz suggèrent que ces dernières sont le produit de la fusion de la croûte et de la cristallisation fractionnée, accompagnées de la subduction d'un magma basaltique dérivé du manteau.

Summary

The Ilgachuz Range is a highly dissected late Tertiary shield volcano that rises about 1200 m above the general level of the Interior Plateau of central British Columbia. The range straddles the Christensen Creek (NTS 93C/11) and Carnlick Creek (NTS 93C/14) map areas which cover an area of about 1800 km^2.

The region was overridden by two major glacial advances which left thick glacial and periglacial deposits in the lowlands and scoured the high peaks of the Ilgachuz Range.

In addition to the Ilgachuz Range the two map areas include pre-Miocene rocks, which are exposed in isolated outcrops on the deeply drift-covered plateau surrounding the volcano, and range in age from Triassic to early Tertiary. The Mesozoic strata include volcanic and sedimentary rocks that are correlative in part with the Triassic-Jurassic Hazelton Group. They exhibit varying degrees of alteration, ranging from unstrained greenschist facies andesite breccia, to strongly foliated amphibolite grade greenstone.

The early Tertiary rocks include felsic volcanics and related subvolcanic intrusions of the Ootsa Lake Group, and mylonitic orthogneisses of the Tatla Lake Metamorphic Core Complex. The latter is derived from a Mesozoic protolith which yields reset, Eocene, K-Ar dates.

Late Tertiary rocks rest unconformably on all of the older strata. They include the Chilcotin Group, which occurs as isolated remnants of flat-lying basalt flows, and the Ilgachuz Group of alkaline volcanic and related intrusive rocks which form the Ilgachuz Range shield volcano.

The Ilgachuz Range is a composite volcanic shield comprising a thick lower section of highly alkaline to peralkaline felsic flows, domes, and hypabyssal intrusions, overlain by a relatively thin outer mantle of alkaline basalt. A small central caldera is filled with pyroclastic deposits, lacustrine beds, and ponded lava. K-Ar dates indicate that the entire volcanic edifice was built in a period of about two million years between 6 Ma and 4 Ma.

The Ilgachuz Range is one of three large shield volcanoes in the central part of the east-trending Anahim Volcanic Belt. Volcanoes along this belt become progressively younger from west to east and probably formed on the American continental plate as it moved westward over a mantle hotspot. The chemistry and stratigraphy of the Ilgachuz Group rocks suggest that they are the product of crustal melting, accompanied by underplating with mantle-derived basaltic magma. Varying degrees of crystal fractionation have affected both the felsic rocks of the lower shield and basalts of the outer shield.

Sommaire

Le chaînon Ilgachuz est un volcan-bouclier du Tertiaire tardif qui est fortement disséqué et qui s'élève à 1 200 m au-dessus du niveau général du Plateau intérieur dans le centre de la Colombie-Britannique. Le chaînon se situe dans les régions cartographiques du ruisseau Christensen (SNRC 93C/11) et du ruisseau Carnlick (SNRC 93C/14) qui couvrent une superficie d'environ 1 800 km^2.

Deux grandes avancées glaciaires ont submergé la région, laissant des dépôts glaciaires et périglaciaires épais dans les basses terres et rabotant les hauts sommets du chaînon Ilgachuz.

Outre le chaînon Ilgachuz, les deux régions cartographiques Contiennent des roches pré-miocènes, qui s'échelonnent du Trias au Tertiaire précoce et se rencontrent dans des affleurements isolés sur le plateau couvert de sédiments glaciaires épais sur lequel se trouve le volcan. Les strates du Mésozoïque comprennent des roches volcaniques et sédimentaires, dont une partie peut être mise en corrélation avec le Groupe de Hazelton (Trias-Jurassique). Elles montrent divers degrés d'altération et varient d'une brèche andésitique non déformée du faciès des schistes verts à des roches vertes fortement foliées du faciès des amphibolites.

Les roches du Tertiaire précoce comprennent des roches volcaniques felsiques et des intrusions subvolcaniques apparentées du Groupe d'Ootsa Lake, et des orthogneiss mylonitiques du Complexe métamorphique interne de Tatla Lake. Ce dernier est dérivé d'un protolithe mésozoïque qui donne des âges K-Ar rajeunis remontant à l'Éocène.

Les roches du Tertiaire tardif reposent en discordance sur toutes les strates plus anciennes. Elles comprennent les roches du Groupe de Chilcotin, qui forment des vestiges isolés de coulées basaltiques subhorizontales, ainsi que les roches volcaniques alcalines et les roches intrusives apparentées du Groupe d'Ilgachuz, qui constituent le volcan-bouclier du chaînon Ilgachuz.

Le chaînon Ilgachuz est un volcan-bouclier composite qui comporte une épaisse tranche inférieure de coulées, de dômes et d'intrusions hypabyssales felsiques, fortement alcalins à hyperalcalins, que recouvre une couche relativement mince de basalte alcalin. Une petite caldeira centrale est remplie de dépôts pyroclastiques, de couches lacustres et de laves endiguées. La datation au K-Ar indique que l'édifice volcanique tout entier s'est formé sur une période d'environ deux millions d'années, il y a entre 4 et 6 Ma.

Le chaînon Ilgachuz est un de trois grands volcans-boucliers dans le centre de la Zone volcanique d'Anahim, à direction est. Les volcans qui se rencontrent dans cette zone sont de plus en plus jeunes d'ouest en est et se sont vraisemblablement édifiés sur la plaque continentale américaine au fur et à mesure qu'elle se déplaçait vers l'ouest au-dessus d'un point chaud mantellique. La chimie et la stratigraphie des roches du Groupe d'Ilgachuz suggèrent que ces dernières sont le produit de la fusion de la croûte et de la subduction d'un magma basaltique dérivé du manteau. Les roches felsiques du bouclier inférieur et les basaltes du bouclier externe ont subi divers degrés de cristallisation fractionnée.

LOCATION AND ACCESS

Carnlick Creek (NTS 93C/14) and Christensen Creek (NTS 93C/11) are adjacent map areas in a sparsely settled region of central British Columbia (Fig. 1, Map 1845A). Anahim Lake, near the southern boundary of the Christensen Creek map area, is the nearest town. The Chilcotin Highway between Williams Lake and Bella Coola passes through the southwestern corner of Christensen Creek map area. A dirt-track summer road along Dean River valley is passable to four-by-four vehicles from Anahim Lake as far north as Rainbow Lake in the southwestern Carnlick Creek area. Native settlements along West Road (Blackwater) River are linked by a network of trails and wagon roads. Although none of these are suitable for motorized vehicles they are part of the Alexander Mackenzie Heritage Trail which is maintained for recreational hiking. It is part of an ancient trade route from the interior to the coast and was followed by Mackenzie (1802) on the last stage of his journey to the Pacific.

Several poorly marked horse trails provide access to the upper slopes of the Ilgachuz Range. They are used intermittently by resident guides and outfitters but are difficult to find without local knowledge. For this study a charter helicopter was used to establish camps in the central Ilgachuz Range and a float plane was used to access the many lakes in the lowlands north of the range.

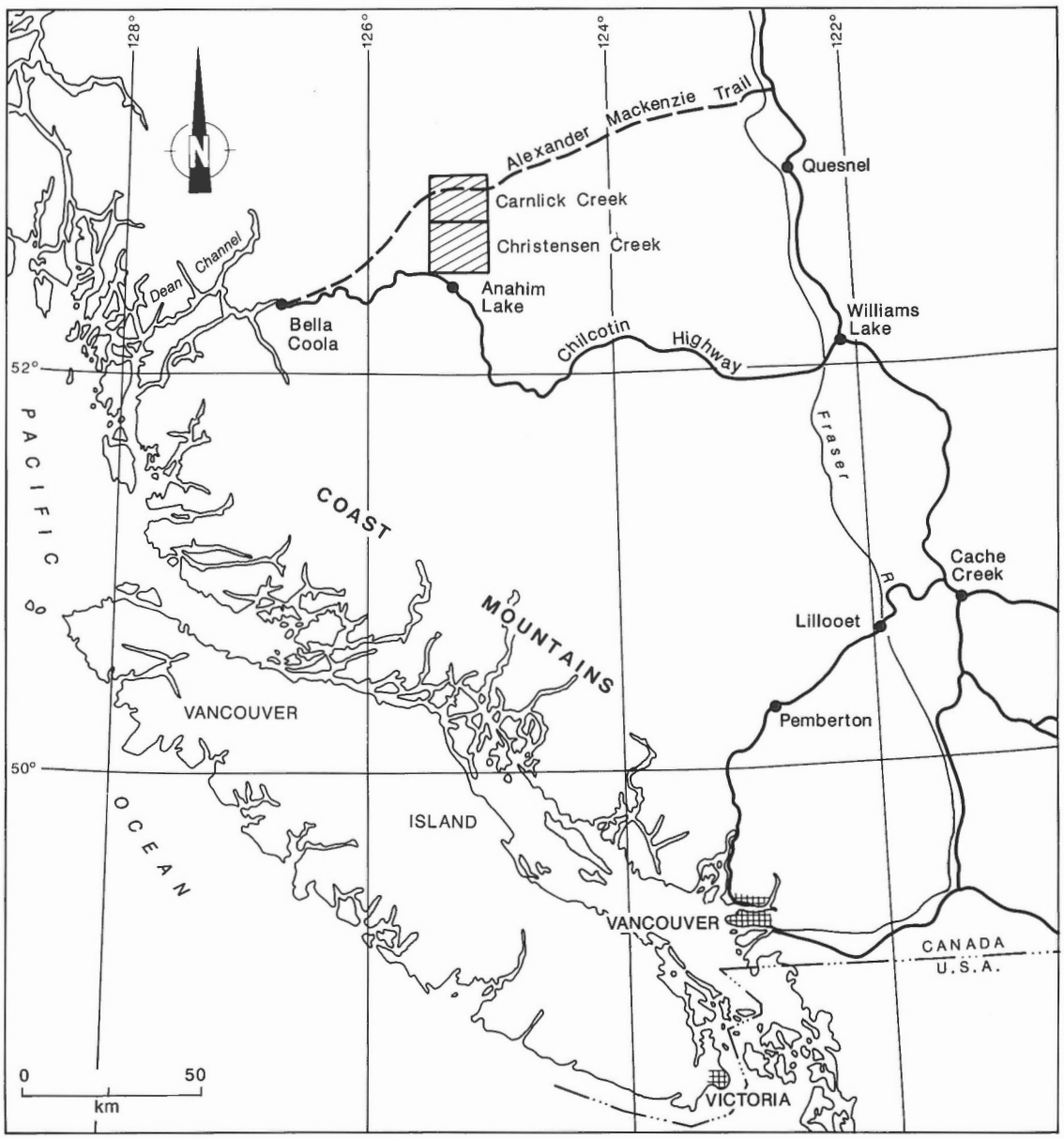

Figure 1. *Index map showing the location of Carnlick Creek and Christensen Creek map areas.*

PHYSIOGRAPHY AND DRAINAGE

Carnlick Creek and Christensen Creek map areas (Map 1845A) encompass the Ilgachuz Range, a deeply dissected shield volcano that rises from the surface of the Interior Plateau to a cluster of peaks over 7000 ft. (2133 m) in elevation (Fig. 2). The base of the shield, as defined by the 5000 ft. contour, is a nearly perfect ellipse with a northwest axis of 30 km and a northeast axis of 20 km. Its western margin is truncated by escarpments facing Dean River valley. Elsewhere the outer perimeter of the shield merges with the surrounding plateau at an elevation of about 4500 ft. (1370 m).

The Ilgachuz Range is on the drainage divide between the West Road (Blackwater) River, which flows east into the Fraser River, and the Dean River, which flows west into Dean Channel. The West Road (Blackwater) River, which heads in the lake-studded flatlands north of the Ilgachuz Range, is a sluggish stream that meanders through a broad valley. The Dean River is also at grade, but it heads in a large drainage area south of the Ilgachuz Range and, north of Anahim Lake, it occupies a broad well defined valley.

A radial drainage system, reflecting the original symmetry of the volcanic shield, dissects the Ilgachuz Range into pie-shaped interfluves separated by deeply incised valleys. Pan, Carnlick, and Blue Canyon creeks, which flow northeast into the West Road (Blackwater) drainage, occupy mature valleys with broad marshy floodplains flanked by steep walls (Fig. 3). In contrast, the westward-flowing tributaries of Dean River have relatively short, steep gradients and are actively eroding their narrow V-shaped valleys. This difference may be due to glacial overdeepening of the Dean River valley during the late Pleistocene, followed by postglacial adjustment of the drainage to a new base level on the west side of the Ilgachuz Range. The truncated spurs and steep escarpment on the west side of the Ilgachuz Range are further evidence of extensive glacial erosion along Dean River valley.

Despite the deeply incised radial drainage, the gently sloping interfluves on the flanks of the Ilgachuz Range shield have not been greatly modified by erosion. When viewed in profile they define a smooth, gently concave surface which is probably close to that of the original lower slopes of the volcano. Where the radial valleys converge in the centre of the range the flat interfluves give way to narrow-crested

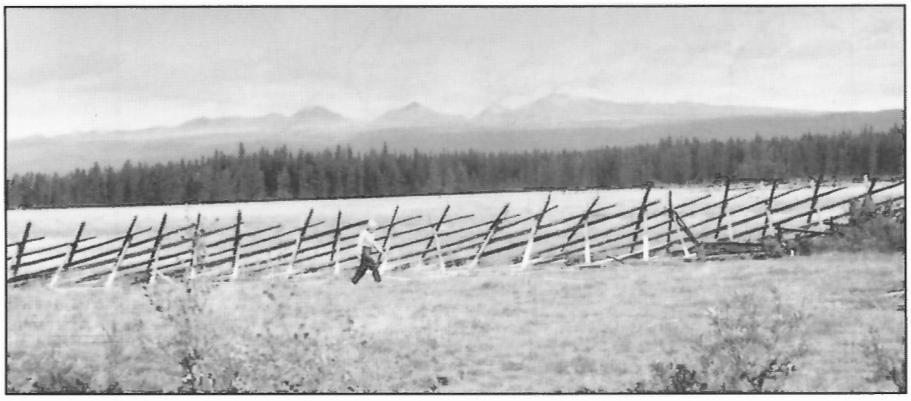

Figure 2.

View looking north from near Anahim Lake at the dissected volcanic shield of the Ilgachuz Range (Go-around Mountain in centre). Flows on the outer flanks of the volcano merge with the nearly flat surface of the adjacent plateau. GSC 1993-184R

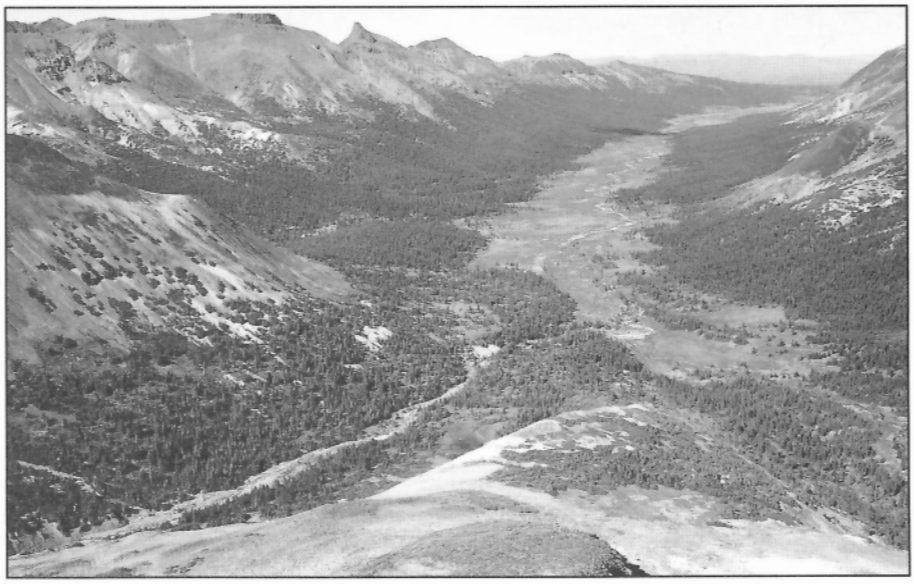

Figure 3.

View looking northeast along Carnlick Creek valley showing broad floodplain and steep valley walls. GSC 1993-184U

ridges and conical peaks (Fig. 4). The form of these erosional remnants appears to be largely controlled by internal structures and variations in the lithology and competence of units within the upper part of the volcanic pile.

GLACIATION

Tipper (1971) recognized two major glacial advances in the Anahim Lake area. During the earlier Fraser Glaciation the Cordilleran ice sheet moved northeastward out of the Coast Mountains onto the Interior Plateau. At its maximum development the Fraser ice was at least 5000 ft. (1524 m) thick over Anahim Lake valley and its northeastward flow was not affected by local topography. Although the Ilgachuz Range must have been completely ice-covered at that time little evidence of Fraser Glaciation is preserved in the upper part of the range. A few erratics were found on interfluves above 6500 ft. (1980 m), but most of the high peaks and ridges have been greatly modified by postglacial erosion that has removed the older surficial deposits. If glacial bedrock features were present they too have been masked by later development of felsenmeer, talus, and solifluction slopes.

Retreat of the Fraser ice sheet was followed by a second buildup of ice in the Coast Mountains (Tipper, 1971). This culminated with formation of the Anahim Lake lobe, a complex of coalesced valley glaciers that spread eastward onto the Interior Plateau. At its maximum, this lobe did not cover the Ilgachuz Range but instead was diverted into the flanking valleys, flowing northward down Dean River valley and eastward along West Road (Blackwater) River valley.

Most of the glacial features preserved within the mapped area were produced by the relatively young Anahim Lake lobe. Low, poorly formed drumlins are developed locally along the Dean and West Road (Blackwater) river valleys and indistinct glacial grooving is present, both in the valleys and on the till-covered lower slopes of the Ilgachuz Range up to an elevation of about 6000 ft. (1828 m) (Fig. 5). Between about 5000 and 6000 ft. (1524 and 1828 m), the slopes of the Ilgachuz Range display a myriad of lateral overflow channels and elongated ridges of lateral moraine that parallel the ice limit at successive stages of retreat (Fig. 6). Extensive development of esker complexes, meltwater channels, and areas of pitted terrane indicate that withdrawal of the Anahim Lake lobe was accompanied by rapidly changing patterns of periglacial drainage and the stagnation of large areas of ice.

Although the Ilgachuz Range was not overridden by the Anahim Lake lobe, valley glaciers must have headed in cirques on the northeast side of the range. Ice probably persisted in the upper reaches of Blue Canyon, Carnlick, and Pan creeks after stagnation and retreat of the main Anahim Lake lobe. Eskers in the lower parts of these valleys were probably formed by periglacial streams flowing out of the Ilgachuz Range after the Anahim Lake lobe had receded to an elevation of about 5000 ft. (1524 m) (Fig. 7). Terminal moraines in Carnlick Creek and Blue Canyon Creek valleys represent the last ice stagnation fronts prior to final retreat of the valley glaciers.

TECTONIC SETTING

On the Terrane Map of the Canadian Cordillera (Wheeler et al., 1988) the Carnlick Creek and Christensen Creek map areas are included in the southern part of Stikinia (Fig. 8). The presence of Mesozoic volcanic and sedimentary rocks correlative with the Hazelton Group (see Tipper, 1963) is consistent with a Stikine affiliation. However, late Tertiary volcanics and Pleistocene glacial deposits cover much of the area and terrane boundaries in that part of the Intermontane Belt (see Gabrielse et al., 1991) are poorly constrained.

Schist and gneiss in the western part of the mapped area appear to be part of a metamorphic core complex that extends south into the Mount Waddington area (NTS 93N) where it

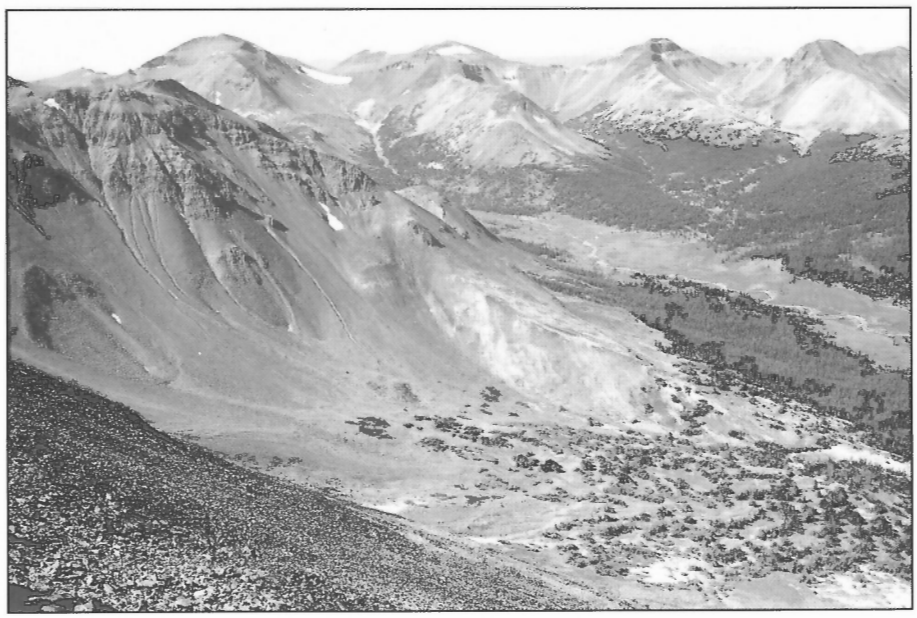

Figure 4.

View looking west from Mount Scot at high peaks in the central Ilgachuz Range. From left to right: Carnlick Mountain, Saxifraga Mountain, Phacelia Peak, Calliope Mountain. The summit of each of the four peaks is capped by a remnant of Amica Lake flows. GSC 1993-184Z

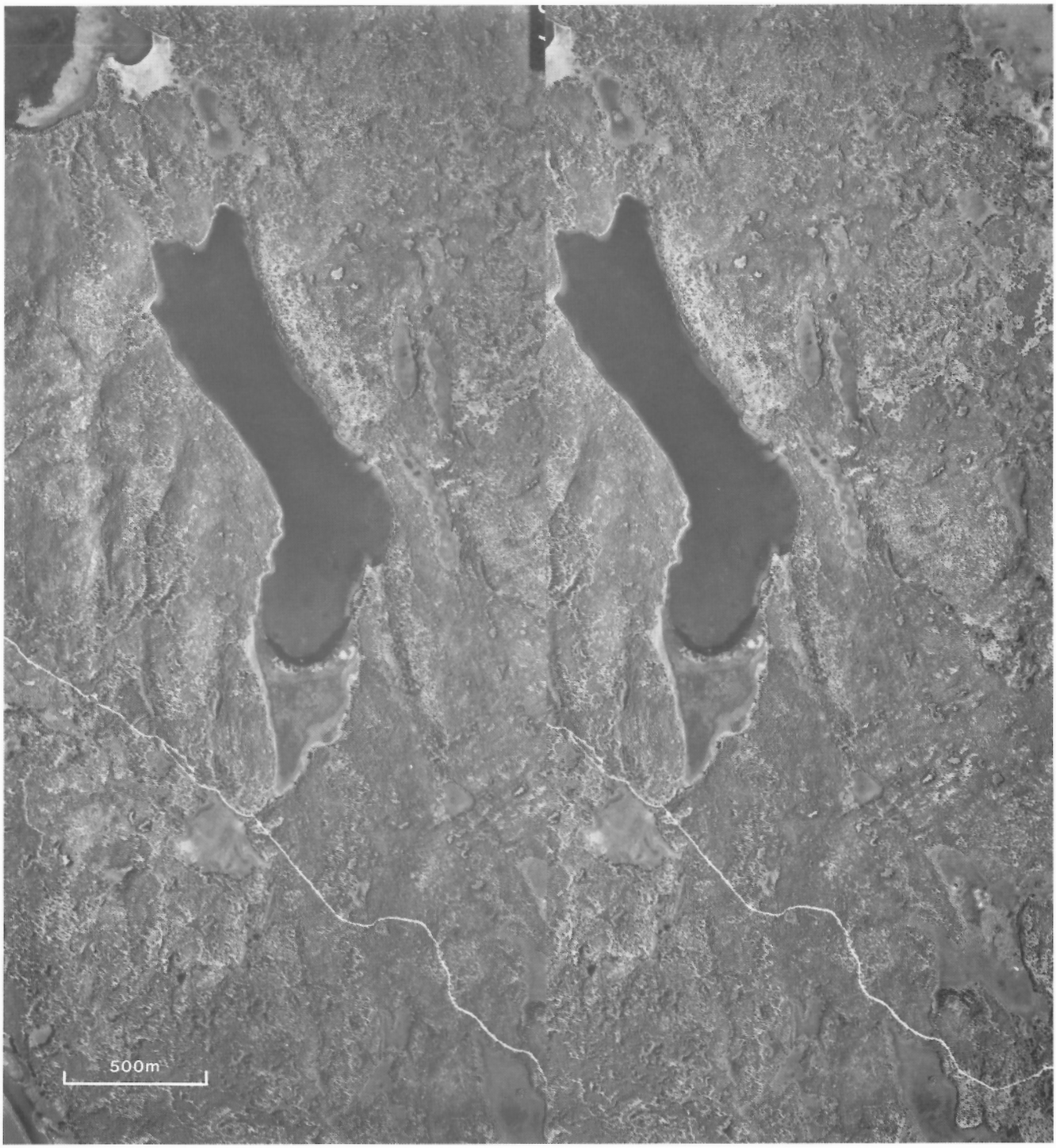

Figure 5. *Stereogram showing pitted terrane and low, north-trending drumlins in Dean River valley near Poison Lakes. Province of British Columbia airphotos BC7730:266 and BC7730:267.*

Figure 6. *Stereogram showing lateral overflow channels on the north flank of the Ilgachuz Range. Province of British Columbia airphotos BC7896:135 and BC7896:136.*

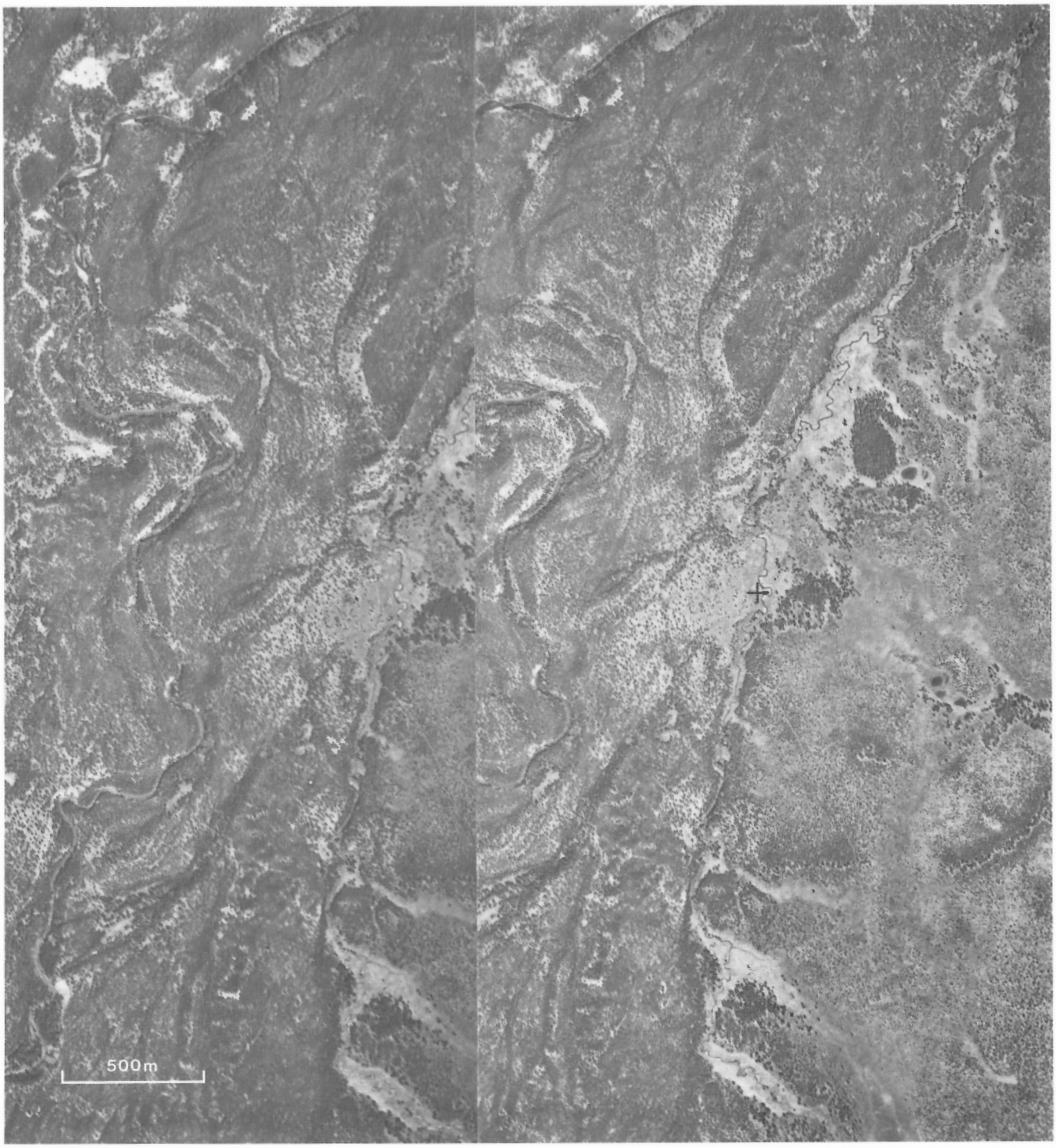

Figure 7. *Stereogram of esker swarm and stream-cut terraces along the lower part of Carnlick Creek valley. Province of British Columbia airphotos BC2975:23 and BC2975:24.*

is bounded on the west by the Yalakom Fault (Fig. 8). It seems likely that an extension of the Yalakom, or a major splay from it, extends northwest through Anahim Lake valley in southwestern Christensen Creek area.

The metamorphic rocks were mapped by Tipper (1969) as part of the Mesozoic Coast Intrusions. However, recent radiometric dating of these rocks indicates a range of K-Ar ages from 53.4 to 45.6 Ma (Friedman and Armstrong, 1988). A predominance of Eocene dates suggests that the metamorphism may have been coeval with eruption of the Ootsa Lake volcanics and that both are manifestations of a widespread thermal event that affected most of the western Cordillera during Eocene time (Armstrong, 1988). The juxtaposition of Eocene metamorphic core complexes with volcanics of approximately the same age is analogous to that reported by Ewing (1981) for the Kamloops Group in south-central British Columbia. There the upwelling of metamorphic core complexes was accompanied by the formation of pull-apart basins in a transtensional environment related to dextral movement on the Fraser Fault zone. A similar tectonic setting related to dextral movement on the Yalakom Fault may have prevailed in the Anahim Lake region during the Eocene thermal event.

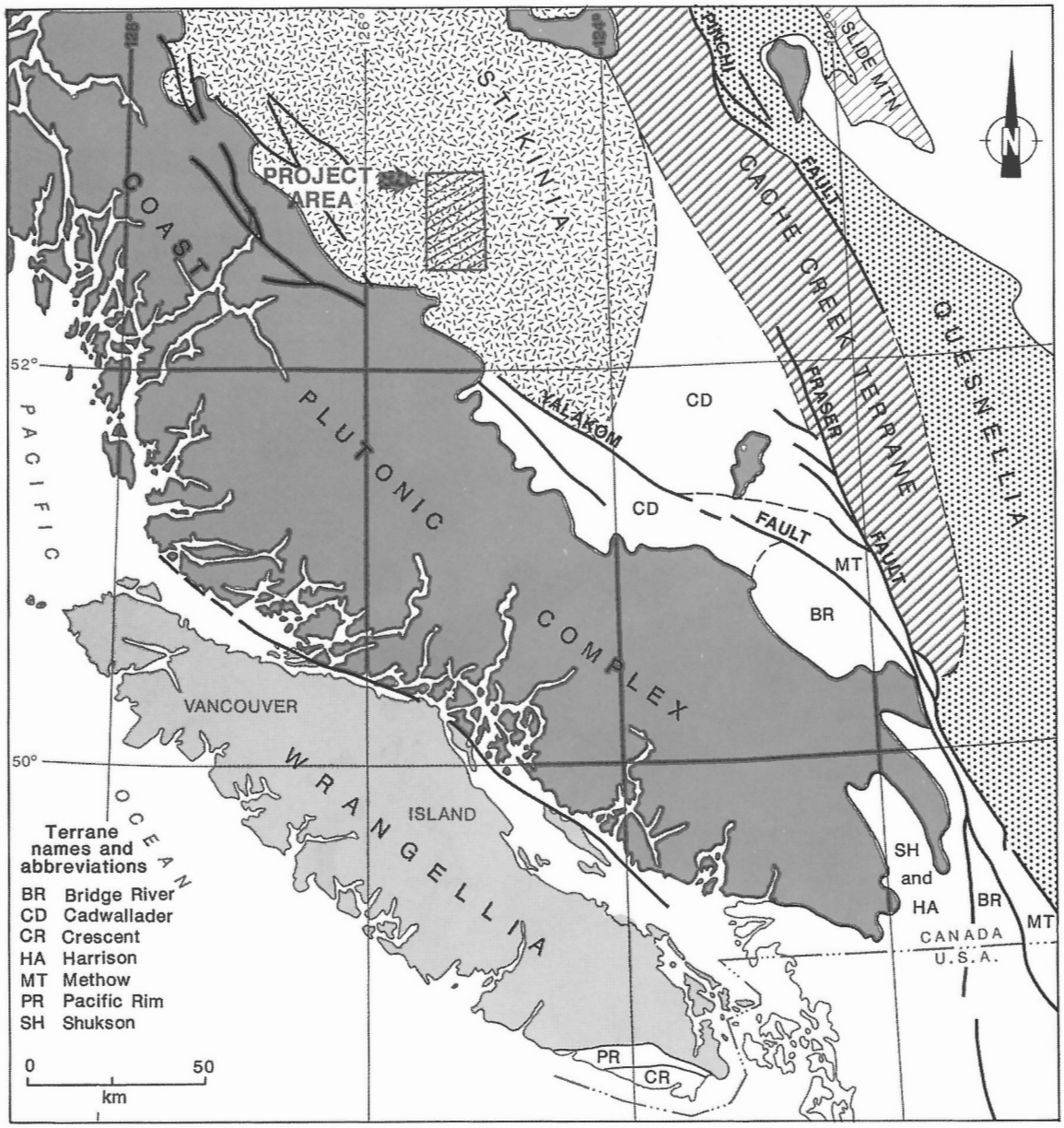

Figure 8. *Terrane map showing the relationship of the project area to major pre-Neogene tectonic elements of the west-central Cordillera (terrane boundaries after Gabrielse et al., 1991).*

The late Tertiary tectonic setting appears to have been independent of older plate boundaries (Fig. 9). Flat-lying, transitional basalts of the Miocene and younger Chilcotin Group are believed to have erupted along a northwesterly trending zone of back-arc volcanism that was parallel to, but inland from, the calc-alkaline, Pemberton-Garibaldi arc (Souther, 1976; Souther and Yorath, 1991). Both the central volcanoes of the Pemberton-Garibaldi arc and the back-arc flows of Chilcotin basalt are related to eastward subduction of the Juan de Fuca Plate (Souther, 1977; Bevier, 1983a, b; Mathews, 1989). In contrast, the Ilgachuz Range is part of an east-trending belt of alkaline to peralkaline central volcanoes, subvolcanic plutons, and dyke swarms that comprise the Anahim Volcanic Belt. Eruption of the Anahim Belt volcanoes overlapped the period of Chilcotin volcanism, but profound differences in composition suggest distinctly different tectonic environments. Whereas the composition of the Chilcotin Group lavas is extremely uniform transitional basalt (alkali basalt to tholeiite), the highly alkaline Anahim Belt lavas vary from picritic basalt to peralkaline rhyolite. The composition of these rocks is characteristic of continental rift and plume complexes (Souther and Yorath, 1991). Moreover, the age of initial igneous activity along the belt becomes progressively younger from west to east. For these reasons the Anahim Volcanic Belt has been interpreted as a hotspot trace, formed by the westward movement of the North American Plate over a mantle plume (Bevier et al., 1979; Souther, 1986; Souther and Yorath, 1991).

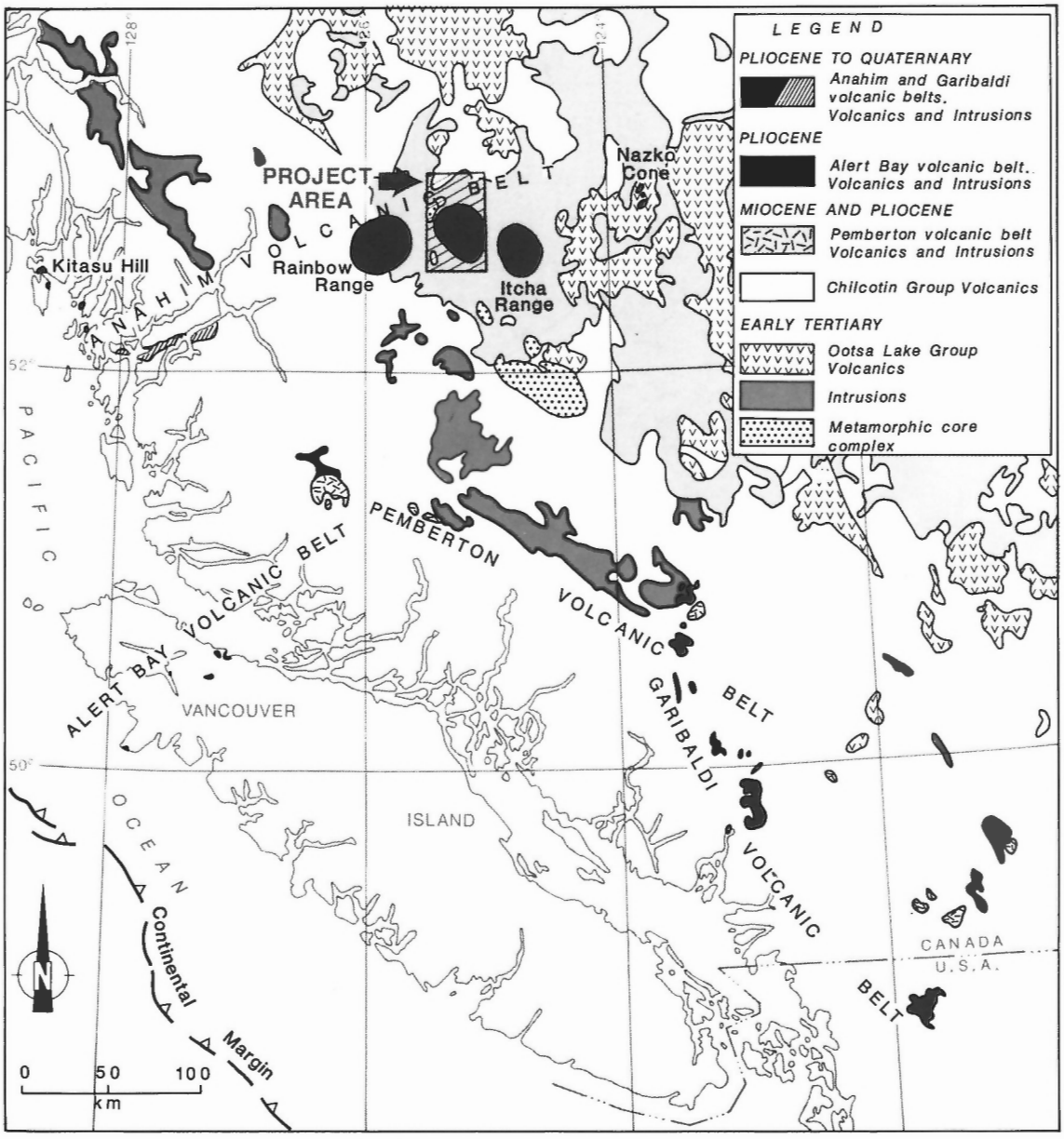

Figure 9. *Map showing the relationship of the project area to Neogene tectonic elements of the west-central Cordillera (modified from Wheeler et al., 1988).*

PREVIOUS GEOLOGICAL WORK

In 1793 Alexander Mackenzie was guided by natives along a network of ancient trading routes that link the central Interior Plateau with the Pacific coast. Part of the route, known as the "grease trail", follows West Road (Blackwater) River valley through the northern part of Carnlick Creek map area. In his narrative Mackenzie (1802) describes the basaltic escarpment along Blackwater River as a "high rocky ridge". More than 80 years later, in 1876, this same route was followed by G.M. Dawson during his exploration of central British Columbia (Dawson, 1878). Dawson (1878) identified the Ilgachuz Range as a Tertiary "volcanic mountain" and his map correctly shows the inlier of Mesozoic rocks, surrounded by Tertiary lavas north of Eliguk Lake. No further geological work was done in the area until H.W. Tipper began systematic mapping of the Anahim Lake area at a scale of 1:250 000. Tipper worked in the area from 1954 until 1957 and his map (Tipper, 1969) is still the most comprehensive summary of the regional geology.

PRESENT STUDY

In 1982 the Ilgachuz Range was visited for one day during a program to collect material for radiometric dating of Tertiary volcanic centres in the Cordillera. The recognition of a possible caldera complex prompted a detailed investigation of the volcano as a target for geothermal exploration. Systematic mapping of the volcanic edifice was started in 1983 and the area was revisited for brief periods during the summers of 1985 through 1988. In 1988 the Geological Survey of Canada received a mandate to investigate the hydrocarbon potential of the Nechako-Chilcotin region as part of the national Frontier Geoscience Program (FGP). Because this area includes the Ilgachuz Range, the original topical study of the Ilgachuz Range volcano was broadened to encompass the entire Carnlick Creek and Christensen Creek map areas. Field mapping in these two areas was completed during the summer of 1990 as one of several subprograms related to the FGP investigation.

ACKNOWLEDGMENTS

Cathie Hickson and Derrick Brown participated in the initial reconnaissance of the Ilgachuz Range in 1982, and Chris Dodds and Steve Irwin assisted with the field mapping in 1985. Computer formatting and machine plotting of the chemical and mineralogical data was done by Paul Metcalfe. Our thanks to all of you.

The success of this project owes much to the skill and good judgment of the pilots who worked with us under often trying conditions. For getting us safely in and out of many difficult spots we thank John Fry, Rob Owens, Mike King, and Rob Skelly.

Our special thanks to Maurice Lambert whose insightful discussion and diligent review of the original manuscript made a substantial contribution to this work.

GENERAL GEOLOGY

The Carnlick Creek and Christensen Creek map areas include rocks ranging in age from early Mesozoic to Pliocene or younger (Table 1; Map 1845A). The pre-Tertiary map units include unfoliated metavolcanic rocks of probable Triassic age and layered sedimentary and volcanic rocks that are probably correlative with the Jurassic Hazelton Group.

Metamorphic rocks comprising mylonitic orthogneiss, pelitic schist, biotite gneiss, and gneissic granodiorite are probably coextensive with the Eocene Tatla Lake Metamorphic Core Complex that lies south of the mapped area (Friedman and Armstrong, 1988). Felsic volcanic rocks of the Eocene Ootsa Lake Group are poorly exposed and one can only speculate that they and the metamorphic core complex may be related to a common thermal event.

Undeformed late Tertiary volcanic rocks cover most of the mapped area. Flat-lying basalt flows of the Miocene-Pliocene Chilcotin Group form low, discontinuous escarpments on the plateau surrounding the Ilgachuz Range. They are coextensive with a vast lava field that extends eastward across much of the Interior Plateau. The Ilgachuz Range is a Late Miocene shield volcano comprising a complex assemblage of alkaline to peralkaline volcanic rocks, the Ilgachuz Group, which range in composition from basalt to rhyolite. The Ilgachuz Group has been subdivided into four formations, each of which includes several map units.

Pliocene or younger pyroclastic cones and associated flows of olivine basalt occur on the flanks of the Ilgachuz Range. They are similar in composition and in form to monogenetic cones scattered along the Anahim Volcanic Belt from Kitasu Hill on the coast to Nazko Cone west of Quesnel.

Triassic (?) and Jurassic Hazelton Group (in part)

In Anahim Lake map area, Tipper (1969) subdivided the Hazelton Group into two map units: a Lower and/or Middle Jurassic unit consisting mainly of dark green andesite and basalt associated with black argillite and chert-pebble conglomerate; and a Middle Jurassic unit consisting almost entirely of varicoloured volcanic rocks. In addition, he recognized an extensive group of pre-Middle Jurassic metamorphosed volcanic and sedimentary rocks, which lie within and along the eastern margin of the Coast Plutonic Complex.

In Carnlick Creek and Christensen Creek map areas, the paucity of outcrop and absence of fossils preclude any direct correlation with Tipper's (1969) units. Instead, the lower Mesozoic rocks within the mapped area have been divided into two units (**TJHm** and **TJHv**)[1] on the basis of their

[1]Technical difficulties preclude the use in this text of the specialized symbols found on map 1845A. However, the use of conventional type to approximate these symbols does not seem to intruduce any unacceptable problems if the legend of map 1845A is used when referring from text to map.

Table 1. Table of formations.

PERIOD OR EPOCH	GROUP FORMATION	UNIT	NAME/LITHOLOGY
Pleistocene and Recent		Q1-Q6	glacial drift, colluvium
Pliocene or younger		Pf	Flank basalt, satellitic cones
	-------- Disconformity --------		
	ITCHA GROUP	PI	comenditic trachyte, basalt
Late Miocene and Early Pliocene	ILGACHUZ GROUP		
	Tundra Mountain Volcanics		
		MPTf	Far Mountain basalt
		MPTg	Go-around rhyolite
		MPTh	Hump Mountain basalt
		MPTn	North Rift basalt
		MPTs	Stonecrop basalt
-------- Disconformity --------			
Late Miocene	Arnica Lake Volcanics	MA, MA	comendite and comenditic trachyte flows and intrusions
	-------- Disconformity --------		
	Carnlick Creek Volcanics		
	(Shield and dome facies)		(Intracaldera facies)
	MCpos Pipe Organ trachyte		MCpo Pipe Organ trachyte
	MCr Rich Creek rhyolite		MCs Saxifraga trachyte
	MCc Calliope rhyolite		MCp Phacelia tuff
	MCm Mizzen Mountain rhyolite		MCpc Pan Creek tephra
	MCps Pan Creek tephra		MCf Festuca comendite
			MCe Epiclastic deposits
	-------- Local disconformity (caldera fault scarp) --------		
	Dean River Volcanics	MD, MD	comendite and comenditic trachyte flows and intrusions
-------- Conformable contact (?) --------			
Miocene and ?younger	CHILCOTIN GROUP	Mc	basalt flows
-------- Angular unconformity --------			
Early Tertiary and/or older	OOTSA LAKE GROUP	TOv, TOg	felsic volcanics, quartz-porphyry intrusions
	-------- Contact relationship unknown --------		
	Tatla Lake Metamorphic Core Complex		
		TT	schist, gneiss, migmatite, mylonite
-------- Locally in fault contact with Hazelton Group --------			
Jurassic (?)		Jq	quartz diorite
Triassic (?) and Jurassic	HAZELTON GROUP (in part)		
		TJHv	andesite breccia and flows
		TJHm	metavolcanics

metamorphic grade and degree of deformation. Unit **TJHm** is probably correlative in part with Tipper's (1969) pre-Jurassic unit whereas unit **TJHv** may include Lower to Middle Jurassic rocks equivalent to both of Tipper's (1969) Hazelton Group units.

Map unit TJHm

Two small areas of low grade metavolcanic and lesser metasedimentary rocks (map unit **TJHm**) are exposed within the mapped area. The larger of the two areas contains scattered outcrops along West Road (Blackwater) valley in the extreme northwest corner of Carnlick Creek map area. There the predominant lithology is greenstone, which varies in its degree of deformation from dark green chloritic schist with no vestige of primary textures to a pale green, platy, subphyllitic rock in which the flattened remnants of breccia clasts up to 50 cm long are still visible. Isolated outcrops of highly deformed, thinly laminated argillaceous sediments occur in the same general area but their relationship to the volcanics is unknown. In most of these outcrops, bedding features are obscured by a pervasive phyllitic fabric. However, minor folds and crenulations defined by original sedimentary laminations were observed locally.

A second, much smaller area of greenstone assigned to map unit **TJHm** is exposed beneath Ilgachuz Group lavas in the canyon of Christensen Creek. It is a dark grey, slightly foliated, randomly jointed rock with quartz-epidote nodes and stringers.

Thin sections of the unit **TJHm** greenstone reveal a fine grained granular mosaic of feldspar and quartz intergrown with chlorite, epidote, and radiating clusters of actinolite crystals. The clastic texture of crystal-lithic tuffs is still visible in some sections. In these rocks broken feldspar crystals and subangular clasts of microphyric andesite are enclosed in a recrystallized matrix of secondary minerals. All but the finest grained associated sediments show original bedding features including laminations due to size sorting. Most of the metasediments comprise elliptical grains of quartz and feldspar in a mesostasis of chlorite, amphibole, and opaque oxide. They appear to have been derived from argillite and argillaceous tuff. Complex minor folds and crenulations are ubiquitous. Foliation due to flattening of clasts and development of secondary micas commonly coincides with bedding. The mineral assemblage indicates a metamorphic grade ranging from greenschist to lower amphibolite.

With the exception of the greenstone in Christensen Creek canyon, the pervasive foliation that characterizes the rocks of unit **TJHm** has a north to northeast trend and steep easterly dip. This contrasts with the easterly trend and steep southerly dip of gneissosity in the nearby Eocene Tatla Lake Metamorphic Core Complex.

Map unit TJHv

Unmetamorphosed volcanic and volcaniclastic rocks (unit **TJHv**) tentatively correlated with the Hazelton Group are exposed in both Christensen Creek and Carnlick Creek map areas. They form prominent rocky knolls and cliffs in the low hills north of the Ilgachuz Range, along West Road (Blackwater) River valley, and are exposed in road cuts in Dean River valley near Poison Lakes.

The predominant lithology is varicoloured green, purple, reddish-brown, to black volcanic breccia with subangular to subrounded clasts up to 40 cm across. Most outcrops display no bedding features. The clasts are commonly unsorted and randomly oriented but bedding is locally defined by variations in clast size and rarely by thin interbeds of lapilli and finely laminated tuff. The clastic rocks are associated with a lesser volume of massive flows. These are commonly highly fractured and veined with quartz-epidote stringers.

Most of the flows and breccia clasts are aphyric or, less commonly, contain randomly oriented feldspar and/or pyroxene phenocrysts up to 2 mm across. Large quartz-chlorite amygdules are developed locally. In thin section, the aphyric rocks are seen to comprise about 50% feldspar in stout, randomly oriented laths (<0.5 mm) in a matrix of pale green chloritized mafic minerals, opaque oxide granules, and variable amounts of recrystallized quartz. Feldspar phenocrysts in the porphyritic phases are intensely altered plagioclase with simple albite twinning. Pyroxene phenocrysts are commonly unaltered euhedral augite twins. The petrography is consistent with an andesitic composition and low greenschist grade of metamorphism. Unlike the strongly foliated rocks of unit **TJHm** no evidence of strain was observed in any of the rocks in unit **TJHv**.

Jurassic (?)

Map unit Jq

Coarse grained granodiorite with widely spaced rectangular jointing is exposed where the West Road (Blackwater) River has cut a steep-sided canyon into the escarpment on the north side of the Ilgachuz Range. The granodiorite is overlain unconformably by Dean River comendite but its relationship to pre-Ilgachuz Group rocks was not observed. Despite its close proximity to the mylonitic gneisses of the Tatla Lake Metamorphic Core Complex the granodiorite is unfoliated and shows no evidence of strain or fracturing.

The granodiorite has a coarse hypidiomorphic-granular texture comprising 15% euhedral and subhedral crystals of hornblende, 5% biotite, 40% feldspar, and 30% clear interstitial patches of quartz. The hornblende is fresh whereas biotite is partly altered to chlorite. Most of the feldspar has been kaolinized, but both albite and K-feldspar with cross-hatched twinning are preserved in small unaltered patches. Wavy extinction of the quartz is the only evidence of strain.

Tatla Lake Metamorphic Core Complex

The name Tatla Lake Metamorphic Complex (TLMC) was adopted by Friedman and Armstrong (1988) to describe a northeasterly trending belt of metamorphic rocks on the southwestern side of the Intermontane Belt. The rocks were originally mapped as part of the Mesozoic Coast Intrusions (Tipper, 1969); however, detailed mapping and extensive

radiometric dating by Friedman and Armstrong (1988) demonstrated that the TLMC is an Eocene metamorphic core complex. In the type area, south of Christensen Creek map area, the complex comprises a core of amphibolite-grade gneiss and migmatite overlain by a thick zone of ductilely sheared metamorphic rocks. The latter are in fault contact beneath an upper plate of low metamorphic grade cover rocks.

Strongly foliated metamorphic rocks (map unit **TT**), exposed beneath late Tertiary lavas in the western part of Christensen Creek and Carnlick Creek map areas, are probably coextensive with the TLMC to the southeast and with similar metamorphic rocks to the northwest. Although exposures are discontinuous, the lithologies are similar to those described by Friedman and Armstrong (1988) in the ductilely sheared zone and low grade cover rocks of the type area.

Rainbow Lake area

Scattered exposures of gneiss outcrop over a large area on the northwest flank of the Ilgachuz Range, near Rainbow Lake. The principal rock type is medium- to coarse-grained mylonitic orthogneiss comprising quartz, feldspar, and amphibole, plus secondary chlorite, sericite, and actinolite developed on the foliation planes (Fig. 10). Variations in the mineral proportions suggest a heterogeneous plutonic protolith ranging from quartz diorite to quartz monzonite. Relatively small areas of calc-silicate and chloritic schist are associated with the orthogneiss indicating that some of these highly strained rocks were derived from sediments and volcanics. The rocks are characterized by a well developed, horizontal to shallowly plunging, east-trending stretching lineation (Ls) defined by quartz and feldspar augen, and a steeply south-dipping mylonitic foliation (Ss) that contains Ls.

A tops-to-the-east sense of shear is indicated by pressure shadows around asymmetric porphyroclasts, shear bands, and vergence of minor folds. In the type area, farther southwest, Friedman and Armstrong (1988) noted that most kinematic indicators give a tops-to-the-west sense of shear. If the two areas are coextensive, then the opposing sense of shear suggests that they may lie on opposite sides of a dome-shaped structural culmination.

Central Ilgachuz Range

Two areas of metamorphic rock are exposed in the central part of the Ilgachuz Range at elevations above 5500 ft. (1675 m). Phyllite associated with chloritized granite occurs in upper Hump Creek valley, and a relatively small slice of orthogneiss is exposed on the northeast flank of Monocephala Peak.

On Hump Creek, lustrous grey phyllite outcrops intermittently along benches west of Saxifraga Mountain. The section is about 150 ft. thick and dips east at about 45 degrees. Below the phyllite, exposed in small creek canyons, is about 200 ft. of coarse grained chloritized granite with a wavy, poorly developed fabric and widely spaced rectangular joints. The contact between the phyllite and the granite was not observed. Thin sections of the phyllite reveal a well developed planar fabric with small (±0.5 mm) lenticular quartz porphyroclasts in a matrix of mica ribbons (Fig. 11). The quartz porphyroclasts are of two distinct types. The more abundant are relatively small attenuated ribbons of recrystallized quartz. Porphyroclasts of the second type are uniformly dispersed throughout the rock and comprise flattened lenticles of clear quartz that show little evidence of recrystallization. A few of the latter are bordered by pressure shadow domains of newly precipitated quartz similar to that of the quartz ribbons. The intense planar fabric of this rock indicates considerable strain. This was probably initiated as ductile shearing, which produced the quartz ribbons and mica foliation and may have culminated in slippage along the resulting foliation planes. The clear quartz porphyroclasts are probably residual cores of larger porphyroclasts, which escaped internal strain when shearing was concentrated along glide planes in the highly foliated surrounding matrix.

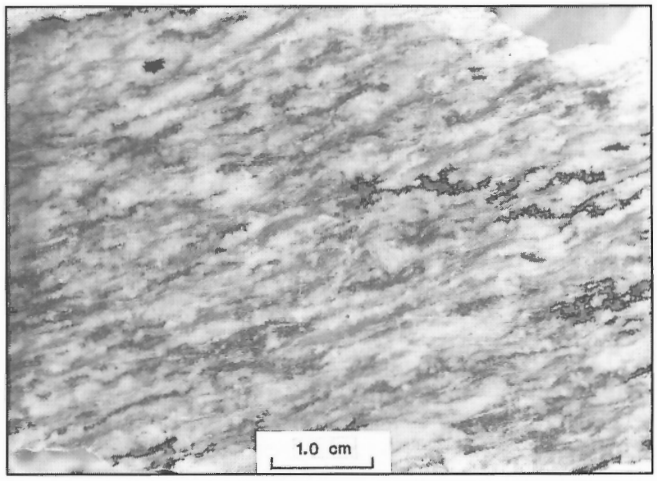

Figure 10. *Photograph of gneiss in the Rainbow Lake area. GSC 1993-184GG*

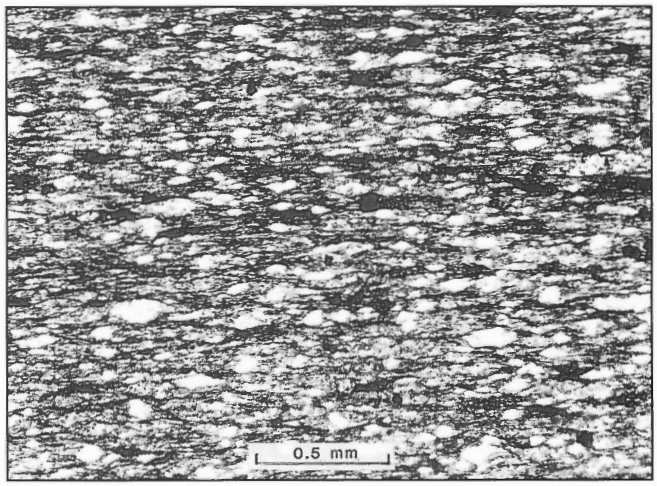

Figure 11. *Photomicrograph of phyllite from under the Ilgachuz Group flows in Hump Creek valley. Rock has well developed mylonitic texture and lenticular quartz porphyroclasts. GSC 1993-184DD*

The granite below the phyllite consists of quartz, perthitic alkali feldspar, and minor muscovite and sodic plagioclase. Thin sections reveal a random network of fractures which give the rock a shattered cataclastic texture on a scale of a few millimetres. The feldspar has deformed by brittle fracturing, whereas the quartz shows evidence of ductile strain and recrystallization (Fig. 12). The fracture zones are up to 3 mm across and comprise a strongly foliated aggregate of secondary mica, recrystallized quartz, and dislocated feldspar fragments.

The phyllite and the underlying granite were probably derived from a common plutonic protolith. The upward increase in the amount of strain suggests that the phyllite may be a mylonite zone related to a southwest-dipping detachment fault. The contrasting behaviour of quartz and feldspar suggest that most of the strain took place at relatively low temperature, in the range of 300° to 450°C where quartz deforms ductilely but feldspar remains brittle (Tullis and Yund, 1977; Sibson, 1983).

On the northeast buttress of Monocephala Peak a narrow screen of fissile, lustrous grey to brown schist lies along the southern contact of a late Tertiary subvolcanic pluton (see section on Pipe Organ trachyte). It is bounded on the north by an intrusive contact with coarse grained Pipe Organ trachyte and on the south by a fault contact with Calliope rhyolite. The rock has a wavy mylonitic fabric and contains lenticular porphyroclasts of quartz and feldspar up to a centimetre long. The foliation is nearly vertical and, in contrast to the easterly trend of Tatla Lake metamorphic rocks elsewhere in the mapped area, it has a northwesterly trend, roughly conformable with the intrusive contact. However, the contact cuts locally across the foliation as does a narrow zone of rusty thermal alteration. The intrusion may have rotated the block of mylonite from its original orientation but it has not affected the internal fabric.

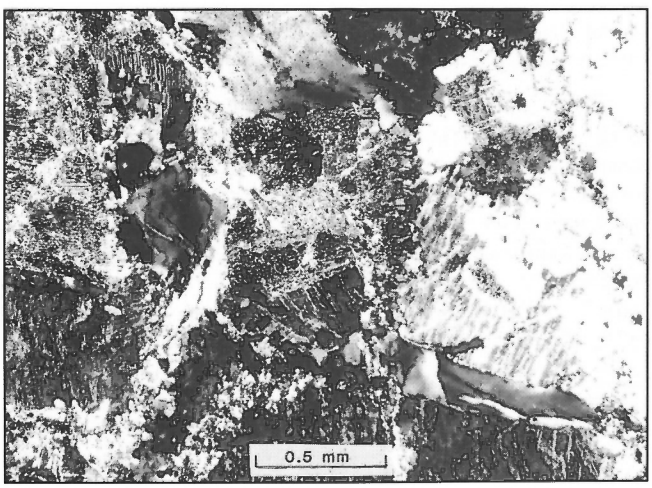

Figure 12. *Photomicrograph showing textures caused by brittle deformation of feldspar and ductile strain of quartz in granitic rock structurally below the phyllite of Figure 11. GSC 1993-184EE*

In thin section the phyllite is seen to have a typical mylonitic fabric. Porphyroclasts of quartz and feldspar have the dynamically recrystallized quartz tails and pressure shadows that are characteristic of ductilely deformed rocks (Fig. 13). Like the rocks in Hump Creek, most of the ductile strain has been absorbed by quartz whereas feldspar has failed by brittle fracturing.

Ootsa Lake Group

The early Tertiary Ootsa Lake Group underlies large areas in Nechako River and eastern Anahim Lake areas where Tipper (1963, 1969) described it as a thick assemblage of nonmarine varicoloured rhyolitic to andesitic flows and pyroclastic rocks. The Ootsa Lake strata in the type area are flat-lying or gently warped, and rest unconformably on all older rocks.

Map unit TOv

Volcanic rocks and associated porphyry intrusions of the Ootsa Lake Group are poorly exposed in the northern part of Carnlick Creek map area and along Dean River valley in the Christensen Creek map area.

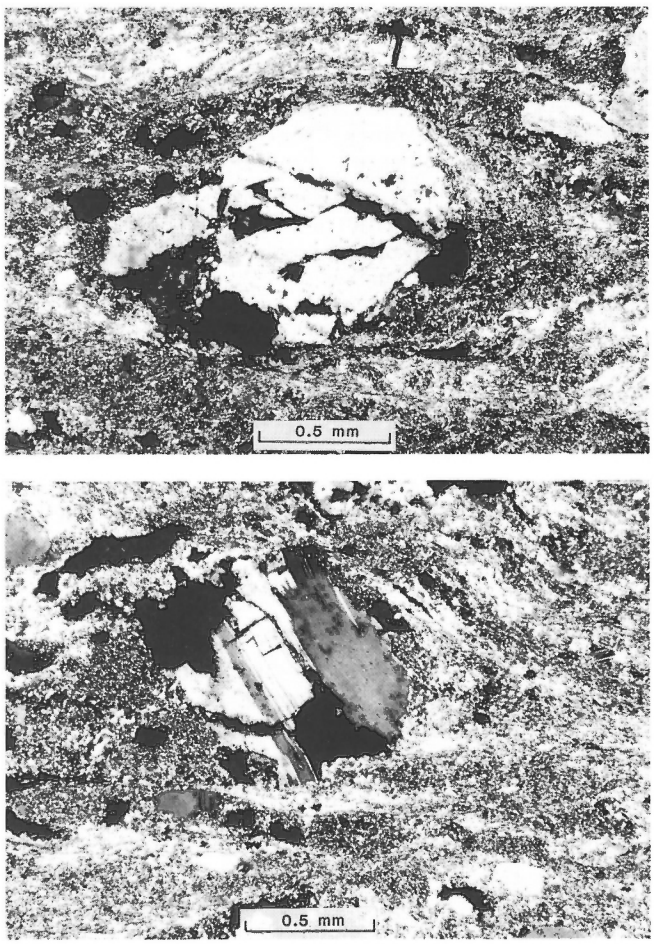

Figure 13. *Photomicrograph of rotated porphyroclasts with quartz pressure shadows in mylonite from Monocephala Peak. GSC 1993-184II*

The outcrops north of Cluchuta Lake and along West Road (Blackwater) River north of Tsetzi Lake are flaggy-weathering, light buff to pale green rhyolite flows. They are very fine grained, either aphyric or sparsely porphyritic with 0.5 to 1 mm phenocrysts of feldspar, quartz, and altered amphibole. Farther west, the Ootsa Lake rocks that outcrop north of West Road (Blackwater) River comprise blocky-jointed rhyolite porphyry. The pale, purplish-grey groundmass is crowded with stout 2 to 3 mm phenocrysts of white feldspar and rounded grains of smoky quartz. The rock lacks any flow structures and its uniform texture over a large area suggests that it may be an intrusion or large dome.

An extensive area of white-weathering, varicoloured rhyolite breccia is exposed in Dean River valley west of Poison Lakes. The fresh rock comprises closely packed, angular to subangular, white, pink, and pale green aphyric rhyolite clasts up to 10 cm across. Clasts are randomly oriented and unsorted suggesting a proximal subaerial source.

No evidence of shearing or folding was seen in any of the Ootsa Lake rocks. However, the poor exposure and lack of bedding features preclude any structural interpretation of these rocks.

Map unit TOg

White-weathering, coarse- to medium-grained, leucocratic quartz porphyry is exposed west of Pettry Lake, in the northwestern corner of Carnlick Creek map area, and between Christensen and Lessard creeks in the southwestern corner of Christensen Creek map area. In both places the contacts are covered, but nearby outcrops of greenstone (map unit **TJHm**) suggest that the porphyries are young intrusive bodies that cut the older, strongly foliated rocks. The quartz phenocrysts, which are up to 3 mm across, are euhedral to subhedral and show no evidence of strain. The feldspar is kaolinized, and clusters of opaque oxides are the only remaining dark minerals. Small quartz-lined miarolitic cavities suggest that the porphyry was emplaced at a shallow depth and that postemplacement alteration has been minor. The lack of alteration and lithological similarity to rhyolite breccias of map unit **TOv** suggest a possible correlation with the Tertiary Ootsa Lake Group.

Chilcotin Group

Basaltic lavas of the Chilcotin Group cover vast areas of the Interior Plateau adjacent to the report area. They are commonly flat-lying and rest unconformably on all of the older rocks of the Intermontane Belt. North of Carnlick Creek map area, in Nechako River area, the flat-lying Tertiary lavas were assigned by Tipper (1963) to the Endako Group. In the Anahim Lake map area (Tipper, 1969) they are referred to informally as the "plateau lavas". The name Chilcotin Group was introduced by Tipper (1978) and adopted by Bevier (1983a) for all of the flat-lying basaltic lava fields of the Interior Plateaus. Mathews (1989) later proposed that the name be formalized "to include the Early Miocene to Early Pleistocene basalts, and the clearly associated pyroclastic and sedimentary rocks, in the southern interior of British Columbia from the Okanagan Highland to the Nechako Plateau but not including the volcanoes of the Anahim Belt or the 'valley basalts' of later Pleistocene to Holocene age." The frequency distribution of nearly 80 K-Ar dates from the Chilcotin basalts (Mathews, 1989) shows distinct clusters in the ranges 14-16 Ma, 6-9 Ma, and 1-3 Ma.

The Chilcotin lavas are mineralogically similar to alkali basalt but intermediate in chemical composition between alkali basalt and tholeiite. The term "transitional basalts", introduced by Bevier (1983b), has been widely adopted.

Bevier (1983a, b) has shown that the Chilcotin lavas issued from numerous separate central vents and coalesced to form a group of overlapping, low-profile shields analogous to the "plains basalts" of Greeley (1982). The relationship between Chilcotin Group lavas and basalts that issued from the Ilgachuz and adjacent Rainbow and Itcha shield volcanoes is poorly understood. Tipper (1969) believed that flows from the shield volcanoes spread out and merge with those of the surrounding plateau – the two being coeval and coextensive. Bevier (1981) and Souther (1984, 1986) showed that the central shield volcanoes of the Anahim Belt are highly fractionated piles ranging from picritic basalt, through trachyte to peralkaline rhyolite, in marked contrast to the uniform transitional basalt composition of the Chilcotin lavas. The peralkaline affiliation and easterly decrease in the age of volcanism along the Anahim Belt lead to its interpretation as a hotspot trace (Bevier et al., 1979; Souther, 1986), whereas the Chilcotin basalts are interpreted as back-arc lavas, related to the subduction of Juan de Fuca Plate, which erupted along a northwesterly trending belt behind the Pemberton and Garibaldi calc-alkaline volcanic fronts (Souther, 1977; Bevier, 1983b).

Despite their many differences, the Anahim Belt and Chilcotin Group lavas overlap in both age and composition. Discriminating between distal basalt flows from the Anahim Belt shield volcanoes and plateau lavas of the Chilcotin Group is difficult, if not impossible, particularly in areas of sporadic outcrop. In the report area only those basalts that occur beyond any topographic expression of the Ilgachuz shield are assigned to the Chilcotin Group (map unit **Mc**).

Basaltic flows along West Road (Blackwater) River (Fig. 14) are coextensive with Chilcotin Group lavas that extend north and east of the report area. Outcrops of similar basalt are exposed intermittently along Dean River valley west and south of the Ilgachuz Range. The basalt occurs in isolated bluffs, rock drumlins, and small patches of glacially-scoured pavement that are invariably surrounded by till and other surficial deposits. Neither the upper nor lower contact of the Chilcotin Group lavas was observed and even individual flow contacts are rarely exposed. Cross-sections of flows are commonly at least 10 m thick and have well formed columns from 1 to 2 m in diameter. Weathered surfaces are covered by a thick, dark reddish-brown alteration rind. The fresh rock is lustrous dark bluish grey to black. Most flows are porphyritic with feldspar phenocrysts from 0.5 to 3 cm across. The proportion of phenocrysts varies from about 20% to essentially aphyric rocks that contain only a few large, widely spaced feldspar crystals. Feldspar is commonly the

only phenocrystic mineral; however, olivine phenocrysts from 1 to 2 mm across were observed in a few outcrops that are interpreted to be part of the Chilcotin Group succession. Vesicles are rare, probably because the upper and lower portions of flows are covered, but where observed they are filled with secondary minerals.

Thin sections of Chilcotin Group basalt reveal little alteration except for devitrification of interstitial glass, mantling of some olivine by iddingsite, and filling of cavities with pale green celadonite. In the feldsparphyric basalts, euhedral to subhedral, partly resorbed phenocrysts of unzoned plagioclase are set in a fine grained subophitic to intersertal groundmass comprising plagioclase, clinopyroxene, opaque oxides, and minor devitrified glass. Olivine is commonly absent. However, in a few thin sections olivine occurs as euhedral 0.5 to 2 mm microphenocrysts that form up to 10% of the rock. It is associated with 1 to 2 mm microphenocrysts of plagioclase in a groundmass of plagioclase laths, interstitial crystals of clinopyroxene, and opaque oxides. Some of these rocks have a diktytaxitic texture in which the intergranular cavities are now filled with secondary minerals.

Ilgachuz Group

The Ilgachuz Group encompasses the assemblage of lava flows, domes, subvolcanic intrusions, and associated pyroclastic and sedimentary rocks that comprise the Ilgachuz Range shield volcano. The group is divided into four formations: the Dean River Volcanics, which form the thick basal part of the comenditic shield; the Carnlick Creek Volcanics, which are divided into a "shield and dome facies" comprising rhyolite domes and flows and an "intracaldera facies" comprising related caldera-filling deposits; the Arnica Lake Volcanics, which form the thick upper part of the comenditic shield; and the Tundra Mountain Volcanics, which form a relatively thin outer mantle of basalt.

The above formations have been further subdivided into 16 map units.

Dean River Volcanics

The oldest exposed rocks of the Ilgachuz Group are assigned to the Dean River Volcanics (map units MDv, MDi). They consist mostly of feldsparphyric comendite and comenditic trachyte flows, and minor pyroclastic breccia (map unit MDv) that form a broad, elliptical platform on which the younger volcanic edifice is built. Distal flows of the Dean River Volcanics form a prominent escarpment along the western perimeter of the Ilgachuz Range and outcrop along the lower benches of radial valleys cut into the Ilgachuz shield. Proximal facies, exposed in the headwaters of radial valleys near the centre of the shield, include flows, breccias, and subvolcanic intrusions, all of which have been more or less altered by hydrothermal activity associated with Dean River and younger volcanism.

The base of the Dean River Volcanics was not observed. The volcanics are overlain both conformably and disconformably by the Carnlick Creek Volcanics and disconformably by the Arnica Lake and Tundra Mountain volcanics.

At least 1000 ft. (300 m) of distal flows and associated flow-top breccia are exposed in the Dean River escarpment and along the northeast side of Carnlick Creek. Individual flows are commonly from 50 to 100 ft. (15-30 m) thick, but

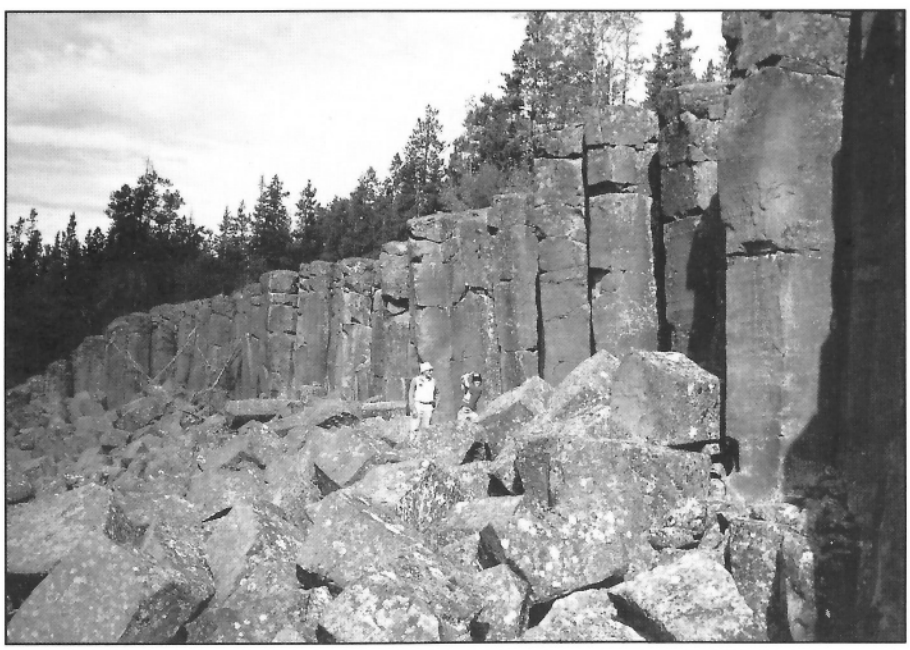

Figure 14.

Chilcotin Group columnar basalt at Basalt Lake. GSC 1993-184Y

flows up to 500 ft. (150 m) thick are present in some sections. Most distal flow units comprise at least 80% lava and 20% or less flow-top and-bottom breccia. A few metres of glass-bearing basal breccia with subvitreous lustre and highly contorted flow layering were observed locally at the basal contact of flows. The upper few metres of most flows is highly oxidized, loosely packed, blocky breccia. Columnar jointing is locally well developed, but on weathered outcrops it is masked by pervasive prominent platy fabric along subhorizontal flow foliation. The Dean River flows are deeply weathered to shades of green, greenish brown, or greenish grey, with prominent clear colourless to yellow-weathering feldspar phenocrysts.

The proximal facies of the Dean River Volcanics is exposed where deep radial valleys have eroded through overlying strata in the central part of the Ilgachuz Range. It is transitional with the distal flows and is characterized by an increased proportion of breccia, greater alteration, fracturing, and veining. In upper Festuca Creek, about 600 ft. (180 m) of mixed Dean River flows and breccia lie disconformably below southwest-dipping flows of the Arnica Lake Volcanics (Fig. 15). The entire succession consists of rusty-weathering, pale grey chaotic breccia, bits of debris-flow or rock avalanche deposits, and spires of rock that are probably remnants of fractured and dismembered flows. Local fracture zones have been healed by a stockwork of silica and calcite veins, indicating that hydrothermal activity was intense.

A multiphase intrusion (map unit MDi) is exposed in canyons at the head of Calliope Creek and on low benches adjacent to Festuca Pass. The body includes several feldspar-phyric phases of varying grain size and a phase with fine grained seriate texture. The porphyritic varieties are crowded with 1 to 2 mm randomly oriented feldspars having a nearly cubic crystal habit, whereas the intergrown, subhedral minerals of the seriate phase include a continuous range of grain sizes up to 3 mm. Crosscutting relationships between phases suggest that the body is the product of multiple episodes of intrusion and fracturing. All of the intrusive rocks are more or less fractured and cut locally by intensely altered breccia zones. Fracture zones within the intrusive body, and in adjacent Dean River flows northeast of Festuca Pass, are cut by a random stockwork of silica veinlets that probably formed during a period of post intrusion hydrothermal activity. The body is distinctly more altered and displays a greater diversity of textures than younger intrusions associated with Arnica Lake volcanism. The seriate texture is unique to this body, and glass, which is commonly present in the Arnica Lake intrusions, is completely absent. For these reasons the body is interpreted to be a subvolcanic intrusion related to Dean River volcanism.

Dean River comendite and comenditic trachytes are indistinguishable in thin sections. Both are porphyritic or microporphyritic rocks containing from 10 to 30% phenocrysts in a fine- to medium-grained, holocrystalline groundmass (Fig. 16).

More than 90% of the phenocrysts are alkali feldspar, which occurs as 1 to 5 mm euhedral to subhedral crystals. Most crystals are unzoned and have simple Carlsbad twinning. Very fine polysynthetic and cross-hatched twinning were noted in a few thin sections. Reaction rims are either absent or poorly developed on the feldspars, although some crystals have fritted overgrowths of clear alkali feldspar containing numerous inclusions.

Phenocrysts of clinopyroxene up to 1 mm across are present in most of the Dean River rocks. They occur as pale green euhedral prisms which are commonly mantled by a darker green, more sodic phase. Average extinction angles of 44° suggest hedenbergite.

Pale yellow fayalitic olivine, commonly mantled by an opaque oxide, is a rare constituent of the Dean River comendite.

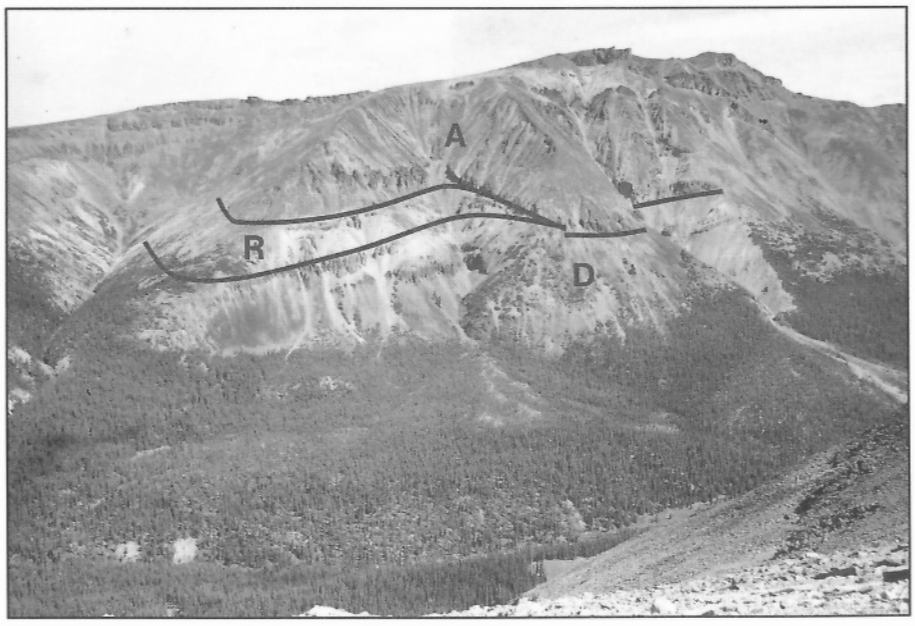

Figure 15.

Proximal flows and breccia of Dean River comendite (D), overlain disconformably by Rich Creek rhyolite (R) and Arnica Lake (A) flows on the northeast side of Festuca Creek valley. GSC 1993-184W

The groundmass of most Dean River rocks is holocrystalline, comprising 75 to 90% feldspar as stout, euhedral laths. Mafic minerals are interstitial to the feldspars and include sodic pyroxene (aegirine-augite, aegirine?), alkali amphibole (mainly arfvedsonite), and aenigmatite. Eutaxitic textures predominate, but in very thick flows and domes both phenocryst and groundmass feldspars are randomly oriented.

In the central part of the Ilgachuz Range, the Dean River rocks have undergone pervasive, low grade hydrothermal alteration resulting in a dispersion of very fine opaque oxide grains and locally in the patchy replacement of groundmass minerals by carbonate and zeolites. Elsewhere the Dean River rocks are unaltered.

Thin sections of the subvolcanic rock reveal evidence of both metasomatic alteration and incipient fracturing on a microscopic scale. Alkali feldspar, which occurs as independent phenocrysts up to 4 mm long and crystal clusters up to a centimetre across, is cut by a crudely oriented network of microfractures. A fine grained mosaic of secondary micas in the central part of each fracture is bounded by a serrated zone

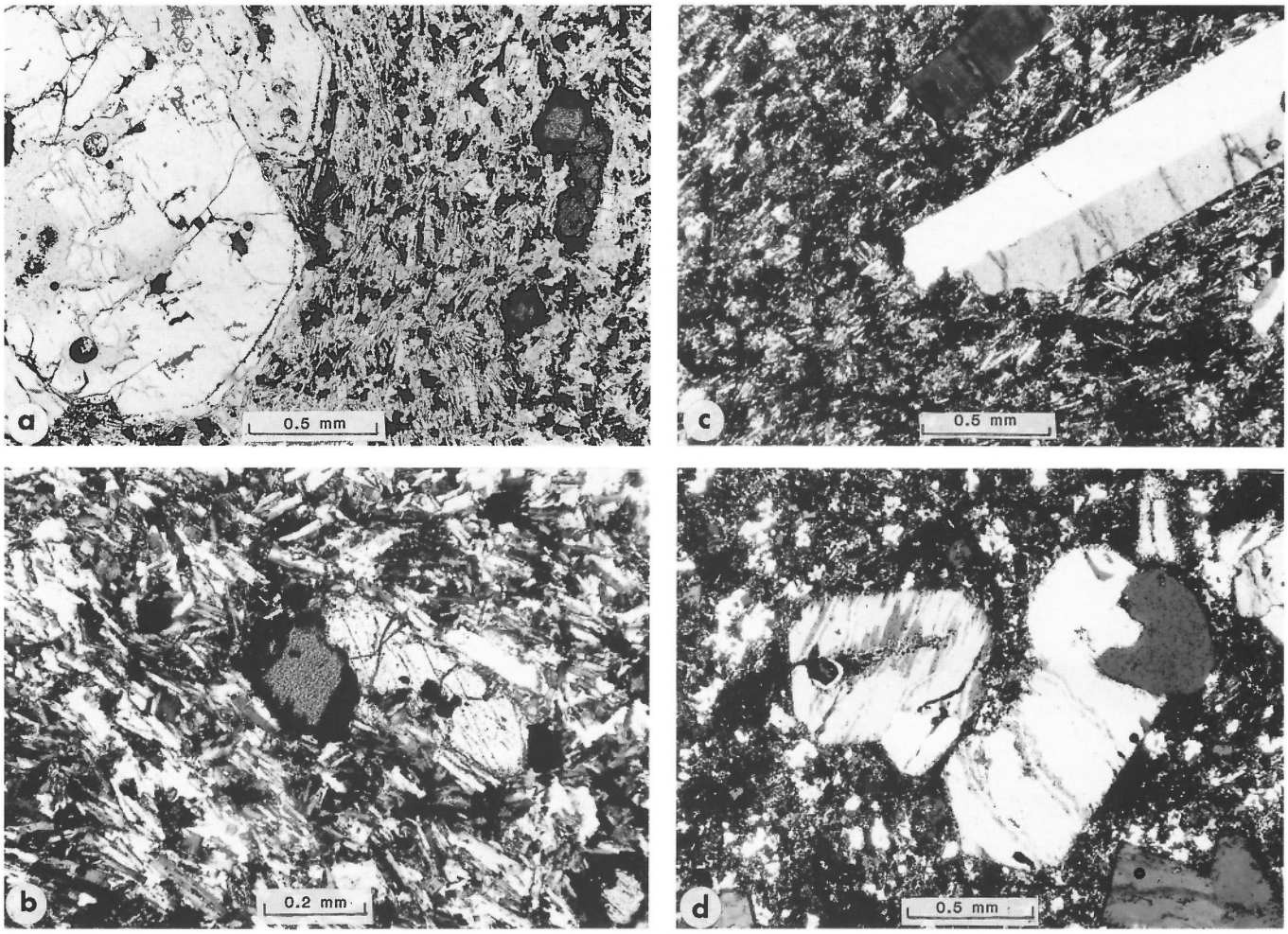

a – Comendite flow. Large alkali feldspar phenocryst and microphenocrysts of sodic hedenbergite and fayalite in a groundmass of alkali feldspar laths, pyroxene, arfvedsonite, and opaques (plane-polarized light);
b – Groundmass of comendite flow. Microphenocrysts of sodic hedenbergite and fayalite in a groundmass of alkali feldspar laths, pyroxene, arfvedsonite, and opaques (plane-polarized light);
c – Comenditic trachyte flow. Large, unzoned phenocrysts of alkali feldspar with simple Carlsbad twins in a groundmass of alkali feldspar laths, pyroxene, arfvedsonite, and opaques (plane-polarized light);
d – Comendite intrusion. Fractured and hydrothermally altered alkali feldspar, and clear quartz in a groundmass of secondary feldspars, quartz, sodic amphibole, and opaque oxides (crossed nicols). GSC 1993-184HH)

Figure 16. *Photomicrographs of Dean River comendite.*

in which the adjacent feldspar, as evidenced by different extinction, has been reconstituted to a more sodic composition (Fig. 16d). Phenocryst boundaries and groundmass feldspars have been similarly altered. In contrast, quartz remains as clear poikilitic patches and some sections retain fairly fresh interstitial aegirine and arfvedsonite, indicative of a strongly alkaline affinity comparable with other rocks in the Dean River assemblage.

The symmetrical distribution of Dean River flows with respect to the elliptical shape of the Ilgachuz Range suggests that the lava issued from one or more vents near the present centre of the shield (Fig. 17). This is reinforced by a radial outward pattern of initial dips, an increase in the proportion of pyroclastic rocks and hydrothermal alteration toward the centre of the range, and by the presence of lithologically

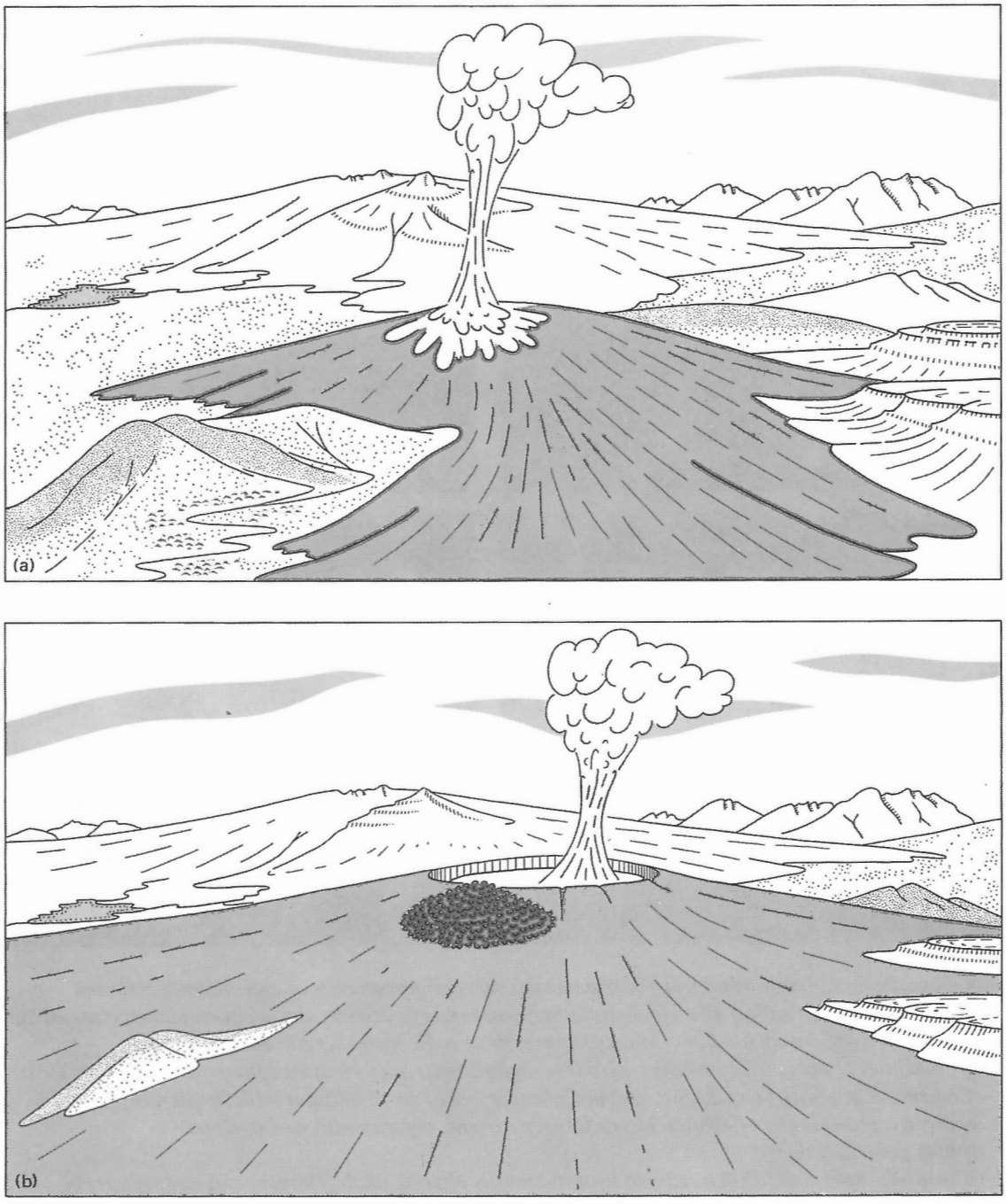

Figure 17. *Conceptual sketches showing: (**a**) An early stage in the formation of the basal (Dean River) shield of the Ilgachuz Range. Older, Rainbow Range shield volcano and Anahim Peak in background. (**b**) Caldera subsidence and eruption of one of the Carnlick Creek rhyolite domes near the centre of the Dean River shield.*

similar subvolcanic bodies in the deeply dissected centre of the Dean River pile. The great thickness and extent of many Dean River flows, the absence of intraflow fluvial deposits, and the narrow range of lithologies are compelling evidence of rapid effusion and little evolution of the primary batch of Dean River magma.

Carnlick Creek Volcanics

The Carnlick Creek Volcanics underlie most of the high peaks and ridges of the central Ilgachuz Range where they occur as thick flows, domes, pyroclastic deposits, and subvolcanic intrusions. The succession is the product of three main eruptive phases: 1) early explosive eruption of rhyolitic tephra (Pan Creek); 2) major effusion of rhyolitic magma (Mizzen Mountain, Calliope, and Rich Creek); 3) effusion and intrusion of trachytic magma (Pipe Organ and Saxifraga).

The stratigraphy of the Carnlick Creek rocks is characterized by rapid facies changes, particularly between sections exposed near the centre and on the flanks of the dissected shield. Whereas Carnlick Creek rocks on the flanks of the shield comprise mostly flows and lava domes, the succession in the central part of the shield includes thick deposits of subaerial and lacustrine tuff. The latter are interpreted to be intracaldera deposits that accumulated in a small central depression that formed either before, or during the early stages of Carnlick Creek activity (see section on Intracaldera facies). The Carnlick Creek rocks have thus been divided into two distinct facies: the "shield and dome facies", which includes the thick flows, domes, and pyroclastic beds that were deposited outside the caldera on the central part of the shield; and the "intracaldera facies", which includes the epiclastic deposits, flows, and pyroclastic rocks that were ponded in the caldera depression. Some units (Saxifraga trachyte, Phacelia tuff, Festuca comendite, and epiclastic deposits) are confined to the "intracaldera facies" whereas others (Pipe Organ trachyte and Pan Creek tephra) occur in both facies.

Shield and dome facies

The shield and dome facies is confined to the central part of the Ilgachuz shield where Pan Creek tephra is overlain by thick piles of Carnlick Creek rhyolite flows. The magma issued from at least three centres. The resulting steep-sided piles of overlapping flows and associated subvolcanic plutons are referred to informally as the Mizzen Mountain, Calliope, and Rich Creek rhyolites.

Pan Creek tephra (map unit MCps). Pan Creek tephra is the basal member of the Carnlick Creek Volcanics. It was deposited as air-fall tuff both within the central caldera (see section on Intracaldera facies) and on the flanks of the surrounding Dean River shield (Fig. 17). Some of the latter was eroded from the surface and redeposited as distal outwash, lahar, and bedded lacustrine tuff deposits beyond the outer limits of the shield. The tephra consists of pumice, lithic, and crystal fragments that were ejected during explosive, precursor activity related to the massive effusions of rhyolite lava that built the Mizzen Mountain, Calliope, and Rich Creek domes. Tephra related to the Festuca activity is probably also present in the Pan Creek succession.

The shield and dome facies of the Pan Creek tephra is a poorly consolidated, recessive horizon that is largely covered by talus from overlying massive flows. Small outcrops are preserved as discontinuous lenses less than 30 m thick in creek beds and cliff faces throughout the central part of the Ilgachuz Range. Sections on the southwest side of Festuca Creek and southeast side of Carnlick Creek were probably deposited near the caldera margin where the primary pyroclastic deposits were rapidly covered and preserved beneath thick flows of Calliope and Mizzen Mountain rhyolite. The dominant lithology is pale green, ochre- to white-weathering tuff consisting mostly of sand- to grit-sized pumice but locally containing up to 20% lithic fragments. The pumice fragments are commonly undeformed and randomly oriented in thick, crudely stratified beds. However, flattening has occurred locally and moderate welding was noted at one locality on the northeast slope of Mizzen Mountain.

The few relatively thin pockets of Pan Creek tuff preserved beneath younger flows on the central shield compared with the great thickness of fine air-fall tuff preserved within the adjacent intracaldera facies, suggests that much of the unconsolidated Pan Creek tephra originally deposited outside the caldera was rapidly washed away and redeposited elsewhere. Bedded tuff, lahar, and outwash deposits on the northeast margin of the Ilgachuz Range contain a large proportion of rounded pumiceous clasts which are consistent with such an origin. These poorly consolidated rocks are well exposed in the lower canyons of Pan Creek, Shag Creek, and Carnlick Creek valleys, where flat-lying sections up to 100 ft. (30 m) thick consist of interbedded lacustrine and outwash deposits. The lacustrine beds are commonly from 1 to 3 m thick with thin laminations defined by graded bedding and density sorting of pumice and lithic grains. Locally well developed crossbedding and channelling suggest a deltaic environment. Grains in the graded lacustrine tuff range in size from coarse grit to fine sand and consist of pumice, bits of obsidian, fine grained rhyolite, and broken crystals of quartz and alkali feldspar. The lacustrine beds are interlayered with fluvial and debris-flow deposits containing unsorted, angular to subrounded, locally-derived cobbles and boulders.

Although most of the material in these lacustrine and fluvial deposits appears to have been derived from Pan Creek ejecta, the rocks may not have been deposited in their present, distal environment until long after Pan Creek activity had ceased. Indeed the events that lead to rapid erosion and redeposition of primary Pan Creek tephra may have been triggered by some later event in the history of the volcano.

Mizzen Mountain rhyolite (map units MCmv1, MCmv2, MCmi). The Mizzen Mountain rhyolite forms a complex of overlapping domes and flows on the extreme eastern margin of the Ilgachuz Range. The deeply dissected western part of the pile rests conformably on Pan Creek tephra, but farther east Mizzen Mountain flows lap directly onto the eroded surface of the older Dean River pile.

The lower part of the pile (unit **MCmv2**) is locally more than 1000 ft. (300 m) thick and consists of light greenish- to purplish-grey rhyolite. Much of the rock is porphyritic with 2 to 4 mm phenocrysts of clear glassy feldspar and tiny black prisms of amphibole and/or pyroxene. Many of the rocks have irregular gas cavities that are commonly bounded by phenocrysts. Euhedral crystals of sodic amphibole and quartz either line or have grown into the voids. The porphyritic rocks are associated with a lesser volume of green aphanitic rhyolite with complex flow banding. Basal breccias are associated with obsidian layers several metres thick, whereas flow-top breccias are commonly porous, highly oxidized, rusty-weathering recessive zones.

The thickness of individual cooling units is extremely variable (Fig. 18). On the ridge southwest of Mizzen Mountain a 100 m thick flow wedges out completely in less than half a kilometre. Similarly rapid changes in thickness occur throughout the lower part of the Mizzen Mountain pile, which consists almost entirely of overlapping, lens-shaped flows and domes.

The upper few hundred metres of the Mizzen Mountain pile (unit **MCmv1**) consist of uniformly aphyric to sparsely feldsparphyric rhyolite flows characterized by fine laminar flow layering. The flows are relatively thin, commonly less than 10 m, and laterally persistent, in marked contrast with the lens-shaped morphology of flows in the lower part of the pile. On ridges both north and south of Pan Creek they form an east-dipping mantle over the extreme eastern side of the Mizzen Mountain pile.

The main source of the Mizzen Mountain rhyolite probably lies beneath the extrusive dome, but a cluster of pipe-like conduits (unit **MCmi**) west and south of Mizzen Mountain are probably satellitic feeders. These small intrusive bodies of pale green rhyolite are characterized by vertical flow layering (defined by trains of microvesicles), by closely spaced subhorizontal columnar jointing, and by thick glassy to subvitreous margins. The relationship between the intrusive and extrusive rhyolite is well exposed near the north end of Dodds Domes, where several thick rhyolite flow lobes are rooted in a vertically sheeted intrusive body that can be traced down through Pan Creek tephra into underlying Dean River rocks. Vertical flow layering in the root zone of the flows turns over to subhorizontal where the magma emerged from the vent and spread laterally onto the surrounding surface (Fig. 19).

Flows and domes in the lower part of the Mizzen Mountain pile include both comendite and comenditic trachytes. Although there is some overlap in petrographic criteria, the two rock types can usually be distinguished in thin section (Fig. 20). Both types are porphyritic, containing from 2 to 10% clear, euhedral, up to 4 mm size phenocrysts of unzoned alkali feldspar with simple Carlsbad twinning, and less than 1% euhedral phenocrysts of hedenbergite up to a millimetre long.

Feldspar and hedenbergite are commonly the only phenocrystic phases present in the comenditic trachytes. In most thin sections the phenocrysts are crudely oriented in a eutaxitic groundmass of subhedral alkali feldspar laths and interstitial grains of pale green aegirine.

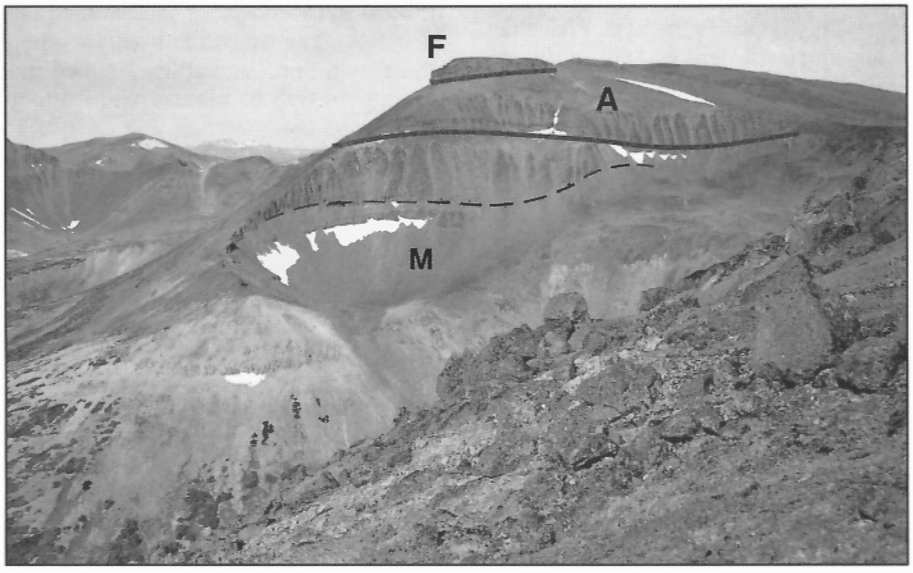

Figure 18. *View south from Mizzen Mountain toward the head of Pan Creek. Thick, lens-shaped flows of Mizzen Mountain comendite (M) are overlain by Arnica Lake comenditic trachyte (A). The ridge is capped by a small remnant of Far Mountain basalt (F). The dashed line separates two individual cooling units of the Mizzen Mountain rhyolite. GSC 1993-184S*

In addition to alkali feldspar and hedenbergite, many of the comendites contain sparse microphenocrysts (up to 0.2 mm) of pale yellow fayalitic olivine. Most of the olivine crystals are euhedral or subhedral, but they are commonly mantled by reaction rims of hematite and/or arfvedsonite. The groundmass of the comendite consists of random to spherulitic intergrowths of alkali feldspar, quartz, and femic minerals. The latter include poikilitic crystals of arfvedsonite, kataphorite (and/or aenigmatite), and aegirine. These skeletal crystals are optically continuous over areas up to 2 mm across.

Glass from the base of comenditic flows contains euhedral microphenocrysts of alkali feldspar and hedenbergite of the same size and proportion as those in the crystalline portion of the flow. The surrounding glass is unaltered and charged with streams of microlites oriented in the plane of flow.

Aphyric comendite in the upper part of the Mizzen Mountain pile has a pronounced eutaxitic texture defined by well oriented, anhedral to subhedral, interlocking grains of alkali feldspar surrounded by poikilitic intergrowths of skeletal arfvedsonite, kataphorite, and aegirine. The femic minerals are concentrated along well defined flow layers which give the rock its prominent macroscopic colour banding.

Intrusive comendite is either aphyric or contains only sparse phenocrysts of euhedral alkali feldspar. Specimens from most of the small necks and cupolas on the east side of Carnlick Creek valley are very fine grained, comprising aphyric intergrowths of alkali feldspar, sodic pyroxene, and sodic amphibole. Many of the intrusive rocks are vesicular, containing small irregular voids partly filled with tridymite.

Calliope rhyolite (map units MCcv, MCci). Calliope rhyolite is extensively exposed in the central Ilgachuz Range where it forms steep lower slopes and sharp-crested spurs in a cluster of high peaks at the head of Carnlick Creek valley (Fig. 21). Like the Mizzen Mountain rhyolite, the Calliope pile consists of thick overlapping flows and domes associated with a relatively small amount of pyroclastic breccia (map unit MCcv). The internal structure is complex. Initial dips and flow directions are random in detail but the overall geometry is that of an elliptical dome centred near Calliope Mountain suggesting an eruptive centre in that area. The Calliope and Mizzen Mountain piles both rest on Pan Creek tephra; however, the contact between the two domes is not exposed and their relative ages are unknown. The contact is taken arbitrarily between Mount Scot, where Mizzen Mountain flows dip south, and Carnlick Mountain, where Calliope flows dip east.

The Calliope eruptive rocks are light green, greenish-grey, to nearly white flows and domes of feldsparphyric rhyolite. The lower contact of the pile is well exposed on the east flank of Hierochloë Peak where the basal flow rests on a thick section of blocky rhyolite breccia and pumiceous tuff. This pyroclastic unit is probably a proximal facies of the Pan Creek tephra erupted during an initial explosion from the Calliope vent. Farther south, near the head of Hump Creek, the glassy base of the lowest Calliope flow rests on a fine grained distal facies of the Pan Creek tephra. Individual lens-shaped Calliope flows are from 50 to 500 ft. (15-150 m) thick and the composite thickness of the pile on Phacelia Peak is nearly 1000 ft. (300 m). Many of the flows have a quenched base of granular obsidian underlain by a few metres of breccia made up of porous oxidized blocks and glass shards sloughed from the flow front.

Figure 19. *Thick proximal lobes of Mizzen Mountain rhyolite near the north end of Dodds Domes. The flows are rooted in a cluster of vertical pipe-like feeders on the south (left) end of the ridge. GSC 1993-184T*

The peak and eastern flank of Calliope Mountain comprise a roughly circular body of rusty-weathering, hydrothermally altered comendite which has the form of a plug dome (map unit MCci), and is probably one of the principal eruptive vents. The rock is light grey to purplish-grey rhyolite with randomly oriented yellow feldspar clusters. A prominent set of rectangular joints extends vertically through about a hundred metres of cliff exposure. The joints are parallel with vertical sheeted trains of small (<1 mm) irregular vesicles, partly or wholly filled with hematite. Adjacent to joint surfaces the rock is bleached and mottled with clusters of secondary minerals to a depth of 5 to 10 cm. This is probably the result of late-stage hydrothermal or gas phase alteration.

In thin section the Calliope eruptive rocks have 20 to 40% euhedral phenocrysts of randomly oriented sanidine up to 4 mm across (Fig. 22). The feldspar is unzoned and forms simple Carlsbad twins. Phenocrysts of green sodic hedenbergite up to 1 mm long form about 1% of most samples. Phenocrystic aenigmatite is present in most thin sections of Calliope rhyolite. It occurs rarely as euhedral crystals up to 2.5 mm long and more commonly as small prisms less than 0.5 mm across. The groundmass comprises a mosaic of tiny sanidine laths intergrown with quartz and poikilitic grains of aegirine, arfvedsonite, kataphorite, and/or aenigmatite. Arfvedsonite also occurs as an overgrowth on both feldspar and pyroxene phenocrysts and as a vapour-phase mineral lining cavities.

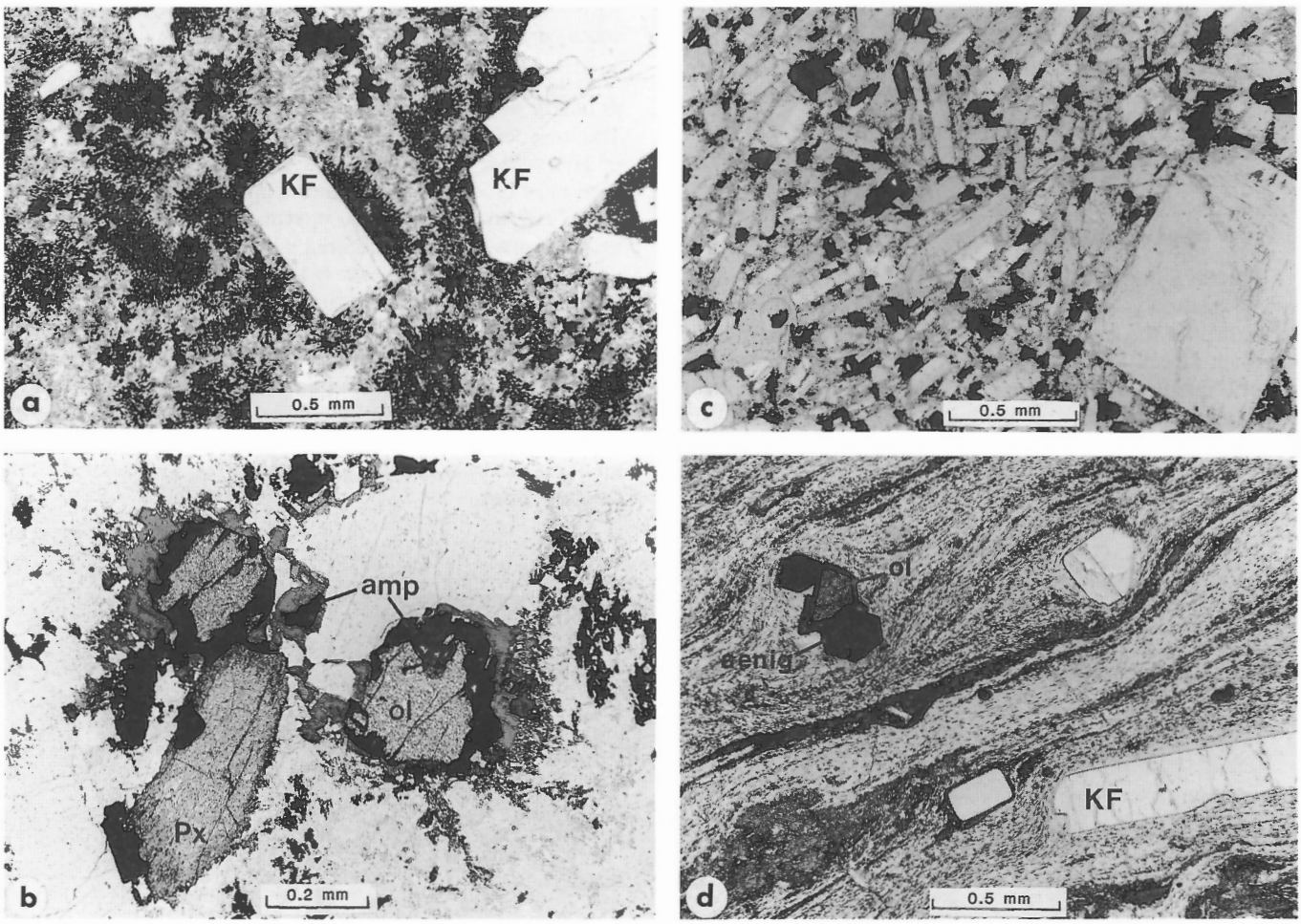

a – Comendite. Euhedral phenocrysts of sanidine (KF) in a spherulitic groundmass of intergrown alkali feldspar, quartz, aegirine, and arfvedsonite.

b – Comendite. Microphenocrysts of sodic hedenbergite (Px) and fayalite (ol) overgrown by arfvedsonite (amp). Groundmass is an intergrowth of alkali feldspar, quartz, minor aenigmatite, and arfvedsonite.

c – Comenditic trachyte. Phenocryst of anorthoclase in a groundmass of euhedral alkali feldspar, interstitial hedenbergite, and opaque oxides.

d – Comenditic trachyte glass. Microphenocrysts of alkali feldspar (KF), fayalite (ol), and aenigmatite (aenig) in a flow-banded, microlite-charged glass. All plane-polarized light. GSC 1993-184X

Figure 20. *Photomicrographs of Mizzen Mountain comendite and comenditic trachytes.*

Glass from the base of a thick Calliope flow is only slightly less porphyritic than holocrystalline rock from the central part of the flow. Euhedral sanidine and aenigmatite are the principal phenocrystic phases whereas only a few tiny grains of pyroxene were found in three thin sections of Calliope glass.

Thin sections from the central plug dome support the field evidence of pervasive alteration. Except for a few remnants of arfvedsonite, the interstitial mafic minerals have been completely replaced by granular dark red to opaque hematite which also lines or fills all vesicles. The groundmass feldspar is relatively unaltered. It consists of randomly oriented, interlocking, euhedral to anhedral grains of unzoned alkali feldspar from 0.2 to 0.5 mm long. Alkali feldspar phenocrysts up to 5 mm across form up to 40% of the rock. Unlike the groundmass feldspar, which is characterized by simple Carlsbad twinning, the phenocrysts display complex cross-hatched and fine polysynthetic twinning as well as Carlsbad twins. Most of the phenocrysts have embayed crystal margins and narrow, zoned overgrowths of more sodic feldspar.

Rich Creek rhyolite (map unit MCr). Rich Creek rhyolite is exposed beneath thick flows of Arnica Lake comendite in the head of Rich Creek valley and on the precipitous northeast side of Festuca Creek valley. Individual cooling units are up to 60 m thick. They have a vitreous base of black obsidian overlain by a 5 to 10 m zone of finely laminated, light grey to purplish-grey, fluidal-banded rhyolite containing sparse feldspar phenocrysts up to 2 mm long. The central part of most flows is massive, medium grained, commonly mottled, equigranular feldsparphyric rhyolite which grades up into porous white to pinkish-white flow-top breccia comprising subangular blocks in a matrix of comminuted rock and pumice.

The source of the Rich Creek rhyolite is unknown. However, the relatively high proportion of vitreous rocks and the presence of coarse rhyolite breccia, containing clasts up to a metre across, suggest that the Rich Creek rhyolite is not a distal facies of the Calliope pile. It was probably erupted from a local centre now covered by younger units.

In thin section the Rich Creek and Calliope rhyolites are similar (Fig. 22, 23). Crystalline rhyolite is porphyritic, containing from 1 to 10% euhedral, unzoned sanidine phenocrysts and a few euhedral prisms of aenigmatite and hedenbergite in a groundmass of subhedral alkali feldspar laths, interstitial quartz, arfvedsonite, and minor aegirine. Related obsidians vary from aphyric glass containing only microlites to glass containing up to 20% phenocrysts of sanidine. More commonly the obsidian contains sparse phenocrysts of alkali feldspar and rarely hedenbergite in a fluidal, vitreous matrix charged with acicular microlites of feldspar and pyroxene. Many of the obsidians contain two generations of feldspar: an early assemblage of relatively large (1-2 mm) partly resorbed crystals, and a younger assemblage of small spherulitic clusters (Fig. 23b). Despite their rounded form the older phenocrysts have sharp contacts and lack any evidence of embayment by or reaction with the surrounding glass. Radiating feldspar crystals, which form the spherulites, have a dendritic habit and are rarely more than 0.2 mm long. Flow layers in the glass are deflected around them, indicating that the spherulites formed prior to quenching and solidification.

Figure 21. *View looking north from Carnlick Mountain at the south face of Calliope Mountain. The massive, vertically jointed rock forming the summit area is a plug dome that was probably one of the principal eruptive centres of the Calliope rhyolite. GSC 1993-184AA*

Pipe Organ trachyte (map unit MCpos). Coarsely porphyritic trachyte flows (map unit MCpos) are exposed on Mount Scot and Go-around Mountain. They are overlain by Arnica Lake Volcanics and, although their base is covered, they outcrop above, and probably rest on, Mizzen Mountain rhyolite. The flows, which contain up to 50% large randomly oriented feldspar phenocrysts, are lithologically similar to the flat-lying ponded flow on Pipe Organ Mountain. Their steep (20-30 degree) south to southeasterly initial dips, however, indicate that they are either from a separate source outside the caldera or that they represent a distal facies of the ponded flow that spilled over the caldera rim onto the flanks of the surrounding shield.

Intracaldera facies

The stratigraphy in the central part of the Ilgachuz Range indicates that some of the Carnlick Creek strata accumulated within a central depression about 5 km across (Map 1845A). This depression is interpreted to be a small caldera which began to subside either before or during the early stages of Carnlick Creek eruptive activity. The deposition of Pan Creek tephra within the caldera depression was at least partly contemporaneous with eruption of Festuca comendite from a vent on the northeast caldera rim, and with the accumulation of epiclastic deposits along the inner margin of the caldera scarp. Thus, despite their distinctive lithologies, the superposition of these three lower units varies from place to place

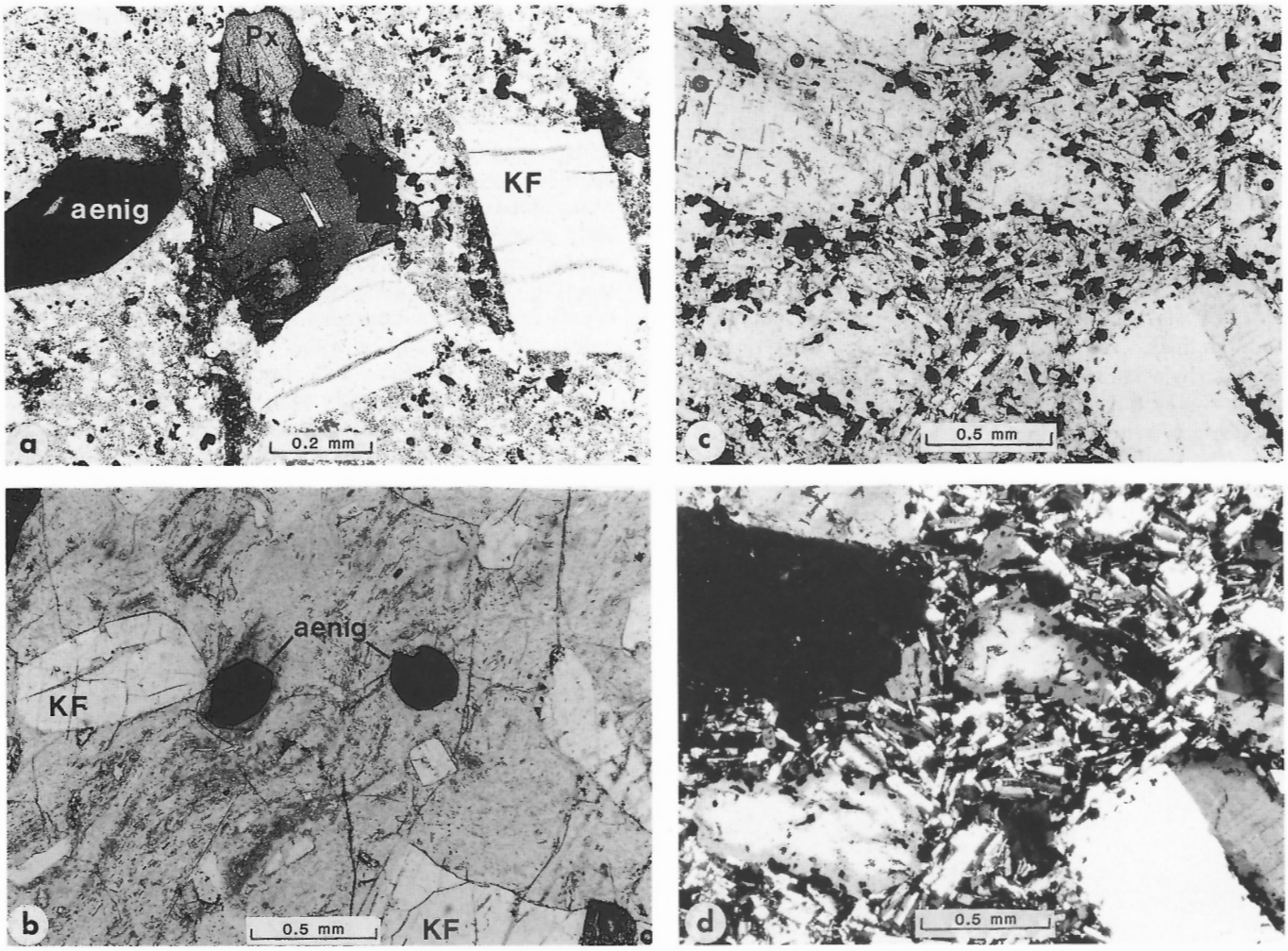

***a** – Comendite flow. Microphenocrysts of sanidine (KF), sodic hedenbergite (Px), and aenigmatite (aenig) in a fine grained groundmass of intergrown alkali feldspar, quartz, sodic pyroxene, and opaque oxides (plane-polarized light).*

***b** – Comenditic glass. Phenocrysts of sanidine (KF) and aenigmatite (aenig) in fluidal-banded glass (plane-polarized light). (c, d) Comendite plug dome. Phenocrysts of anorthoclase with deeply embayed crystal margins. Groundmass comprises euhedral alkali feldspar laths and interstitial opaque alteration products*

***c** – Plane-polarized light,*

***d** – crossed polars. GSC 1993-184CC*

***Figure 22.** Photomicrographs of Calliope rhyolite.*

depending on their proximity to eruptive vents and location relative to the caldera scarp. They are overlain by Phacelia tuff and Pipe Organ trachyte, which was subsequently ponded in the upper part of the caldera (Fig. 24). The latter may have spilled over the caldera rim onto the south slope of the shield (see section on Shield and dome facies).

Epiclastic deposits (map unit MCe). On Cindercone Peak and the adjacent ridge south of Crumble Mountain, the basal member of the intracaldera assemblage is a poorly consolidated epiclastic deposit that mantles the scarp around the northern edge of the caldera (Fig. 25). Most of the deposit is a chaotic jumble of unsorted, angular to subrounded volcanic clasts in a sparse, poorly compacted matrix of comminuted rock debris. Crudely developed stratification with steep (≈ 20 degree) southerly dips is visible locally. The thickness on Cindercone Peak is estimated to be at least 300 ft. (100 m). Most of the clasts are green feldsparphyric comendite, apparently derived from Dean River flows that form the inner walls of the caldera scarp. However, clasts of subvitreous comendite are also present. These are lithologically similar to clasts in Festuca breccia on nearby Stonecrop Ridge and are interpreted to be primary Festuca ejecta. Clast size is commonly less than 1 m, but several individual boulders up to 3 m across were noted, and one block of shattered comendite more than 30 m across is suspended in the boulder deposit on the ridge south of Crumble Mountain.

The lack of sorting, sparse matrix, and extreme range of clast sizes that characterize the epiclastic deposits suggest they are the product of rock avalanches, debris flows, and landslides. Their steep inward dip, and location between Dean River flows on the shield and lacustrine tuff (Phacelia tuff) ponded within the caldera suggests that they were sloughed from the inner walls of the caldera during its initial collapse. The presence of primary, subvitreous clasts in the basal part of the epiclastic wedge suggests that subsidence was preceded or accompanied by at least local eruptions of Festuca comendite.

Festuca comendite (map unit MCf). The Festuca comendite comprises an assemblage of flows, pyroclastic rocks, minor intrusions, and associated epiclastic rocks exposed on the south side of Pipe Organ Mountain and adjacent parts of Stonecrop Ridge, and in box canyons extending down almost to Carnlick Creek valley. In contrast to gently north-dipping Dean River flows on the adjacent shield and flat-lying Pan Creek tephra within the caldera, the Festuca succession dips consistently southwest at 10 to 30 degrees. Flows were seen only at mid and high elevations within the pile, whereas breccias are present throughout. However, the attitude of the rocks, which is almost parallel to the slope on which they are exposed, precludes any estimate of thickness.

Most of the flows consist of composite, steeply dipping pahoehoe toes with narrow, lensoid cross-sections 5 to 10 m across. Many are detached, suspended as rootless lobes of lava in a chaotic mass of collapsed flow breccia. Although most of the flow breccias comprise blocky unwelded clasts, evidence of welding and clast deformation was observed locally. Both the flows and clasts in the associated flow breccia are very fine grained to subvitreous rocks containing sparse, 1 to 2 mm phenocrysts of clear feldspar.

At lower elevations, beds of unsorted to crudely graded breccia from 8 to 10 m thick have southerly initial dips of 10 to 15 degrees (Fig. 26). Clasts, commonly less than 30 cm across, are angular to subrounded and consist entirely of subvitreous comendite similar to that forming the flows and flow breccias exposed at higher elevations. The matrix is a granular mixture of the same material plus a small amount of granular glass. Locally the breccia is interstratified with beds of fine air-fall tuff similar to, and probably coextensive with, adjacent Pan Creek tephra.

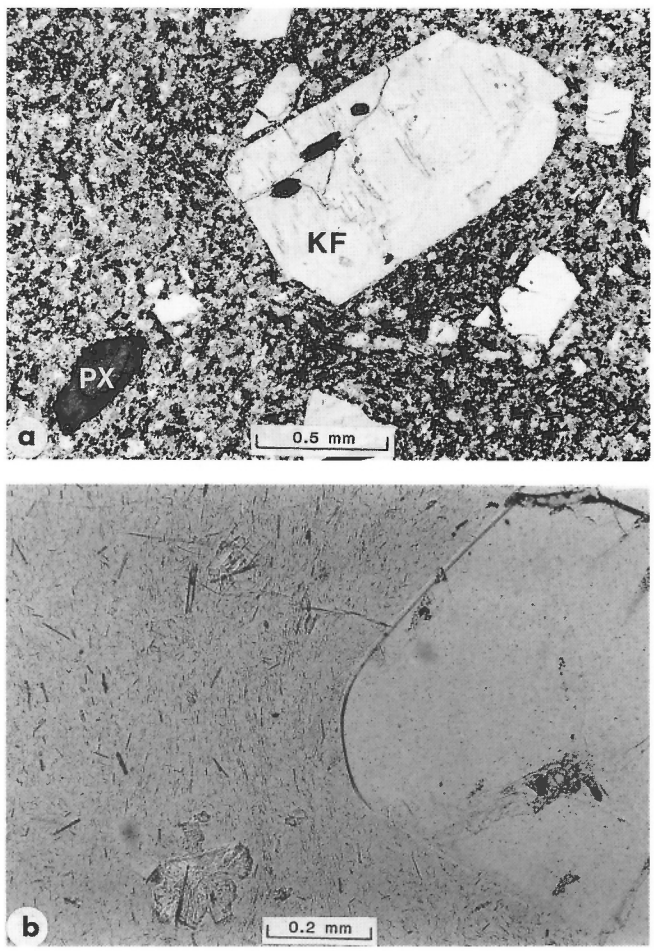

Figure 23. *Photomicrographs of Rich Creek rhyolite. (**a**) Comendite flow. Euhedral phenocryst of sanidine (KF) and subhedral crystal of sodic hedenbergite (PX) in a fine grained groundmass of alkali feldspar, quartz, sodic clinopyroxene, arfvedsonite, minor aenigmatite, and opaque oxides. (**b**) Comendite glass showing two generations of feldspar: older, partly resorbed large phenocryst; and younger, spherulitic cluster. Both plane-polarized light. GSC 1993-184BB*

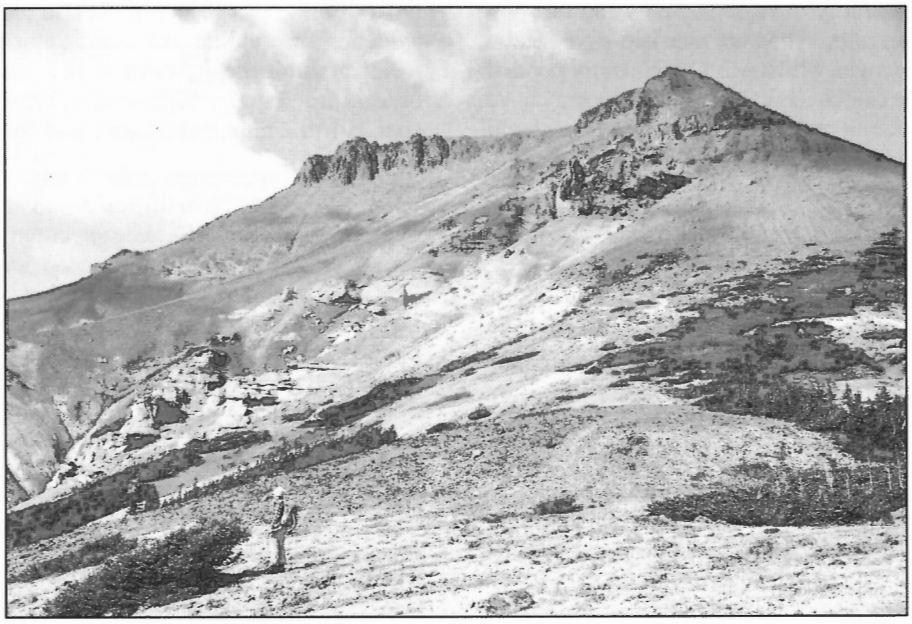

Figure 24. *View of the southeast side of Pipe Organ Mountain showing flat-lying beds of the intracaldera succession. Light coloured beds at the base are Pan Creek tephra. They are overlain successively by thin, dark coloured beds of Phacelia tuff, and the massive, ponded flow of Pipe Organ trachyte, which forms the summit cliffs. GSC 1993-184V*

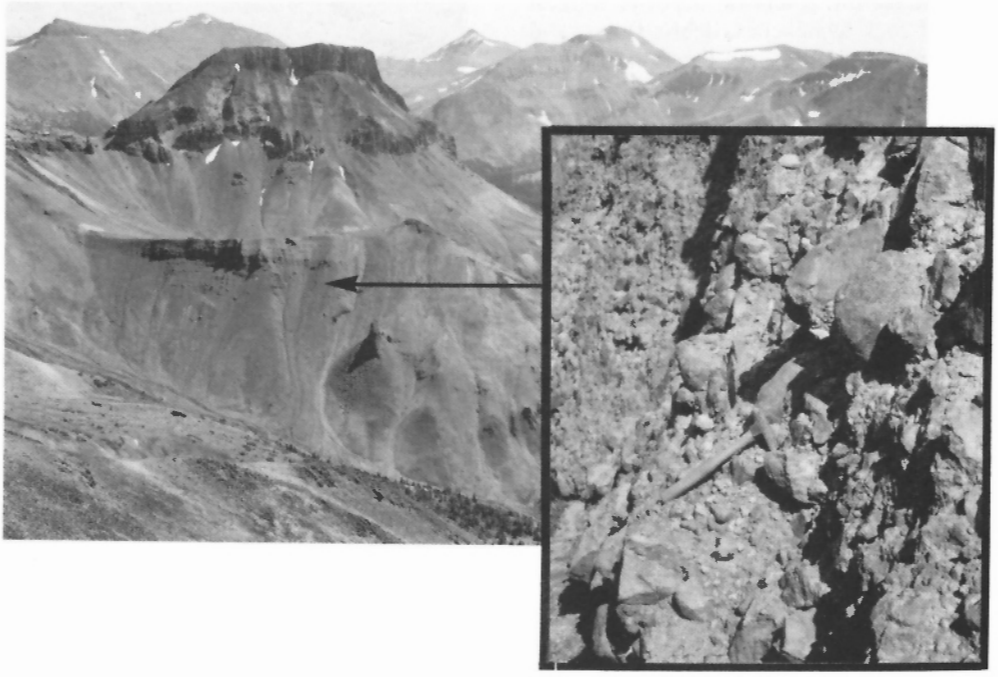

Figure 25. *View looking south from Far Mountain across crudely stratified epiclastic beds forming Cindercone Peak (foreground ridge) to the thick intracaldera trachyte flow that forms the flat-topped summit of Pipe Organ Mountain (middle distance). Inset shows detail of epiclastic deposits comprising unsorted blocks of comenditic trachyte, probably eroded from Dean River flows. GSC 1993-184FF*

The Festuca succession was clearly deposited on a steep southwest-facing slope, toward the inferred central caldera. Indeed the activity was probably concentrated along the northeastern caldera margin where successive eruptions of Festuca comendite built an edifice that lapped onto the caldera rim near Nana Peak and mantled the adjacent inner wall of the caldera depression (Fig. 27a). The thick, crudely graded breccias that mantle the lower slopes were probably deposited as block flows and lahars that originated from episodic collapse of the unstable pile of flows and flow breccia accumulating on the slope above. The presence of air-fall tephra, interlayered with the lahars near the present valley bottom, suggests that the caldera depression must have been dry during most or all of the period of Festuca activity.

In thin section, the Festuca lavas and breccia fragments are uniformly porphyritic (Fig. 28). Randomly oriented euhedral to subhedral crystals of sanidine up to 4 mm across form 10 to 20% of most samples. The feldspar is unaltered and forms simple Carlsbad twins. Pale green hedenbergite is ubiquitous, but rarely forms more than 1% of the rock. It occurs as euhedral prisms up to 2 mm long. Rare pseudomorphs of olivine are present in some sections.

The groundmass varies from perlitic glass containing microlites of feldspar and pyroxene to an aphanitic, microcrystalline mesostasis of feldspar crystallites and opaque minerals.

Pan Creek tephra (map unit MCpc). The intracaldera facies of the Pan Creek tephra is best exposed on the lower slopes of Pipe Organ Mountain and adjacent Stonecrop Ridge where the flat-lying, poorly indurated beds form cliffs with spires, hoodoos, and fantastic wind-sculptured ledges (Fig. 29). On the south side of Pipe Organ Mountain, near Festuca Pass, the basal tuff rests directly on hydrothermally altered Dean River flows and breccia. North of Pipe Organ Mountain, near the northern limit of the intracaldera facies, the tuff beds overlap a steeply south-dipping wedge of epiclastic rocks, and east of Pipe Organ Mountain they interdigitate with southwest-dipping block-flows, lahars,and pyroclastic deposits of Festuca comendite (Fig. 27a).

On the south side of Pipe Organ Mountain the Pan Creek succession is 205 m thick (Fig. 30). It consists mostly of fine grained tuff. Interbeds of lapilli tuff and coarser breccia are concentrated in the lower part and occur sporadically throughout the section. Much of the fine tuff is graded. Laminated sequences with graded beds 1 to 10 cm thick alternate with sequences of 0.5 to 1 m beds having lapilli-sized material at the base and grading up into fine darker coloured tuff at the top. The graded sequences are interlayered with thick (up to 10 m) beds of massive, uniformly fine grained tuff with prominent liesegang banding but poorly defined bedding. Relatively coarse units include lapilli tuff and beds of matrix-supported breccia containing clasts up to 30 cm across. Clasts in these coarser units are pumice, lithic fragments, and obsidian. Pumice clasts, which are the most abundant, form porous, slightly flattened to irregular fragments the same colour as the enclosing white or pale green tuffaceous matrix. The lithic clasts, which consist entirely of subvitreous, feldsparphyric comendite, are concentrated in local, clast-supported lenses within the pumiceous breccia. The obsidian clasts, which are mostly between 2 and 20 cm across, are sparsely and randomly distributed throughout the coarse units. Like the lithic clasts they are feldsparphyric and lithologically similar to the

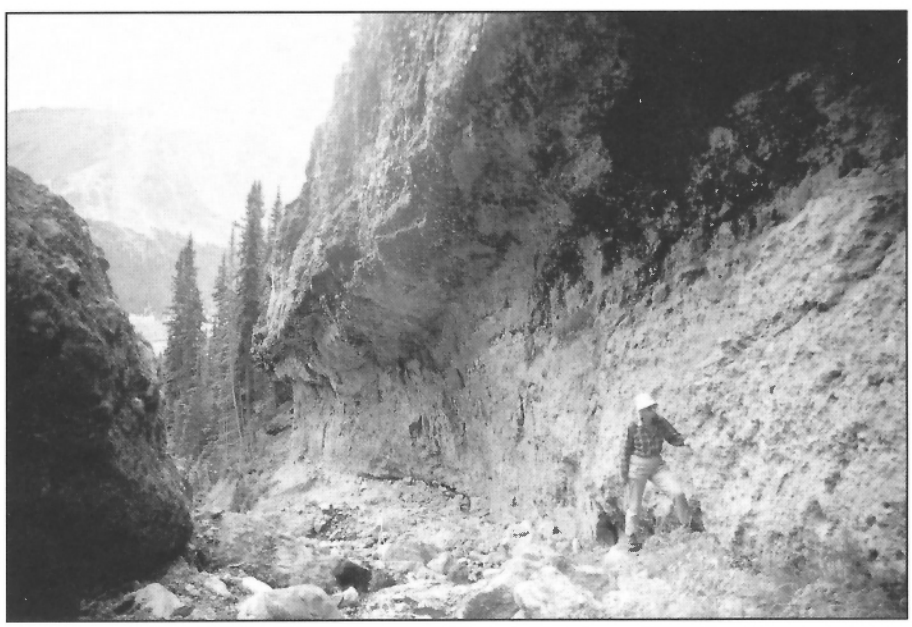

Figure 26. *Steeply inclined block-flow of Festuca comendite exposed in a box canyon south of Stonecrop Ridge. Initial dips indicate that the flow was deposited on a south-facing slope of 20 to 30 degrees. GSC 1993-184NN*

quenched flows and glassy breccia fragments of Festuca comendite. The uppermost unit in the Pipe Organ Mountain section is a coarse breccia containing clasts up to a metre across. Many of these have thick red or yellow oxidation rinds, suggesting that they may have been exposed to subaerial weathering prior to deposition of the overlying Phacelia tuff.

A relatively coarse, proximal facies of the Pan Creek tephra is exposed on the southeast side of Carnlick Creek valley where the basal tuff rests directly on hydrothermally altered and veined autobreccia of Dean River comendite and is overlain by a thick lobe of Mizzen Mountain comendite. The section is at least 200 ft. (60 m) thick and comprises lapilli tuff interbedded with pyroclastic breccia containing pumice blocks up to 5 cm across and a variety of lithic clasts. The latter include subrounded pebbles of green to black feldspar-phyric comendite, small blocks of granular obsidian, and bomb-like globules of subvitreous rhyolite with central gas voids and concentric vesicle trains. Interlayered with the pyroclastic breccia and tuff is a dark brown-weathering lahar or debris flow deposit at least 22 m thick (Fig. 31). It consists mostly of unsorted angular to subrounded volcanic blocks up to half a metre across. However, cryptic fluvial bedding is

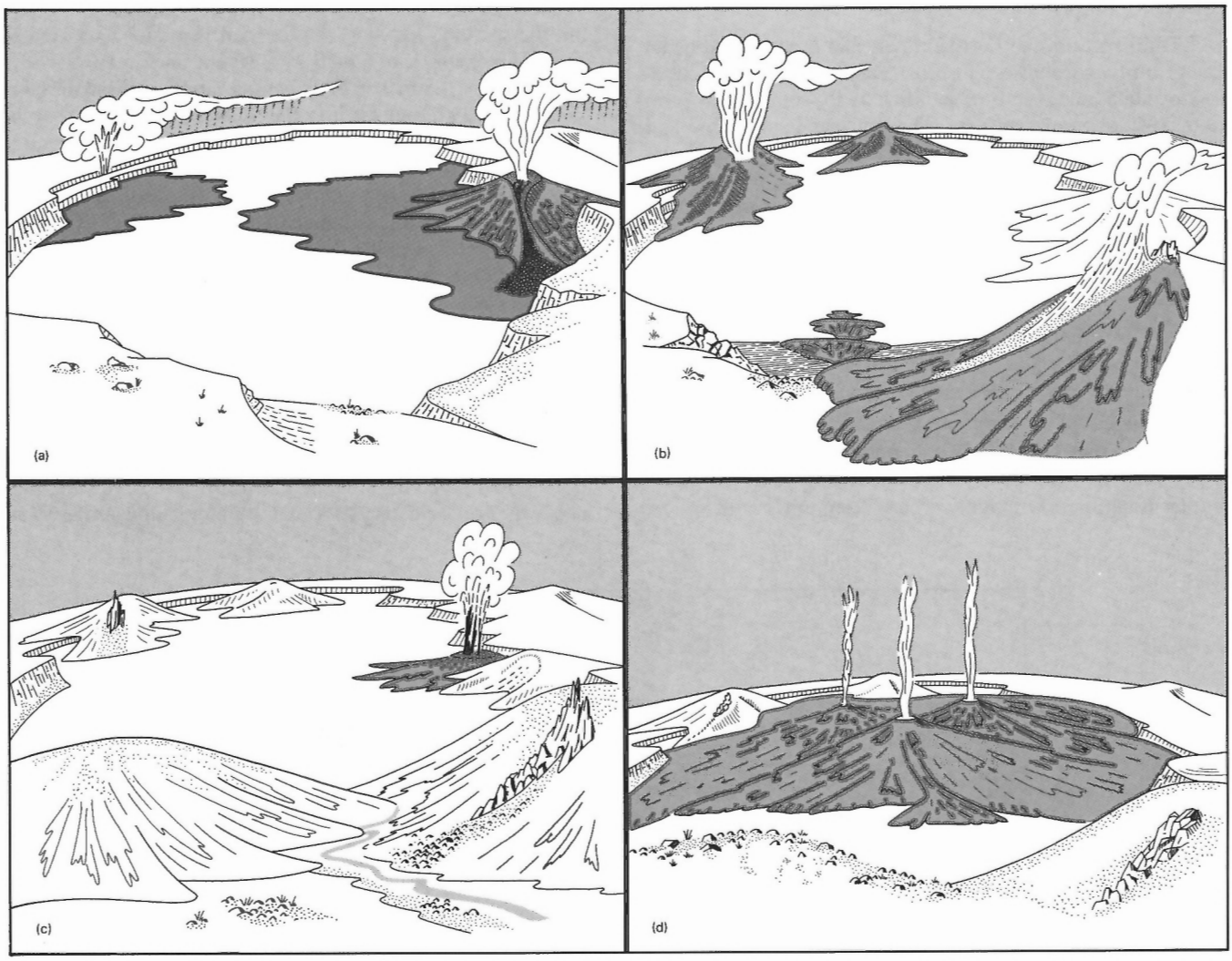

***a** – Caldera collapse accompanied by eruption of Festuca comendite from a vent on the east (right) margin, and accumulation of Pan Creek air-fall tephra within the caldera.*
***b** – Eruption of alkali rhyolite domes (Carnlick Creek Volcanics) from vents around the caldera margin. Rich Creek rhyolite (background), Calliope rhyolite (left), Mizzen Mountain rhyolite (right foreground).*
***c** – Ponding of water in the caldera and eruption of basalt to produce the Phacelia tuff.*
***d** – Eruption of Pipe Organ trachyte from several vents within the caldera to produce a thick, ponded flow.*

***Figure 27.** Conceptual sketches showing the development and infilling of the central caldera.*

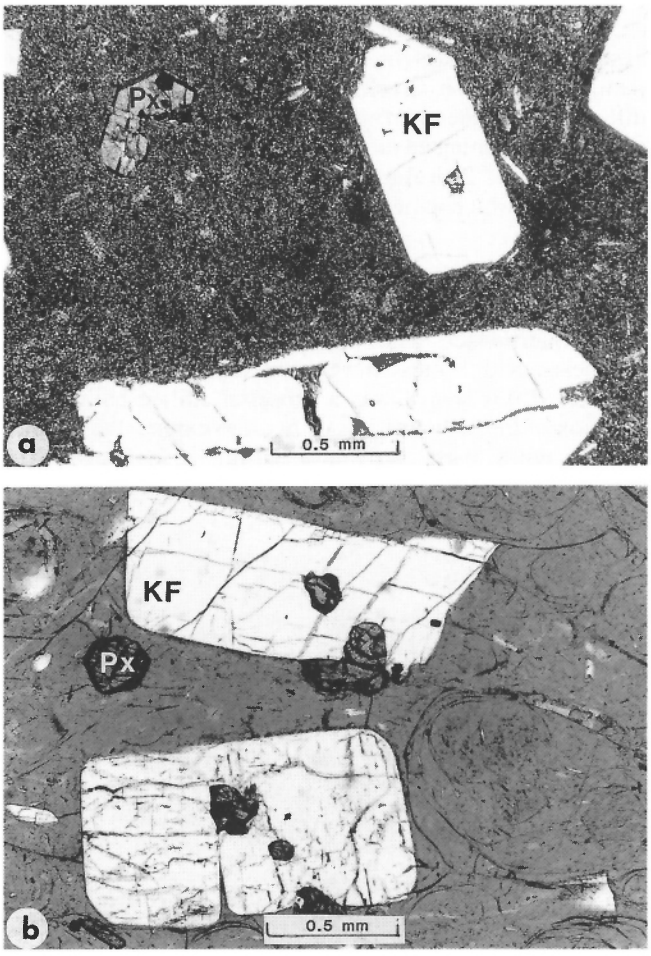

Figure 28. *Photomicrographs of Festuca comendite block-flow. (**a**) Euhedral phenocrysts of sanidine (KF) and hedenbergite (Px) in a fine grained mesostasis of feldspar crystallites and opaque oxides. (**b**) Euhedral sanidine (KF) and hedenbergite (Px) phenocrysts in perlitic glass (Both plane-polarized light. GSC 1993-184PP*

present in local pockets of grit-sized material, indicating that water played a role in its deposition. The coarse grained facies of Pan Creek tephra in the Carnlick Creek section and similar beds at the head of Pan Creek were probably deposited on or near the margin of the caldera during the initial Mizzen Mountain activity (Fig. 27b).

Similar beds of coarse pyroclastic breccia and tuff west of Festuca Pass are overlain by thick flows of Calliope comendite and probably represent a proximal facies of the initial, explosive, Calliope activity.

In thin sections the Pan Creek tephra is seen to be almost completely vitreous (Fig. 32). The pumice consists of clear unaltered glass with open, tubular vesicles. In addition to pumice, most sections include from 5 to 10% alkali feldspar as euhedral or broken crystals, minor quartz, and rare euhedral crystals of sodic pyroxene. Lithic clasts are nearly opaque in thin section, consisting of a dark subvitreous mesostasis enclosing small randomly oriented crystals of clear alkali feldspar.

Phacelia tuff (map units MCpl, MCpf). The Phacelia tuff is confined to Pipe Organ Mountain and adjacent Stonecrop Ridge where it lies conformably on intracaldera Pan Creek tephra and laps against inward-dipping wedges of Festuca comendite and epiclastic deposits. It consists entirely of waterlain clastic deposits and includes both lacustrine (MCpl) and fluvial (MCpf) facies. The Phacelia rocks were probably deposited in a lake and on alluvial fans that occupied the caldera depression during the latter stages of its evolution (Fig. 27c).

The lacustrine facies (MCpl) is from 30 to 50 m thick and consists of thin bedded, fine grained vitric tuff (Fig. 33). Freshly broken surfaces are conchoidal, nearly black, and have a waxy, subadamantine lustre. Internal textures are visible only on weathered surfaces where complex bedding

Figure 29.

Thick beds of intracaldera Pan Creek tephra on the southeast slope of Pipe Organ Mountain. GSC 1993-184OO

features are etched out in varying shades of brown and grey. The bedding is characterized by fine complexly graded and crossbedded laminations resembling those in fine grained turbidite successions (Fig. 34). The basal beds of the lacustrine succession rest directly on the Pan Creek succession of intracaldera air-fall deposits (Fig. 30). The contact is sharp but undulatory, indicating that relief on the caldera floor was as much as 30 m prior to flooding.

Shards in the lacustrine deposits are well sorted and mostly less than 0.5 mm across. They contain abundant spherical vesicles which are relatively large compared with the thin pipe vesicles in the underlying Pan Creek pumice beds. The shards show little or no evidence of reworking and redeposition. Even thin cusps of glass show no evidence of rounding or abrasion. The grains are loosely packed in clast-supported beds containing virtually no matrix. Areas between grains are either void or filled with secondary carbonate and/or zeolites.

Isolated, well rounded dropstones up to 60 cm across are randomly distributed throughout the lacustrine deposits (Fig. 35). They are lithologically similar to Dean River trachyte flows which outcrop on the shield north of Pipe Organ Mountain. Their rounded form and absence of pyroclastic features suggest that they are fluvial boulders, probably derived from erosion of Dean River flows, rather than primary ejecta. Their sparse, random distribution precludes a rockfall or debris-flow origin, and their presence near the centre of the thin bedded tuff deposit, up to a kilometre from any apparent source, precludes their origin as isolated boulders rolling from adjacent cliffs. This raises the possibility that they may have been rafted into the caldera lake on small icebergs calved from summit glaciers.

On the south side of Stonecrop Ridge the lacustrine beds interdigitate with coarse volcaniclastic deposits of Phacelia tuff fluvial facies (map unit MCpf). There, laminated beds of coarse to fine vitreous lapilli are interlayered with volcanic conglomerate and sedimentary breccia containing well rounded to angular pebbles and cobbles up to 15 cm across (Fig. 36). Differential weathering has etched out a complex internal structure of large-scale current crossbedding and channelling. The deposit is clearly of fluvial origin and was probably formed on a delta prograding into the lake from the eastern rim of the caldera. The lithology of the lapilli and larger fragments is similar to vitreous and subvitreous grains, which occur locally as grit layers in the lacustrine beds. Crossbedding and channelling indicate that streams feeding clastic debris onto the delta had their source on the eastern flank of the caldera.

Thin sections from both coarse- and fine-grained facies of the Phacelia tuff comprise unwelded shards of brown vesicular glass, sparse grains of broken feldspar, and rare lithic clasts (Fig. 37). A few grains of pumice, probably derived from the underlying Pan Creek tephra, were found in one section. In contrast to the Festuca and Pan Creek rocks, in which sanidine is the principal feldspar, feldspar grains in the Phacelia tuff are almost all plagioclase with well developed polysynthetic twinning. This is consistent with bulk chemical analyses of the Phacelia lacustrine tuff which, although subject to contamination by secondary minerals, is basaltic. The differences in colour and vesiculation of glass in the Phacelia tuff compared with pumice in the Pan Creek tuff also suggest compositional differences. Rather than an extension of comenditic magmatism, which dominated the early history of caldera formation, eruption of the Phacelia tuff was a precursor to more basic magmatism which increased during the latter stages of shield building.

The vent area of the Phacelia tuff was not found and may have been removed by erosion. Lenses of coarse angular clasts interbedded with the fluvial deposits (MCpf) on Stonecrop Ridge must have been eroded from a nearby source. If this source was a subaerial edifice built by the eruption of Phacelia tuff it is difficult to explain the absence of lava flows, particularly in a basaltic assemblage. The

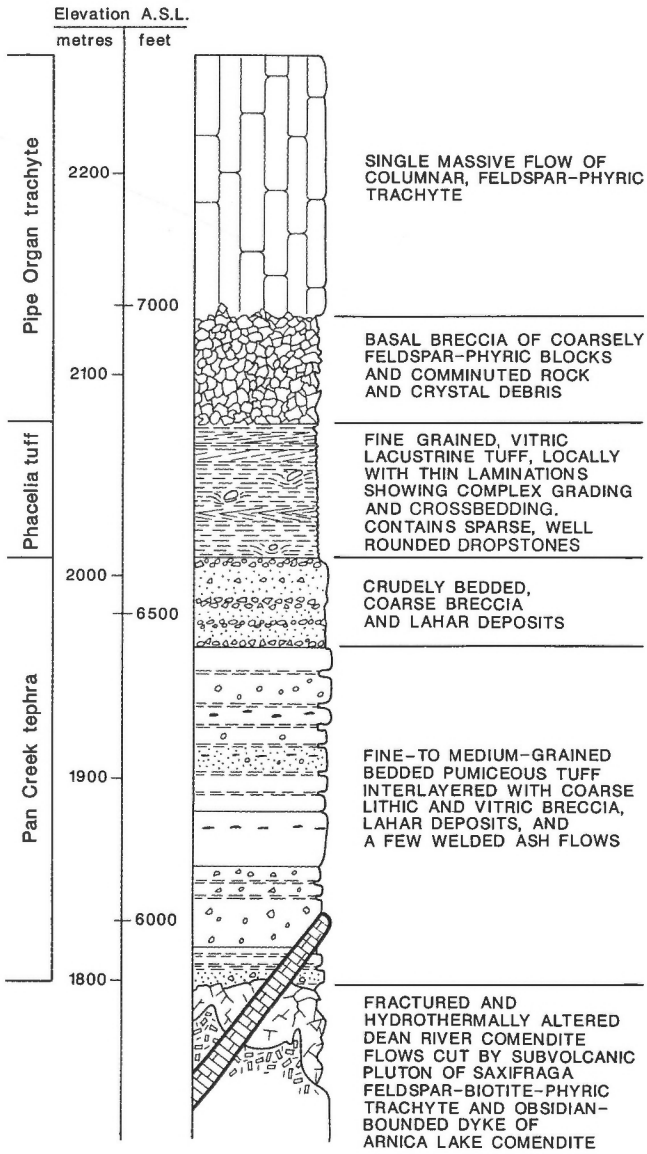

Figure 30. Stratigraphic section, Pipe Organ Mountain.

abundance of glass shards and lapilli in both the lacustrine and fluvial deposits suggests that the vent may have been subject to quenching and repeated phreatic explosions, producing a large volume of glass shards and a low profile tuff-ring in the source area. Such an origin is consistent with the presence of summit glaciers when the Phacelia tuff was deposited, as suggested by dropstones in the lacustrine deposits. Indeed, glacial ice may have helped to contain the summit lake and served as the principal source of water.

Pipe Organ trachyte (map units (MCpov, MCpoi). Intracaldera flows of Pipe Organ trachyte (map unit **MCpov**) are exposed on the upper part of Pipe Organ Mountain and adjacent Stonecrop Ridge (Fig. 38), and subvolcanic intrusions (map unit **MCpoi**) of lithologically similar trachyte are located either within or adjacent to the central caldera. Both intrusive and extrusive phases of the Pipe Organ trachyte contain from 30 to 50% randomly oriented phenocrysts of clear, white, or amber-coloured feldspar up to 1.5 cm across.

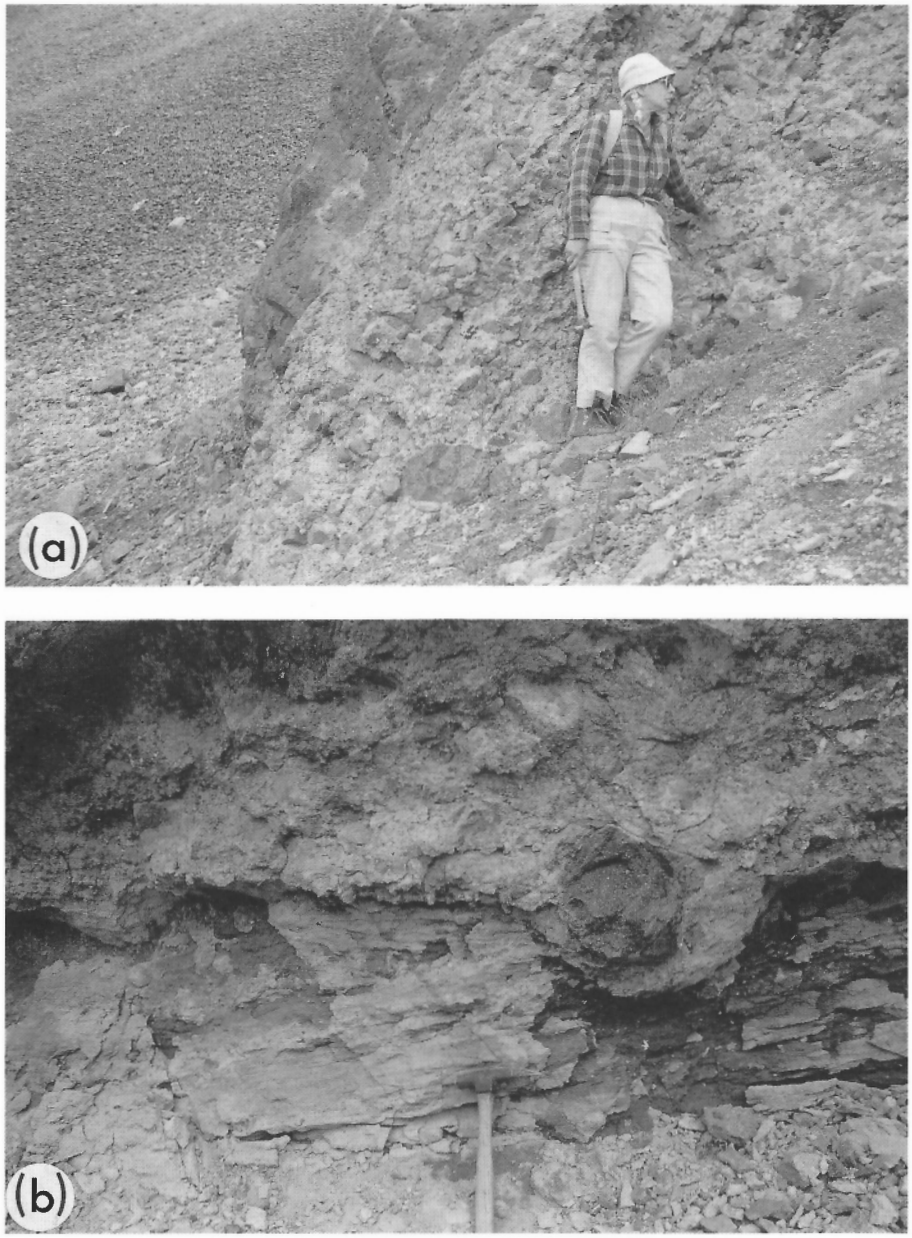

Figure 31. *Lahar deposit near the base of the Pan Creek tephra on the southeast side of Carnlick Creek valley.* ***(a)*** *Unsorted debris near centre of deposit;* ***(b)*** *sag structure near base. GSC 1993-184VV*

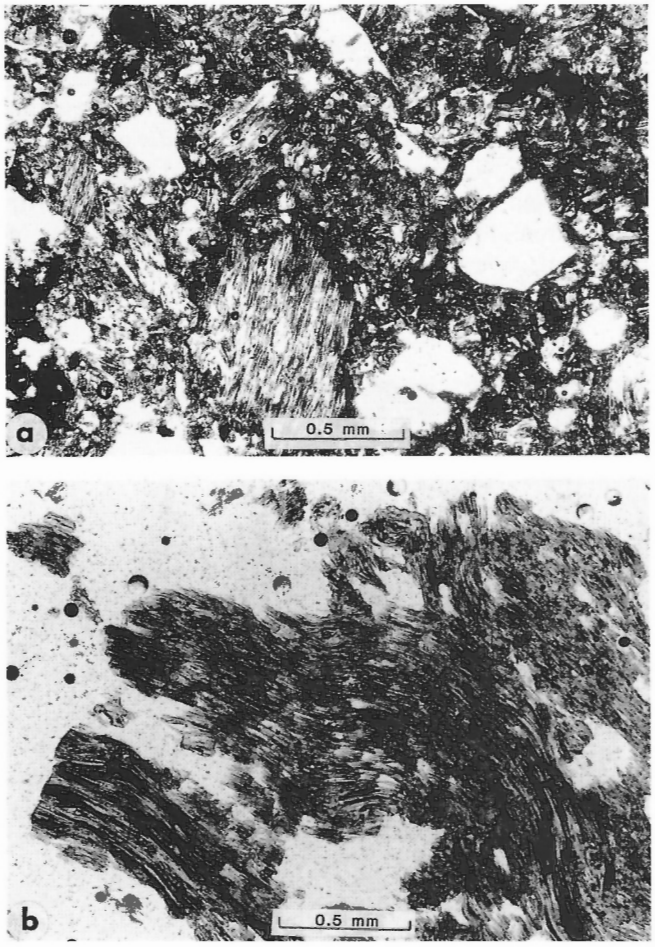

Figure 32. *Photomicrographs of Pan Creek tephra. (**a**) Fine grained crystal-vitric tuff comprising unsorted clasts of pumice and broken crystals of sanidine. (**b**) Detail of pumice fragment showing tubular vesicles. GSC 1993-184QQ*

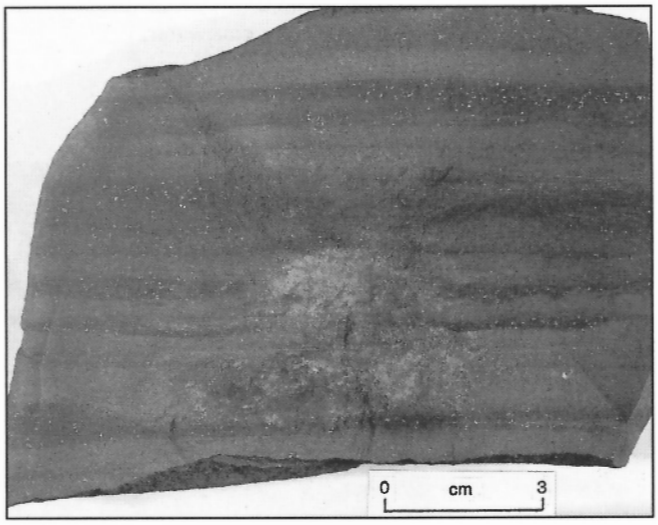

Figure 34. *Specimen of Phacelia tuff showing bedding detail. GSC 1993-184SS*

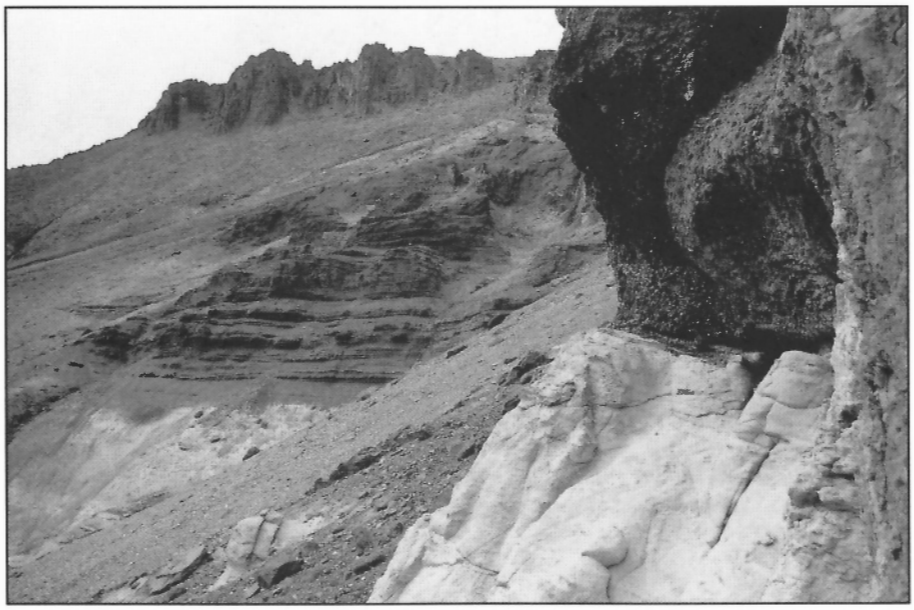

Figure 33.

Phacelia thin bedded lacustrine tuff overlying Pan Creek tephra (white) near the summit of Pipe Organ Mountain. GSC 1993-184LL

On Pipe Organ Mountain, the Pipe Organ trachyte forms a single massive flow that was probably ponded within the caldera depression (Fig. 27d). It comprises about 200 ft. (60 m) of basal breccia that grades upward into more than 500 ft. (150 m) of columnar lava (Fig. 30). The basal breccia consists of subangular blocks up to 4 m across in a matrix of granulated and hydrothermally altered trachyte. In most places the basal breccia rests conformably on undeformed, thinly laminated lacustrine or fluvial beds of Phacelia tuff, and the contact is horizontal and extremely sharp. However, on the south side of Pipe Organ Mountain the basal breccia and underlying tuff are tilted 30° toward the north (Fig. 38), indicating that eruption of the trachyte was followed by differential subsidence and local tilting of the caldera floor. Also, isolated chunks of Pipe Organ breccia up to 60 ft. (20 m) across are partly enclosed within the upper part of the Phacelia tuff. This suggests that the tuff was semiconsolidated when the Pipe Organ trachyte was erupted, and that large masses of flow breccia, spalled from the advancing flow front, were partly enveloped by the underlying tuff. The massive portion of the flow displays three distinct zones: a lower colonnade, about 50 ft. (15 m) thick, which forms cliffs with widely spaced, crudely columnar to rectangular jointing; a central entablature, about 400 ft. (120 m) thick, which forms the recessive central part of the flow and has complex random jointing; and an upper colonnade, about 100 ft. (30 m) thick, which has massive columns up to 2 m in diameter and forms vertical cliffs surrounding the summit. The summit is nearly flat and is probably close to the original upper surface of the flow.

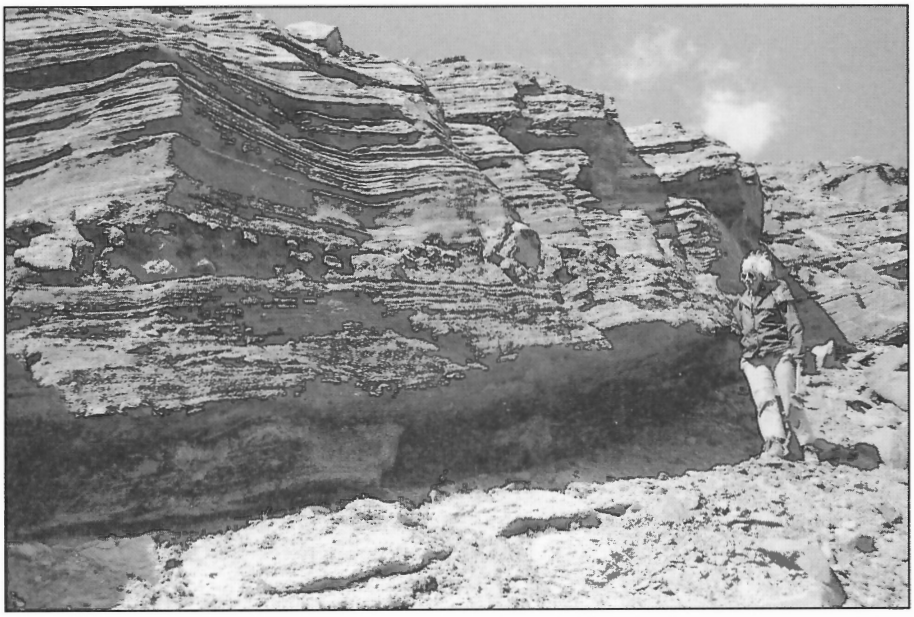

Figure 35.

Large dropstone suspended in thin bedded Phacelia tuff. GSC 1993-184MM

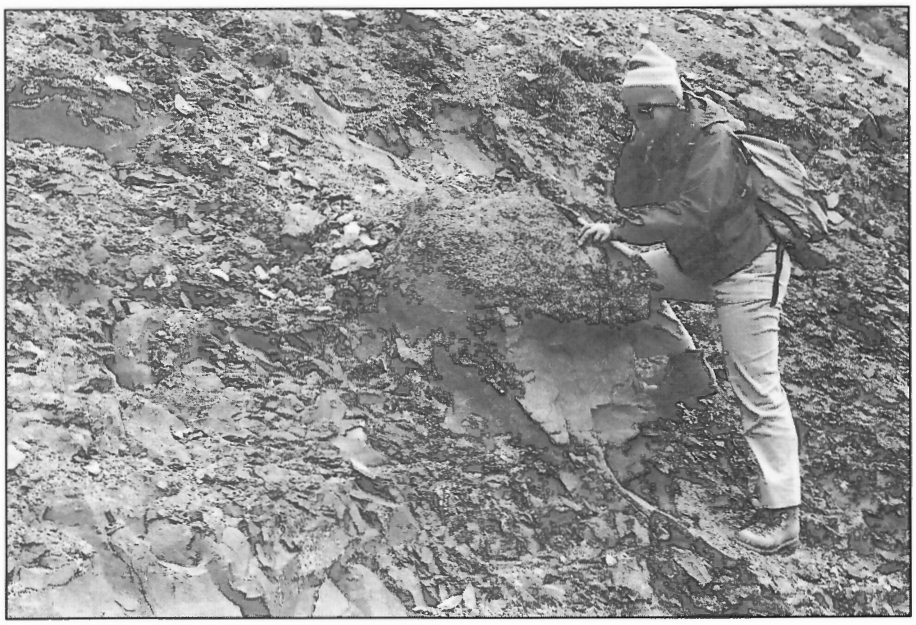

Figure 36.

Thick bedded fluvial facies of Phacelia tuff, northeast of Pipe Organ Mountain. GSC 1993-184RR

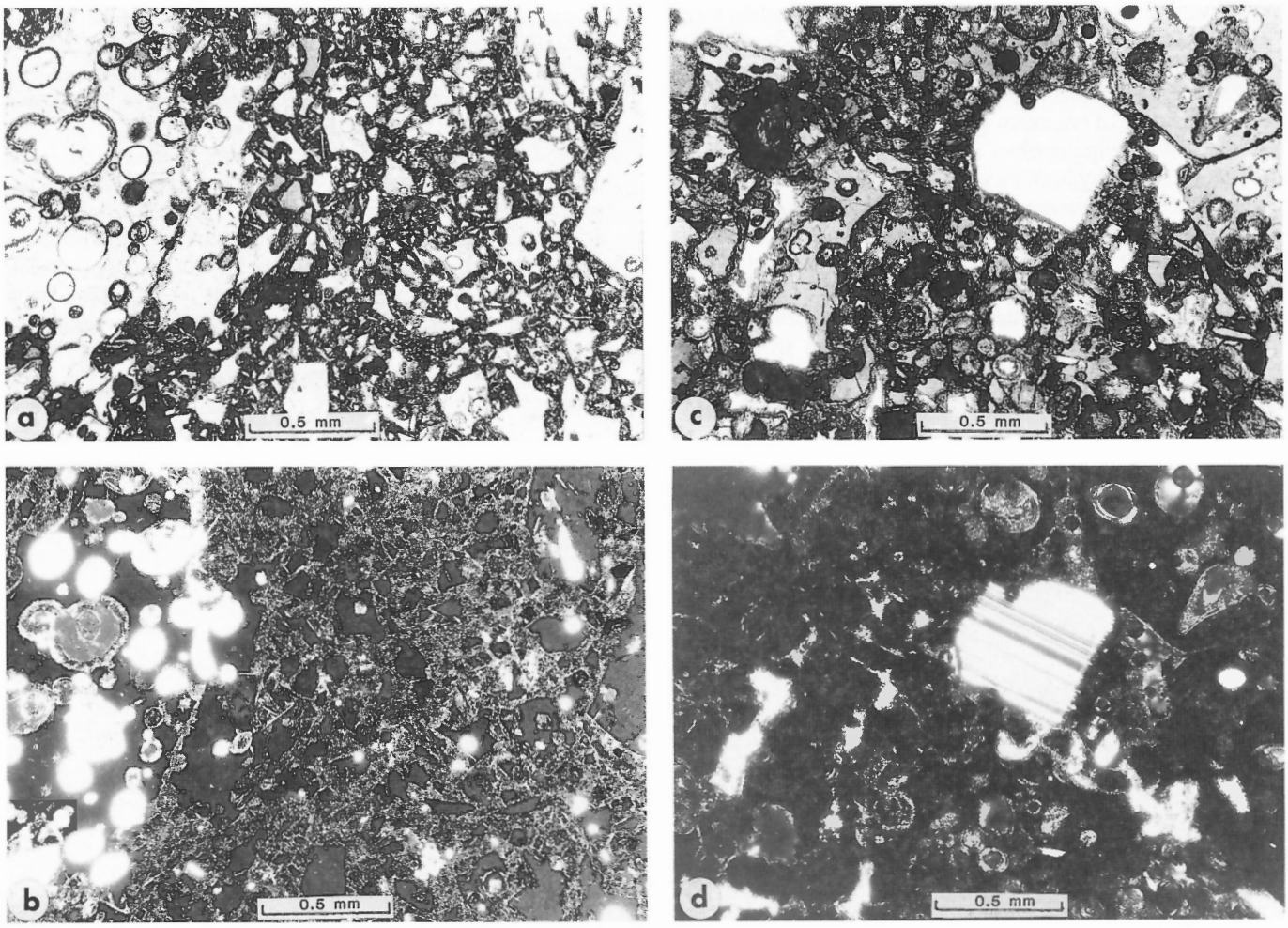

Figure 37. *Photomicrographs of Phacelia tuff. (a, b) Typical vitric tuff showing unsorted glass shards with sharp, cusps (**a**) plane-polarized light, (**b**) crossed polars. (c, d) Vitric tuff containing broken crystal of plagioclase (**c**) plane-polarized light, (**d**) crossed polars. GSC 1993-184JJ*

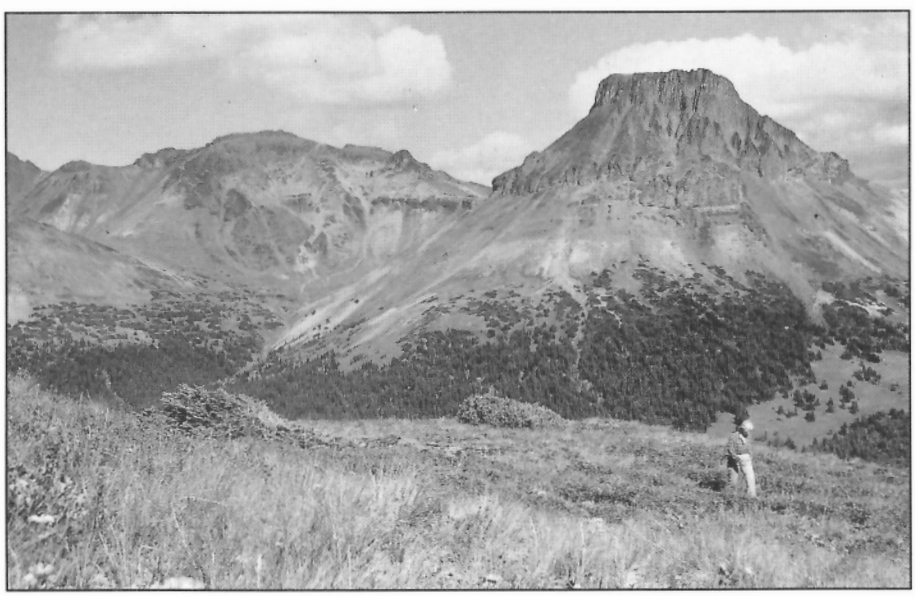

Figure 38.

View looking northeast across Festuca Pass at Pipe Organ Mountain. A single massive flow of Pipe Organ trachyte, underlain by thin bedded Phacelia tuff, forms the upper part of the mountain. Note inward-tilted block on the south (right) side of the mountain. GSC 1993-184KK

Subvolcanic equivalents of the Pipe Organ trachyte flows (map unit MCpoi) are exposed as randomly oriented tabular and irregular intrusions within and adjacent to the central caldera. They are lithologically similar to the flows, containing about 50% clear feldspar phenocrysts up to a centimetre across. Coarse phenocrysts are present right up to the contacts, indicating that the trachyte was emplaced as a crystal mush or cumulate. Most of the intrusive bodies have well developed columnar jointing normal to the contacts. The amount of contact alteration varies depending on the size of the intrusion. The relatively small tabular bodies have sharp contacts that display little or no alteration of either the adjacent intrusion or the wall rock. One of the largest subvolcanic bodies is exposed on the northeast spur of Monocephala Peak. It is about half a kilometre across and consists of massive, dark greenish-brown comenditic trachyte with abundant, randomly oriented feldspar phenocrysts from 5 to 10 mm long. Widely spaced rectangular joints are the only internal structure, but the margins of the body are tectonically fractured and hydrothermally altered. The southern margin of this small pluton intrudes mylonitic schist of the Tatla Lake Metamorphic Core Complex. Bright red hematitic alteration has affected the schist in a contact zone about half a metre wide adjacent to the intrusive contact. The schist is probably a slice of basement rock that was dragged up along the margin of the pluton during the latter stages of viscous or near-solid intrusion.

Thin sections of Pipe Organ trachyte from both flows and intrusions show little variation in texture or mineralogy (Fig. 39). The rock contains from 30 to 50% randomly oriented feldspar phenocrysts as independent subhedral crystals, broken remnants of larger crystals, and as intergrown crystal clusters. Sizes range from 0.5 to 1.5 cm. Crystal outlines are commonly rounded and slightly embayed. Both alkali feldspar and plagioclase are present. In most of the sections examined, unzoned sanidine with simple Carlsbad twinning

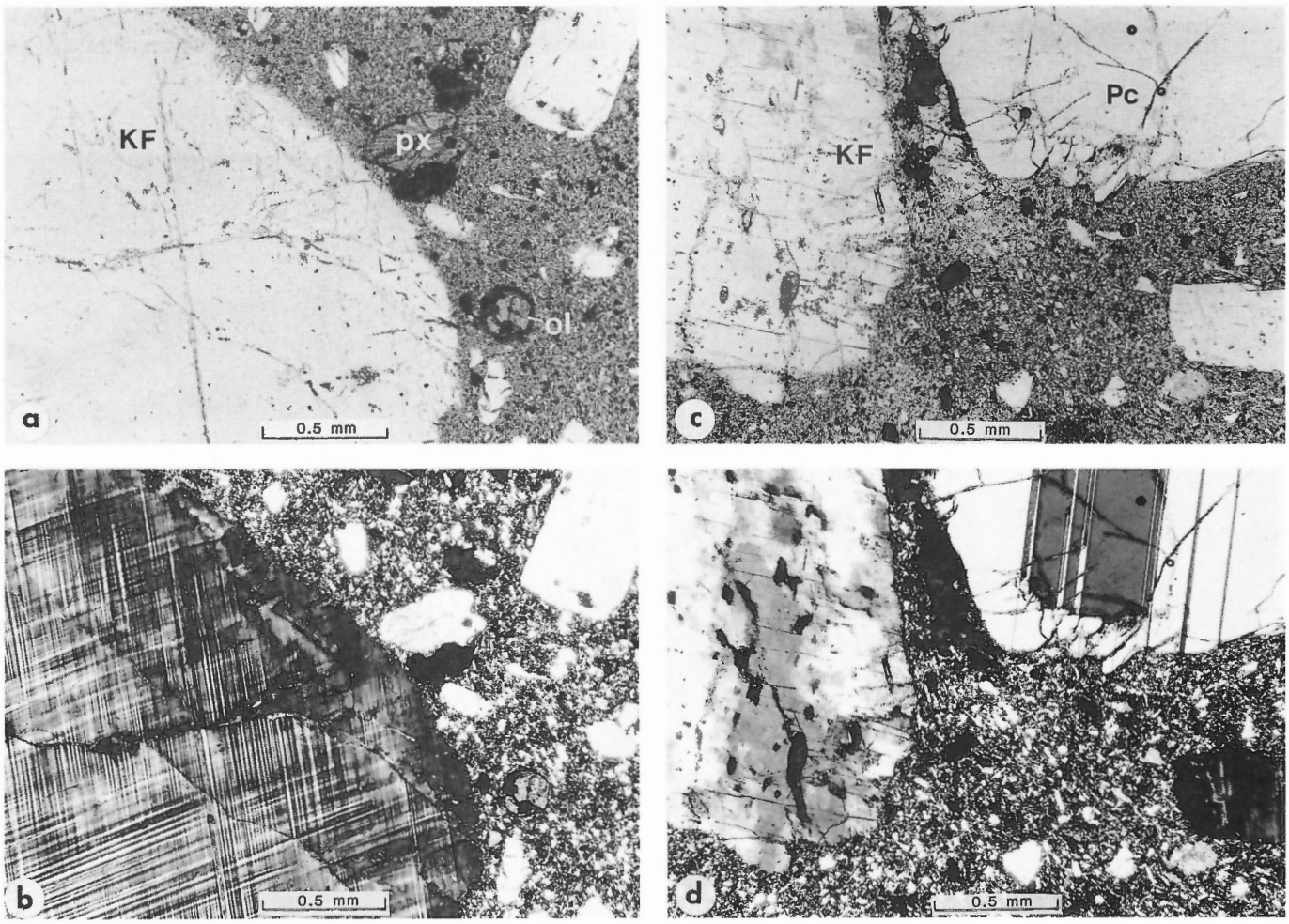

Figure 39. *Photomicrographs of Pipe Organ trachyte. (a, b) From ponded trachyte flow. Large partly resorbed phenocryst of anorthoclase (KF) and microphenocrysts of fayalite (ol) and hedenbergite (px) in a fine grained groundmass of feldspar, clinopyroxene, and opaque oxides*
*(**a**) plane-polarized light, (**b**) crossed polars. (c, d) From trachyte subvolcanic intrusion. Partly resorbed and altered phenocryst of alkali feldspar (KF) coexisting with sodic oligoclase (Pc) in a fine grained groundmass of feldspar, clinopyroxene, and opaque oxides*
*(**c**) plane-polarized light, (**d**) crossed polars. GSC 1993-184UU*

coexists with anorthoclase having fine cross-hatched twinning, and a lesser amount of plagioclase (sodic oligoclase) having coarse albite twinning. The texture of these rocks, with their abundance of unzoned feldspars, suggests that they are cumulates.

Pale brown, nonpleochroic clinopyroxene (ferrosalite) is a ubiquitous phenocryst phase, but it rarely forms more than 1% of the rock. It occurs as euhedral or broken crystals up to 1 mm long. Crystal boundaries are sharp and show no evidence of reaction with the groundmass.

A trace of fayalitic olivine is present in about half of the sections examined. It occurs as pale yellow subhedral grains up to 1 mm across. These are commonly surrounded by opaque reaction rims and have red alteration zones bounding internal fractures.

The groundmass is extremely fine grained and consists of about 85% feldspar as closely packed, stubby, euhedral crystals. Tiny grains of pale green pyroxene and finely disseminated opaque oxides constitute the remaining 15% of the groundmass.

Saxifraga trachyte (map unit MCs). Saxifraga trachyte forms the prominent northeastern spur of Saxifraga Mountain and a group of smaller outcrops in canyons and benches on the southeastern flank of Pipe Organ Mountain (Fig. 4). It is a distinctive, light coloured porphyry comprising about 50% white feldspar phenocrysts up to a centimetre across and about 1% biotite in an aphanitic, light grey to white groundmass. Irregular open cavities, up to 2 mm across, are sparsely but uniformly distributed. Deep weathering, characterized by rusty liesegang banding, is ubiquitous.

On the upper part of the spur the light grey to almost white, rusty-weathering trachyte forms serrated cliffs broken by steep narrow gulleys filled with loose, blocky talus. Vertical, rectangular to crudely columnar jointing is the only internal structure. Individual joint blocks from 0.5 to 1.5 m across extend vertically for up to 10 m without any crosscutting fractures or joint surfaces. Joint-controlled mass wasting has resulted in anomalously high rates of talus production and in downslope movement of larger rock masses. An axial depression up to 20 m deep, which runs along the crest of the spur for

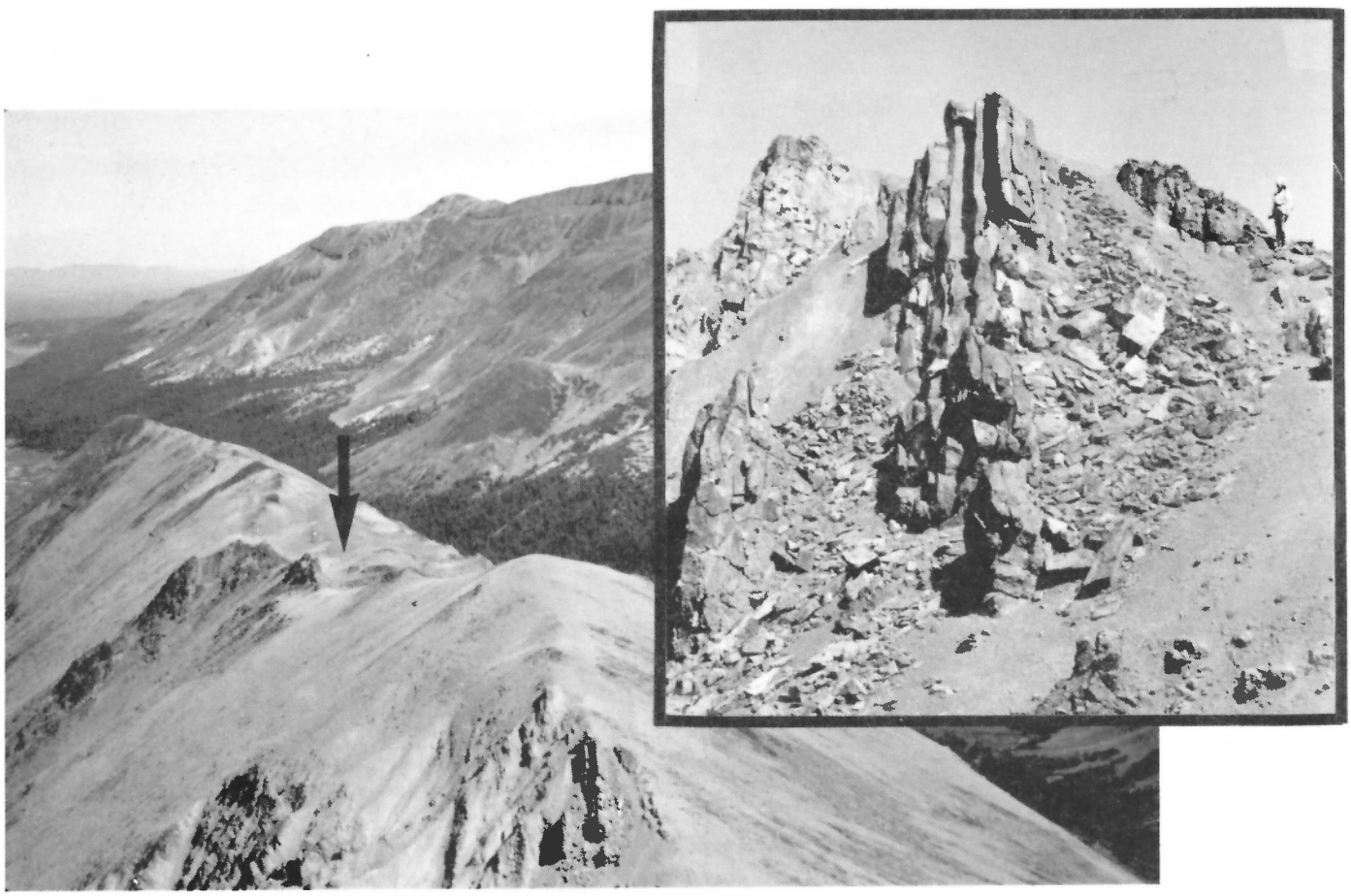

Figure 40. *View along the felsenmeer-covered northeast spur of Saxifraga Mountain. The entire ridge comprises a coarsely jointed subvolcanic intrusion of biotite trachyte. The arrow indicates the area of summit depressions caused by rapid mass-wasting and incipient slope failure. Inset shows detail of well developed vertical jointing responsible for slope instability. GSC 1993-184TT*

more than half a kilometre, is probably a graben bounded by gravity faults related to slow-moving landslides on the south-eastern side of the ridge (Fig. 40).

Except for one short interval, the Saxifraga trachyte is completely surrounded by talus. Only at the southwestern end of the ridge on Saxifraga Mountain is the Saxifraga trachyte exposed in close proximity to other units. There a narrow coll, about 20 m across, separates massive Saxifraga trachyte from southeast-dipping Calliope flows. The coll is filled with unconsolidated, yellow-weathering, clay-like material containing rounded chunks of altered fine grained trachyte. Although the nature of the contact is inconclusive, its steep attitude suggests either a fault or an intrusive contact.

Exposures of Saxifraga trachyte on Pipe Organ Mountain are confined to small discontinuous outcrops in canyons and terraces along a south-flowing tributary of Phacelia Creek. The lithology, jointing, and weathering characteristics of these outcrops are similar to those on Saxifraga Mountain. Although no contacts were observed, exposures of older rocks within 100 m of the Saxifraga outcrops are intensely altered, brecciated, and bleached to a yellow or white material similar to that in the contact zone on Saxifraga Mountain.

Below a thick alteration rind the Saxifraga trachyte is remarkably fresh. Thin sections show little or no alteration of either phenocryst or groundmass minerals (Fig. 41), indicating that the ubiquitous oxidized rind is the result of deep surface weathering rather than deuteric or hydrothermal activity. Feldspar phenocrysts, which form 35 to 50% of the rock, are typically stout euhedral crystals up to a centimetre across. Crystal boundaries are sharp and lack any evidence of reaction with or embayment by the groundmass. Some crystals are slightly zoned and most are microcline with gridiron twinning. Although biotite forms less than 1% of the rock, it is uniformly distributed as randomly oriented euhedral crystals up to 1.5 mm across. Like the feldspar phenocrysts, it is unaltered and shows no evidence of reaction with the groundmass. The groundmass, which has a pronounced eutaxitic texture, consists mostly of interlocking feldspar laths about 0.1 mm long, rare biotite, and unidentified opaque oxides.

The limited distribution, rectangular jointing, and uniform lithology of the Saxifraga trachyte through a vertical distance of at least 1200 ft. (360 m) suggest that it is a subvolcanic intrusive body. With the exception of biotite, which is ubiquitous in the Saxifraga trachyte but absent in the Pipe Organ trachyte, the two lithologies are remarkably similar in chemistry, mineralogy, and texture. Both rocks are typical orthocumulates (McBirney, 1984), and the possibility that they are comagmatic is suggested by their proximity to the central caldera. However, the presence of biotite in the Saxifraga trachyte suggests a closed system intrusive phase which retained some of its volatile component. In contrast, the Pipe Organ trachyte and associated high level feeders erupted on or near the surface where volatiles were rapidly lost and no hydrous minerals formed.

Arnica Lake Volcanics

The Arnica Lake Volcanics comprise thick outward dipping flows (map unit **MAv**), which form much of the symmetrical upper part of the Ilgachuz shield, and a central cluster of related intrusions (map unit **MAi**). The flows are preserved as isolated remnants, capping the higher peaks in the centre of the range and forming broad, gently sloping interfluves around the perimeter of the plateau (Fig. 4). In the central part of the range, where the Arnica Lake flows rest on steep-sided rhyolite domes of the underlying Carnlick Creek Volcanics, initial dips are up to 20 degrees. The more distal flows extend beyond the central domes of the Carnlick Creek

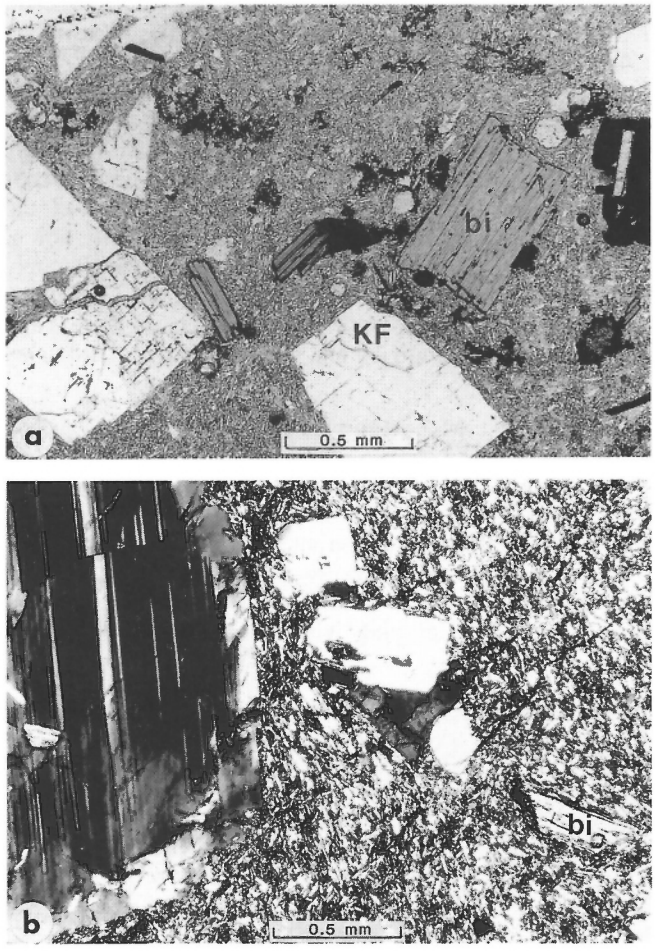

Figure 41. *Photomicrographs of Saxifraga trachyte. (**a**) Euhedral phenocrysts of alkali feldspar (KF) and biotite (bi) in a fine grained groundmass of feldspar laths, minor biotite, and opaque oxides (plane-polarized light). (**b**) Large phenocryst of sodic oligoclase overgrown by alkali feldspar, and microphenocrysts of biotite (bi) in a groundmass of feldspar laths and opaque oxides (crossed polars). GSC 1993-184F*

Volcanics and overlap gently dipping Dean River flows around the periphery of the shield. Most of the Arnica Lake comendite contains between 10 and 30% feldspar phenocrysts as clear, euhedral crystals from 1 to 3 mm long. Where the Carnlick Creek rhyolite is missing, the Arnica Lake flows are difficult to distinguish from the underlying Dean River flows, thus some contacts shown on the map are poorly constrained.

The central rhyolite domes of the Carnlick Creek Volcanics were only slightly modified by erosion prior to eruption of the Arnica Lake Volcanics. In most places the Arnica Lake flows (map unit **MAv**) mantle the initial surfaces of the older composite domes. An exception is seen on the north side of Festuca Creek where basal lobes of Arnica Lake comendite truncate at least 400 ft. (120 m) of underlying Rich Creek and Dean River flows along a steep southwest-dipping unconformity (Fig. 15). Other evidence of erosion prior to eruption of Arnica Lake comendite is found on the east side of Monocephala Peak where the basal Arnica Lake flow occupies an old valley eroded into underlying Calliope flows and an intrusive body of Pipe Organ trachyte. Well rounded, locally-derived cobbles are present along the unconformity. Similarly, on the ridge east of Hump Mountain, a 7 m thick recessive unit at the base of the Arnica Lake section comprises moderately well consolidated fluvial conglomerate (Fig. 42). The clast-supported cobbles and boulders of volcanic rock up to 0.6 m across are crudely shingled and surrounded by a sandy clay matrix.

On Crumble Mountain, near the centre of the Ilgachuz Range, the Arnica Lake Volcanics are about 1100 ft. (335 m) thick. Individual flows are mostly between 20 and 100 m thick, but a few flows are as thick as 150 m. The lower few metres of most flows are coarse autobreccia comprising angular clasts of glass and bleached crystalline rock in a cataclastic flow-layered matrix. In some flows the basal breccia comprises up to 5 m of platy vitreous rock containing well developed, 2 to 10 cm lenticular fiamme. These probably represent incandescent shards spalled from the advancing flow front. The massive to crudely columnar central core of most flows is light to dark olive green feldsparphyric comendite with prominent flow foliation. This grades up into a relatively thin flow-top breccia comprising a few metres of porous green spatter and broken slabs of fine grained comendite with contorted flow layering.

The concentric, outward-dipping symmetry of the Arnica Lake flows indicates a central source from a vent or group of vents that formerly rose to an elevation of at least 7700 ft. (2300 m) (Fig. 43). Erosion has destroyed almost the entire summit area of this once symmetrical volcano. However, remnants of the conduit system are preserved in a complex of dykes, cupolas, and irregular intrusions (map unit **MAi**), which cut all the intracaldera rocks up to and including the Pipe Organ trachyte. The feeders are concentrated within the caldera and some of the larger dykes have an arcuate trace that mimics the caldera margin, suggesting that their emplacement was influenced by pre-existing ring fractures related to caldera collapse.

The intrusive bodies include both pale green aphyric comendite and greenish-grey comendite with a few clear feldspar phenocrysts. The bodies range in size from dykes a few metres thick to irregular, crudely tabular bodies more than 100 m across (Fig. 44). Most contacts are vertical or near vertical and have well developed glass selvages up to half a metre thick. Both the glass and adjacent crystalline comendite contain numerous accidental inclusions, and locally fiamme-like flow structures have developed parallel to the contacts. The central portion of most intrusions is characterized by small diameter, subhorizontal columns, vertical flow layering, and trains of small irregular vesicles. The pronounced vertical flow foliation gives most outcrops a flaggy fabric that promotes rapid mechanical erosion and the formation of copious talus.

Figure 42.

Boulder and cobble layer at the base of the Arnica Lake succession on Hump Mountain. GSC 1993-154M

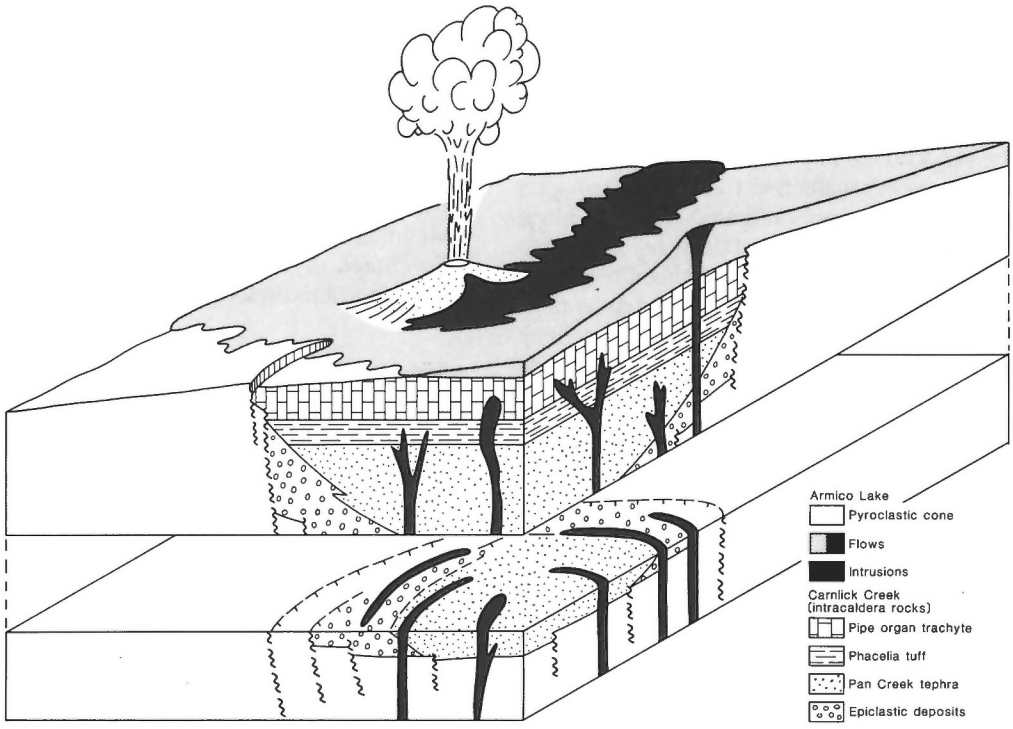

Figure 43. *Block diagram showing the relationship of Arnica Lake flows and intrusions to the caldera structure. The Arnica Lake lava, which overlaps the old caldera margin, was erupted from central vents fed by irregular and concentric, crescent-shaped intrusions that cut the older caldera rocks.*

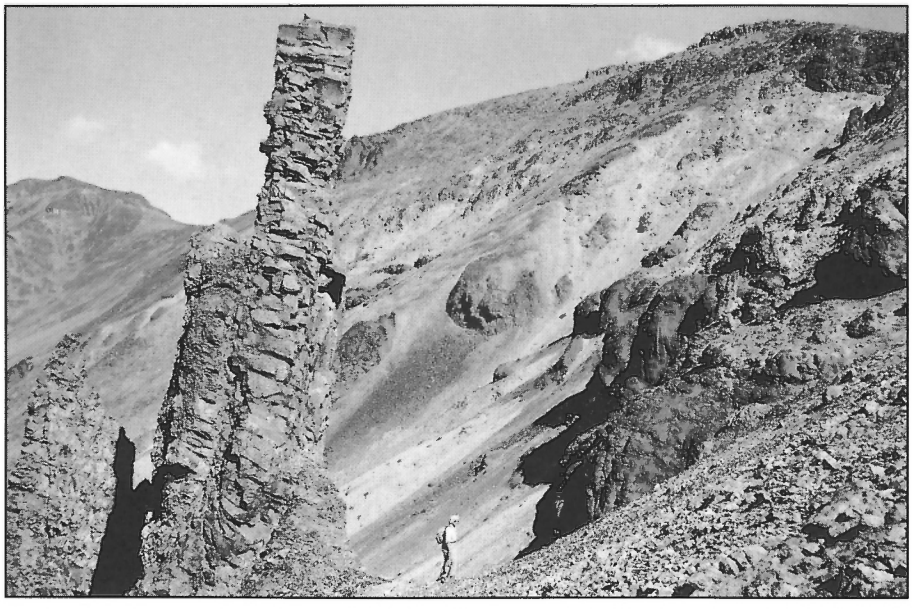

Figure 44.

Erosional remnant of Arnica Lake comendite dyke cutting Phacelia tuff (dark coloured bluffs to right of photo) on the north ridge of Pipe Organ Mountain. GSC 1993-154L

The only vestige of a surface vent related to Arnica Lake comendite feeders is exposed on the east side of Pipe Organ Mountain where Pipe Organ trachyte is cut by a complex of green glassy comendite dykes and a large irregular body of subvitreous comendite and obsidian at least 200 m in cross-section. The glassy portion of this body is exposed in a series of grottos where the gallery walls rise 10 to 15 m through a breccia of closely fitted, randomly oriented blocks of black obsidian (Fig. 45). The obsidian is overlain by at least 100 m of pale yellow to red breccia of oxidized comendite blocks. Although contact relationships are largely obscured by talus the proximity of the breccia to underlying glass dykes (map unit MAi) suggests that they may be vent-filling breccias formed during eruption of the Arnica Lake Volcanics.

The Arnica Lake comendite is remarkably uniform in texture and mineralogy (Fig. 46). Most thin sections have about 20% sanidine phenocrysts as unzoned euhedral crystals from 2 to 4 mm long. Euhedral phenocrysts of green hedenbergite, commonly less than 1 mm long, form about 1% of most thin sections, and pale yellow fayalitic olivine is a sparse but widely distributed phenocrystic phase. Unlike olivine phenocrysts in the underlying Carnlick Creek Volcanics, those in the Arnica Lake rocks show no evidence of reaction with the groundmass of intergrown alkali feldspar laths, quartz, and skeletal grains of poikilitic arfvedsonite and kataphorite. Anomalously thick flows of Arnica Lake comendite, such as those on the northeast side of Blue Canyon Creek, are relatively coarse grained but are otherwise similar to the more common fine grained facies.

Comenditic obsidian from the grottos on the east side of Pipe Organ Mountain is colourless in thin section. It has well developed perlitic structure and sparse euhedral laths of sanidine, which are the only phenocrysts (Fig. 46d). The groundmass of subvitreous comendite from an adjacent lava dome has pronounced eutaxitic flow structure defined by closely packed feldspar microlites. The texture and phenocryst composition of the dome are otherwise identical to those of the glass, and the two are probably cogenetic phases of the same extrusion with slightly different cooling histories.

Thin sections from Arnica Lake subvolcanic intrusions exhibit the same range of textures and mineralogy observed in the extrusive rocks. Most are porphyritic with from 5 to 20% phenocrysts of euhedral sanidine from 1 to 4 mm long. Small prisms of green hedenbergite and rare microphenocrysts of fayalitic olivine are present in some sections (Fig. 46c). The groundmass commonly has a pronounced eutaxitic fabric and comprises sanidine laths and interstitial quartz, arfvedsonite, kataphorite, and bright green sodic pyroxene (aegirine?). Glass selvages are commonly colourless in thin section and contain sparse sanidine phenocrysts only. Several of the intrusions are vesicular. The voids are unfilled and have ragged boundaries defined by groundmass crystals, indicating an absence of late stage vapour phase crystallization or hydrothermal activity.

Tundra Mountain Volcanics

The Tundra Mountain Volcanics consist mostly of basalt flows that issued from several vents on the upper slopes of the Ilgachuz Range and coalesced to form a thin basaltic mantle over the northern and southern portions of the underlying comenditic shield. In addition to four distinctive basalt units – the Stonecrop, North Rift, Hump Mountain, and Far Mountain basalts – a thin felsic unit of limited extent, the Go-around rhyolite, is interlayered with basalt in the upper part of the succession.

Stonecrop basalt (map units MPTsv, MPTsi).

Stonecrop basalt, a dark grey fine grained, feldsparphyric basalt, is the oldest unit of the Tundra Mountain Volcanics and represents the first major eruption of basalt in the Ilgachuz

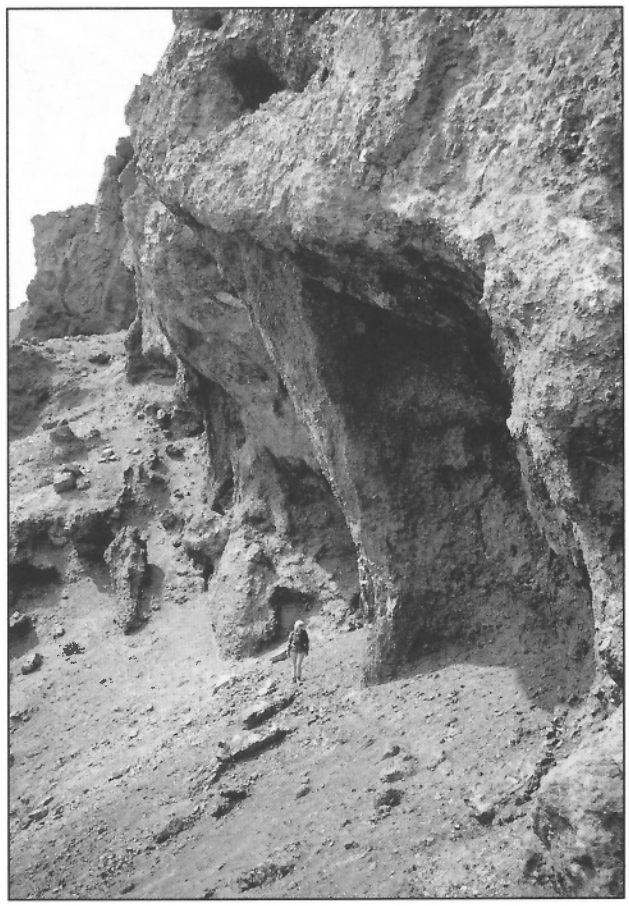

Figure 45. *Grottos in glass on the east flank of Pipe Organ Mountain. The glass and associated dykes and cupolas of green comendite are related to one of many Arnica Lake conduits in the central part of the Ilgachuz Range. GSC 1993-184C*

Range (Fig. 47). Its present distribution is limited to a few flow remnants (map unit **M**PTsv) on Stonecrop Ridge and an elliptical neck (map unit **M**PTsi) on the south slope of Crumble Mountain. However, the thickness of the flows suggests that it may have originally covered a much larger area of the central Ilgachuz Range. The remnant on the east end of Stonecrop Ridge is part of a single flow more than 15 m thick, and the remnant on the west end of the ridge comprises four flows with a composite thickness of 75 m. The flows are separated and underlain by mixed flow-top breccia and primary scoria, suggesting proximity to a fountaining vent. A neck of massive, spheroidal-weathering columnar basalt (map unit **M**PTsi), which straddles and extends down both sides of the ridge on the south side of Crumble Mountain, was probably the main conduit.

The Stonecrop flows rest disconformably on both intracaldera units (Pipe Organ trachyte and epiclastic deposits) and parts of the adjacent shield (Dean River Volcanics), and the neck of Stonecrop basalt cuts Arnica Lake Volcanics. Thus an erosion surface that extended across the caldera margin must have been developed after the eruption of Arnica Lake comendite and before the onset of Stonecrop basaltic volcanism.

Thin sections of Stonecrop basalt reveal little mineralogical variation but considerable difference in texture depending on cooling history (Fig. 48). All of the sections examined contain between 2 and 5% plagioclase phenocrysts (calcic labradorite) as euhedral laths up to 4 mm long. Olivine microphenocrysts up to 1 mm across are also ubiquitous and form between 1 and 2% of the rock. Purplish-brown clinopyroxene (titaniferous augite) is a rare phenocrystic phase.

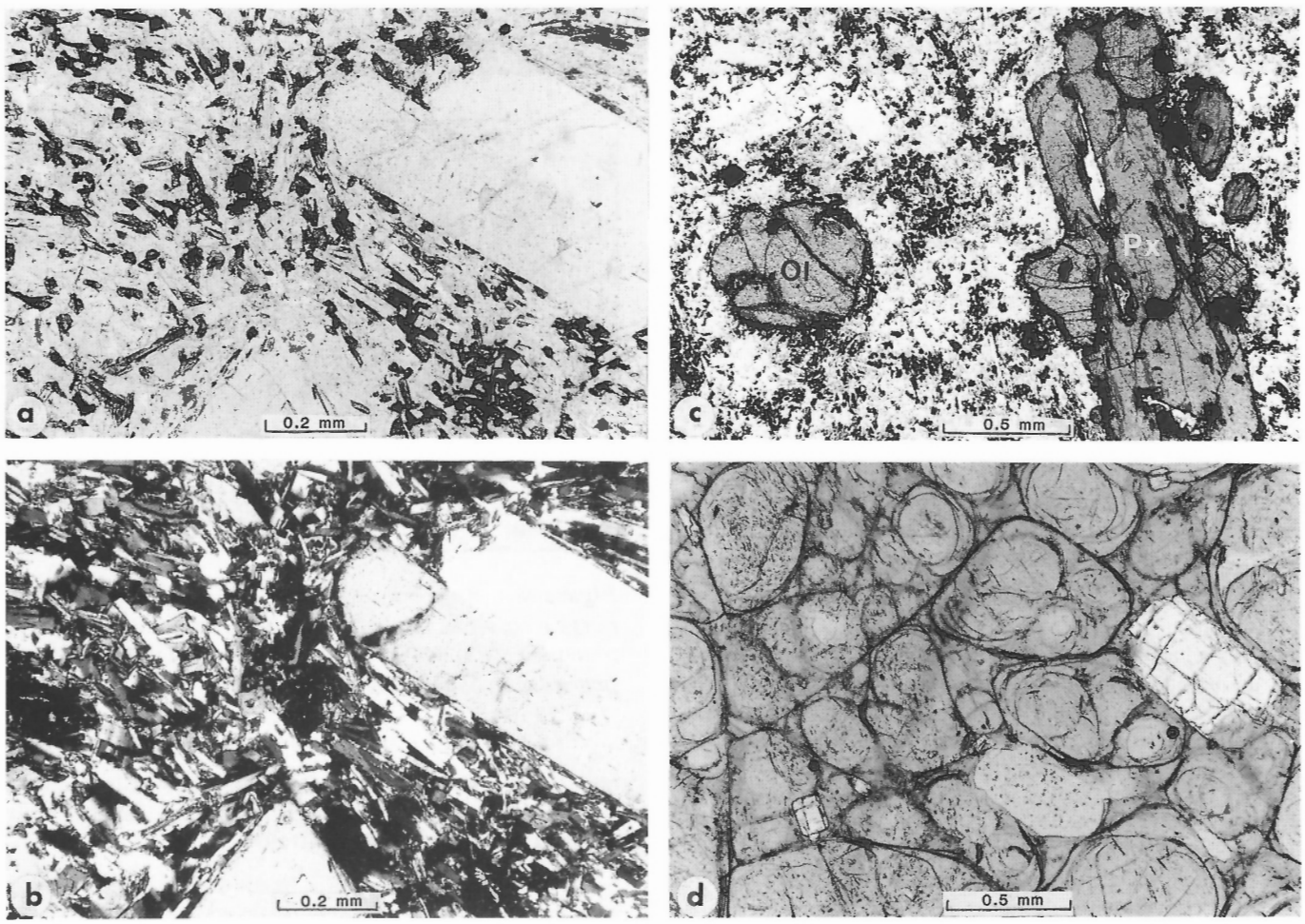

Figure 46. *Photomicrographs of Arnica Lake comendite. (a, b) Comendite flow. Anorthoclase phenocryst with simple Carlsbad twinning in a groundmass of euhedral alkali feldspar laths, interstitial sodic hedenbergite, minor arfvedsonite, and kataphorite (**a**) plane-polarized light, (**b**) crossed polars. (**c**) Comendite subvolcanic intrusion. Microphenocrysts of sodic hedenbergite (Px) and fayalite (Ol) in a fine grained groundmass comprising spherulitic intergrowths of alkali feldspar, aegirine?, arfvedsonite, and kataphorite (plane-polarized light). (**d**) Glass from the "grotto". Euhedral sanidine phenocrysts in clear, perlitic glass (plane-polarized light). GSC 1993-154O*

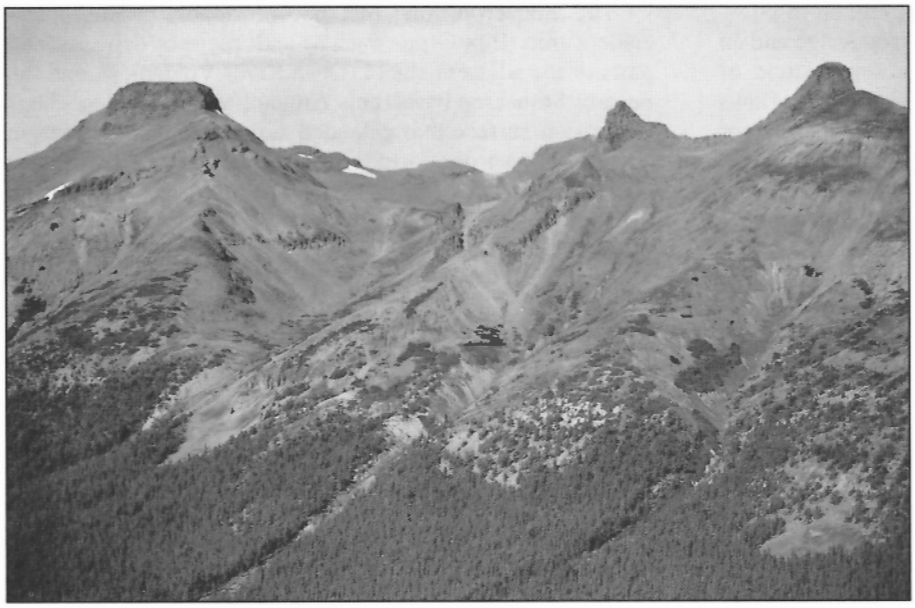

Figure 47.

View looking west from Dodds Domes at Stonecrop Ridge (flat-topped summit on left). The single basalt flow capping the east end of the ridge is more than 15 m thick. GSC 1993-184D

The groundmass assemblage comprises about equal proportions of plagioclase, clinopyroxene, and opaque oxides, and a smaller proportion of olivine. Textures range from medium grained granular, in which clinopyroxene and plagioclase occur as separate subhedral crystals, to intersertal textures in which the feldspar laths are enclosed by ophitic grains of clinopyroxene up to 2 mm across.

North Rift basalt (map units MPTnv, MPTni)

The North Rift basalt flows (map unit MPTnv) rest disconformably on Arnica Lake comendite and are overlain locally by both Go-around rhyolite and Far Mountain basalt. The rock is a distinctive light grey, highly porphyritic basalt containing abundant phenocrysts of clear feldspar up to 1 cm across, and sparse phenocrysts of lustrous black clinopyroxene from 1 to 2 mm across.

A pile of proximal flows and pyroclastic beds on Far Mountain can be traced northward to remnants of distal flows on the broad interfluvial plateau between Festuca and Blue Canyon creeks. On Far Mountain the proximal facies of the North Rift basalt is approximately 100 m thick. The basal flow rests directly on Arnica Lake comendite and dips gently toward the northeast. It is about 35 m thick and consists of loosely agglutinated pyroclastic beds. Thin (0.5-1 m) layers of lightly welded basaltic lapilli, spatter, and vesicular bombs are interlayered with thin discontinuous flow lobes up to a metre thick. The pyroclastic sequence is overlain by a succession of lava flows from 1 to 3 m thick, separated by thin layers of hackly, red flow-top breccia.

Remnants of distal flows on the plateau northwest of Far Mountain include individual cooling units up to 20 m thick. In contrast, the flows northeast of Far Mountain are relatively thin and appear to have spread uniformly across the gently outward dipping surface. This difference may be due to local

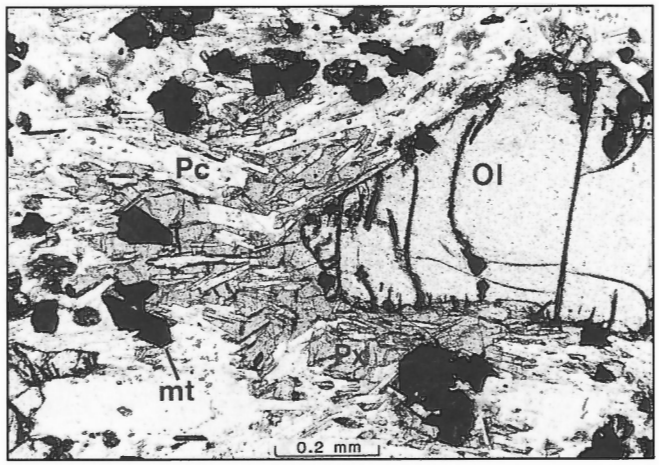

Figure 48. *Photomicrograph of Stonecrop basalt flow. Large phenocryst of olivine (Ol) in a groundmass of ophitic titanaugite (Px), labradorite laths (Pc), and titanomagnetite (mt) (plane-polarized light). GSC 1993-184H*

ponding and channelling of flows into depressions on the surface of the shield. However, no fluvial deposits were observed beneath the North Rift flows.

The source of the North Rift basalt was probably a fissure, represented now by a swarm of northwesterly trending dykes (map unit MPTni) on the steep upper slope of Festuca Creek near proximal pyroclastic deposits on Far Mountain (Fig. 49). The largest or main dyke (North Rift dyke, Map 1845A) pinches and swells between 5 and 10 m in thickness and is continuously exposed as a prominent rib that extends along the slope for about one kilometre. The elevation of the dyke is about 60 m below the projected base of pyroclastic deposits on the adjacent ridge (Fig. 50). This probably accounts for

the great thickness of the dyke. At such a shallow depth the intrusion probably flared out in response to decreased confining pressure near the surface.

Thin sections of North Rift basalt reveal no significant differences in mineralogy or texture between the dykes and flows (Fig. 51). Euhedral phenocrysts of plagioclase (sodic labradorite) up to 0.5 cm long form between 15 and 40% of most sections. In addition to plagioclase, some sections contain partly resorbed grains of alkali feldspar (anorthoclase) with rounded, embayed, and fritted boundaries (Fig. 51b). These are probably xenocrysts incorporated from the underlying comenditic rocks. Clinopyroxene phenocrysts, which form about 2% of most specimens, are rarely more than 1 mm across. They occur as euhedral to subhedral,

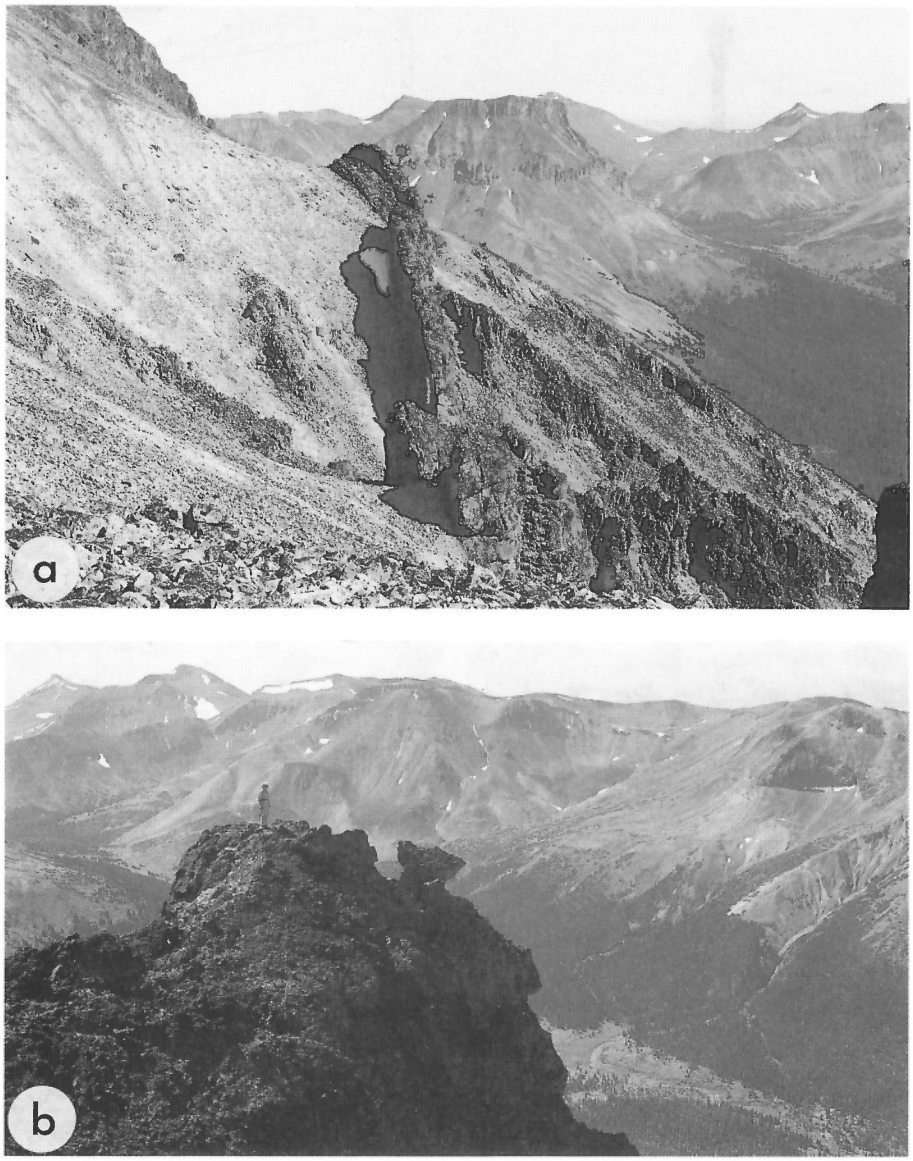

Figure 49. *(**a**) View looking southeast at the main North Rift dyke on the west flank of Far Mountain. At this location the dyke is 10 m thick and is one of the principal feeders for the North Rift basalt flows. Pipe Organ Mountain is in the background. (**b**) Proximal pyroclastic breccia (foreground) of North Rift basalt on the ridge above and to the northeast (left) of the dyke shown in Figure 49a (see Fig. 50). Monocephala Peak is in the centre background. GSC 1993-154Q*

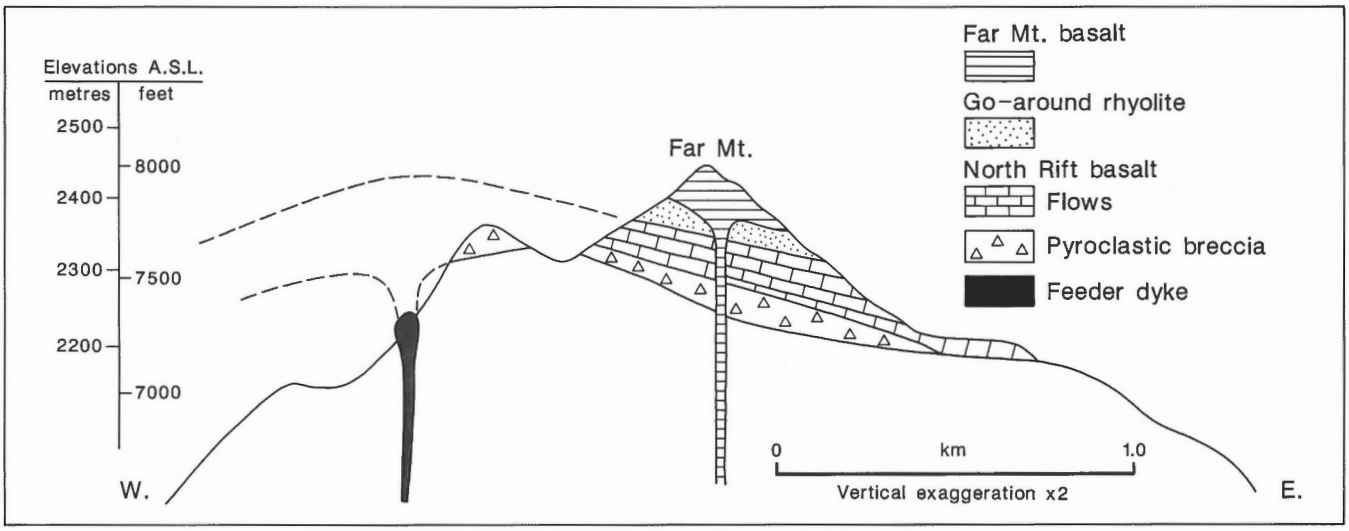

Figure 50. *Cross-section showing the relationship of the North Rift dykes to proximal flows and pyroclastic deposits (see Fig. 49).*

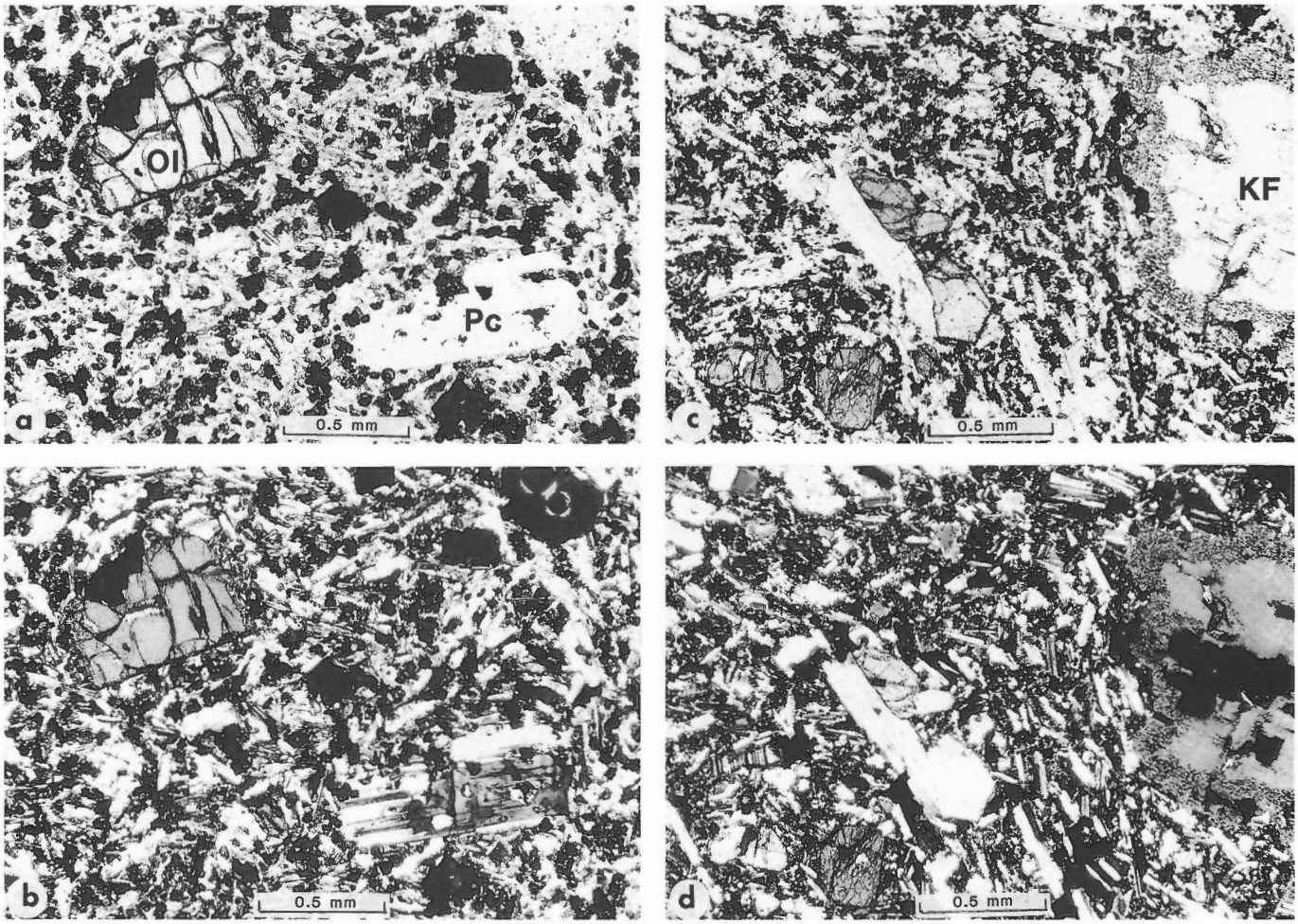

Figure 51. *Photomicrographs of North Rift basalt. (a, b) Flow. Phenocryst of olivine (Ol) and labradorite (Pc) in an intergranular groundmass of plagioclase, augite, and titaniferous magnetite (**a**) plane-polarized light, (**b**) crossed polars. (c, d) Dyke. Xenocryst of alkali feldspar (KF) with fritted reaction rim, enclosed in olivine-plagioclase-phyric basalt (**c**) plane-polarized light, (**d**) crossed polars. GSC 1993-154N*

pale brown, nonpleochroic crystals (salite) that show no reaction with the groundmass. Olivine phenocrysts up to 2 mm across vary in abundance from 0 to about 2%. The proportion of olivine and feldspar phenocrysts appears to be antipathetic, suggesting that olivine abundance may be controlled by in situ crystal settling – the larger olivine phenocrysts being cumulus crystals.

The groundmass comprises an intergranular assemblage of euhedral to subhedral plagioclase laths, small subhedral grains of clinopyroxene and olivine, and finely disseminated opaque oxides. The rock is unaltered and vesicles are unfilled.

*Hump Mountain basalt (map unit **MPTh**).*

Flows of Hump Mountain basalt are extensively exposed in the southern quadrant of the Ilgachuz Range where they form cap rocks on several of the higher peaks, and cover broad areas of the adjacent plateau (Fig. 52). The rock is light grey on both fresh and weathered surfaces, and most outcrops have a flaggy aspect resulting from well developed flow foliation. Pronounced subhorizontal flow layering, foliation, and fracture-cleavage are characteristic features of the Hump Mountain basalt as are large, flat talus slabs which produce a resonant ringing sound when struck with a hammer. Most of the Hump Mountain basalt is aphyric or contains only a few sparse phenocrysts of plagioclase, pyroxene, or olivine. However, a single porphyritic flow containing about 40% phenocrysts of plagioclase, pyroxene, and olivine is interlayered with the aphyric flows on the east flank of Hump Mountain.

The Hump Mountain flows are commonly between 1.5 and 6 m thick and separated by relatively thin layers of ropy, red flow-top breccia. Most of the remnants on the plateau comprise only one or two flows, but the section on Hump Mountain includes at least 10 cooling units with a composite thickness of 75 m. The basal flow in this section rests on a 10 m thick layer of unconsolidated fluvial gravel with rounded boulders up to 30 cm across in a sandy to earthy matrix. Similar, but thinner, gravel deposits were noted under the Hump Mountain succession at several other locations. All of the clasts are locally derived from comenditic rocks in the underlying shield.

The source of the Hump Mountain flows was not located. Based on initial dips, which are symmetrically disposed around the head of Carnlick Creek valley, their source has probably been completely removed and any associated subvolcanic bodies covered by deep colluvium that fills this major valley.

Thin sections of aphyric Hump Mountain basalt display a well developed trachytic texture that reflects the characteristic megascopic flow foliation (Fig. 53). Slender, closely aligned laths of plagioclase up to 0.5 mm long form about 60% of most sections. The remaining 40% comprises about equal proportions of subophitic clinopyroxene, intergranular crystals of olivine up to 0.3 mm across, and disseminated grains of opaque oxides. Rare microphenocrysts of olivine up to 0.5 mm across are present in some thin sections.

A thin section of the anomalously porphyritic flow on Hump Mountain lacks the well developed trachytic texture of the aphyric flows. Crudely aligned phenocrysts of plagioclase, clinopyroxene, and olivine from 1 to 4 mm across are surrounded by a fine grained pilotaxitic groundmass of the same minerals plus disseminated opaque oxides. Both the plagioclase and pyroxene exhibit complex oscillatory zoning.

*Go-around rhyolite (map units **MPTgv, MPTgi**)*

Go-around rhyolite is the only felsic unit within the otherwise basaltic Tundra Mountain Volcanics. It was found at only two locations, on the summit of Go-around Mountain and interlayered with basalt units on Far Mountain.

The remnant on Go-around Mountain (map unit **MPTgv**) is about 60 m thick and rests conformably on Hump Mountain basalt (Fig. 54). A 15 m recessive interval at the base consists

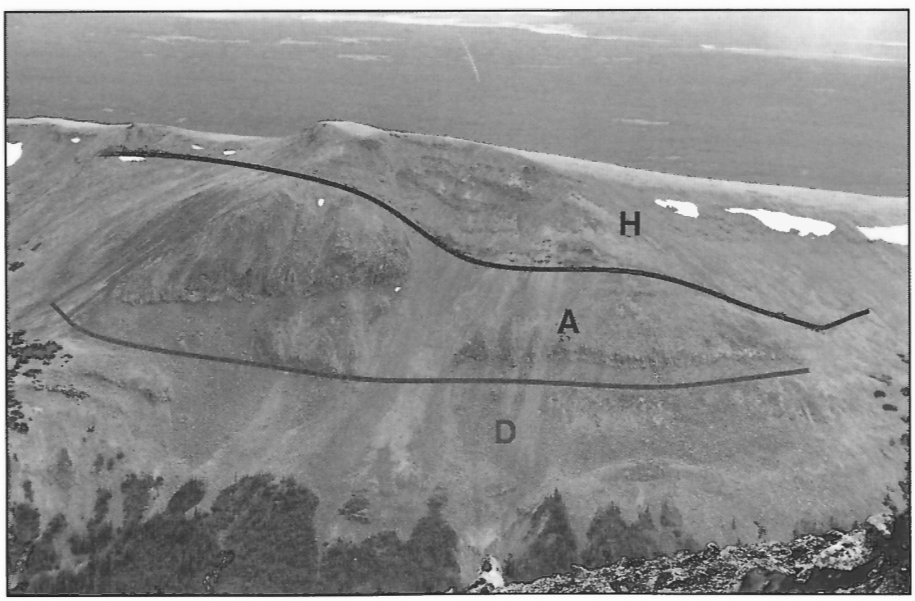

Figure 52.

Thin flows of Hump Mountain basalt (H) capping the ridge west of Hump Mountain. Arnica Lake comendite (A) forms the prominent dome-shaped lobe below the peak. Dean River flows (D) outcrop on the lower part of the slope. About 400 m of section are exposed. GSC 1993-184E

of fine, moderately indurated pumice, which grades up into coarser, agglutinated subangular lapilli (±3 cm). The lapilli is overlain by pale grey, fine grained, platy rhyolite which forms the upper 45 m of the summit.

On Far Mountain, the Go-around rhyolite (map unit **MP**Tgv) is 65 m thick. It rests conformably on northeast-dipping North Rift basalt flows and is overlain conformably by the basal pyroclastic beds of Far Mountain basalt. The lower 1.5 m consist of very fine, yellow, poorly indurated ash. This is overlain by 30 cm of granular obsidian which grades up into a 5 m thick subvitreous horizon with well developed fiamme. The pronounced eutaxitic fabric of this horizon disappears upward, grading into pale grey, flow layered, aphyric rhyolite which forms the upper part of the unit. The massive rhyolite appears to be a lava flow. However, the welded, basal eutaxitic horizon may have been deposited as a proximal pyroclastic flow.

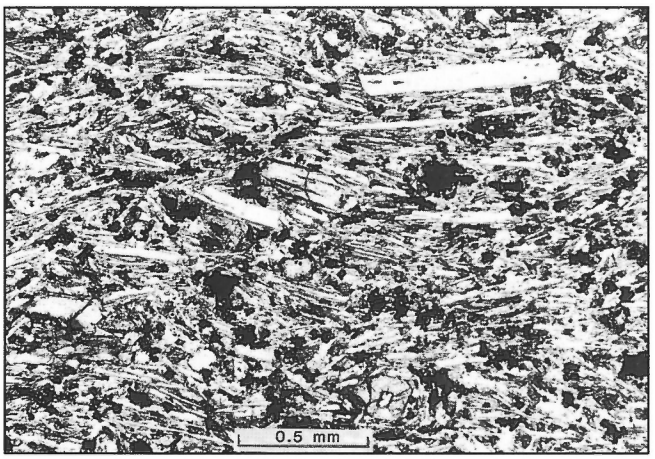

Figure 53. Photomicrograph of Hump Mountain aphyric basalt with prominent flow foliation defined by orientation of labradorite laths. Small grains of olivine, clinopyroxene (augite), and magnetite are interstitial to the feldspar. GSC 1993-184I

Thin sections of Go-around rhyolite from the Go-around Mountain and Far Mountain flows have similar textures and mineralogy (Fig. 55). The holocrystalline rhyolite is either aphyric or contains sparse euhedral phenocrysts of clear, unzoned, sanidine up to 2 mm long and rare microphenocrysts of bright green clinopyroxene (ferrohedenbergite) as euhedral prismatic crystals or crystal clusters. In addition, the rhyolite on Far Mountain contains rare microphenocrysts of fayalite surrounded by successive overgrowths of arfvedsonite and aegirine. The groundmass consists of crudely aligned or radiating clusters of alkali feldspar laths partly enclosed by ophitic grains of pleochroic blue and dark reddish-brown alkali amphibole (arfvedsonite and kataphorite), and bright green, highly pleochroic alkali pyroxene (aegirine?). Silica (probably tridymite) occurs as clear, late stage interstitial patches charged with tiny prisms of alkali feldspar.

Go-around obsidians contain sparse euhedral to slightly rounded phenocrysts of unzoned sanidine up to 2 mm long, and rare bright green euhedral prisms of ferrohedenbergite in a completely vitreous, fluidal-banded glass.

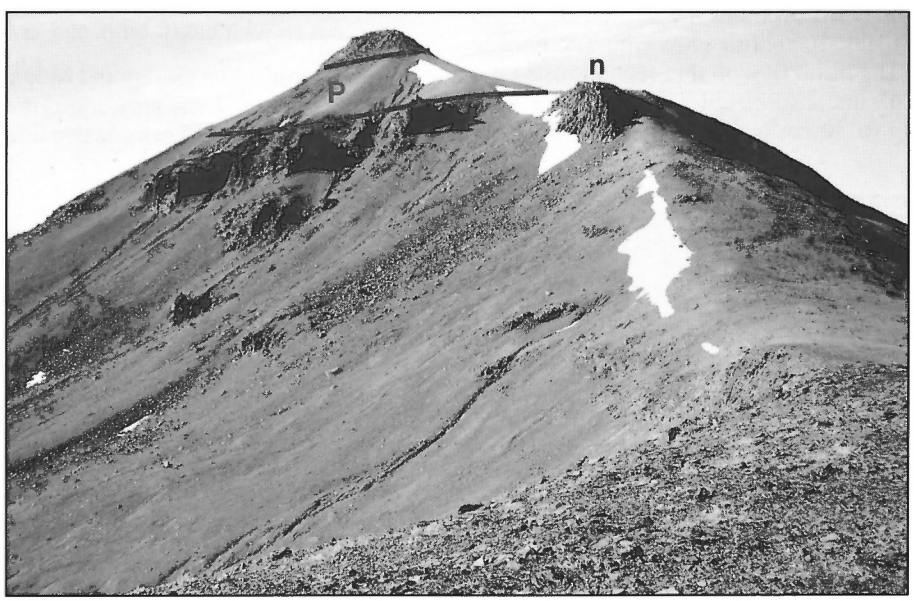

Figure 54 . *North slope of Go-around Mountain. Pumice (P) overlain by a thick flow of rhyolite form the conical upper part of the summit. This is one of two localities where felsic rocks occur within the Tundra Mountain succession. The small neck (n) on the west side of the peak is interpreted to be a local source. GSC 1993-154P*

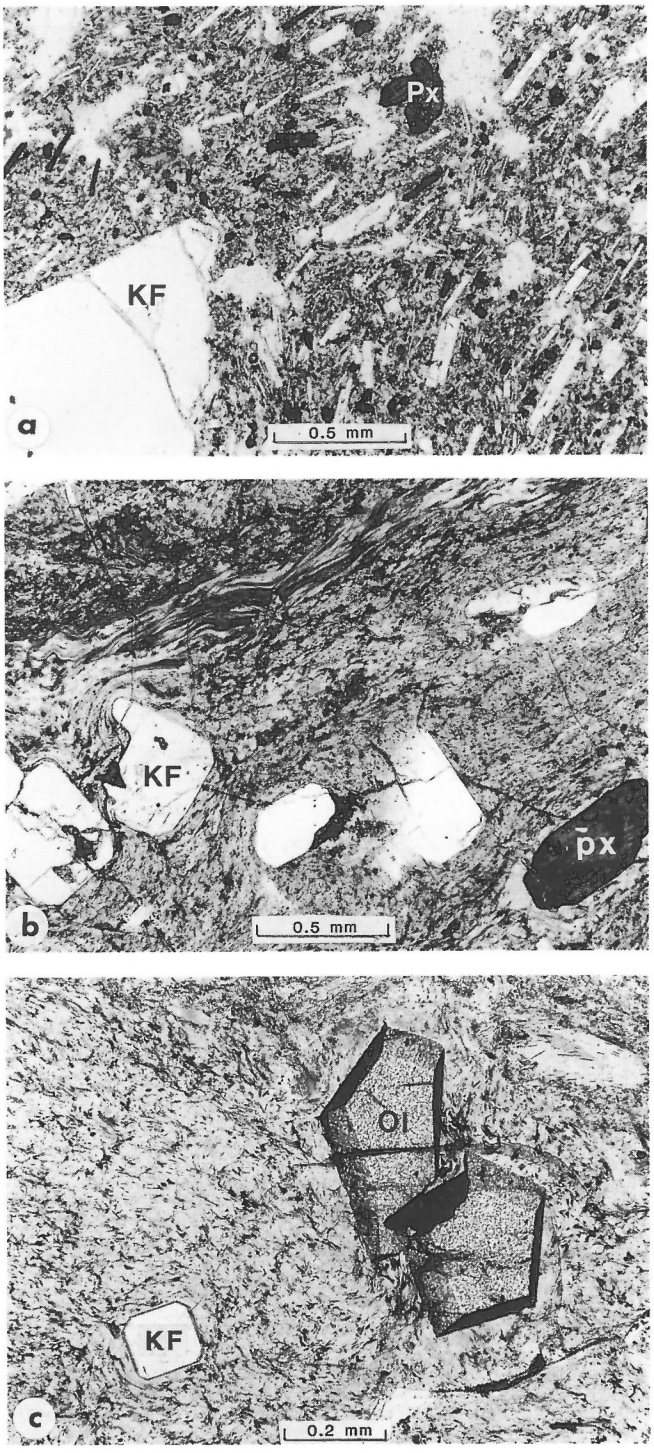

Figure 55. *Photomicrographs of Go-around rhyolite. (**a**) Comendite flow. Large sanidine phenocryst (KF) and microphenocrysts of hedenbergite (Px) in a fine grained groundmass of crudely aligned alkali feldspar laths, sodic clinopyroxene, and opaque oxides. (**b**) Microphenocrysts of sanidine (KF) and hedenbergite (px) in fluidal banded glass. (**c**) Euhedral microphenocrysts of fayalite (Ol) and sanidine (KF) in microlitic glass. All plane-polarized light). GSC 1993-184G*

A small circular neck of felsic rock (map unit **MPT**gi) exposed on the northwest flank of Go-around Mountain may be the source of the summit deposits. The source of Go-around deposits on Far Mountain was not found. They probably issued from a nearby vent and it is doubtful that they or the correlative deposits on Go-around Mountain are remnants of a formerly widespread rhyolite succession. They more likely represent small, approximately coeval eruptions of residual, silicic magma inherited from an earlier, more extensive episode of rhyolitic volcanism.

*Far Mountain basalt (map units **MPT**fv, **MPT**fi)*

Far Mountain basalt is the youngest unit of the Tundra Mountain Volcanics. Flows of Far Mountain basalt (map unit **MPT**fv) are extensively exposed in the northern half of the Ilgachuz Range where they form the upper surface of broad interfluves between Festuca and Blue Canyon creeks (Fig. 56). Smaller remnants form caps on adjacent ridges, and related subvolcanic intrusions (map unit **MPT**fi) are exposed in the headwaters of deeply incised radial valleys. On Far Mountain, proximal flows and pyroclastic deposits of Far Mountain basalt rest conformably on Go-around rhyolite, and on Tundra Mountain they conformably overlie flows of North Rift basalt. Elsewhere the Far Mountain basalt rests disconformably on an erosion surface that truncates successively older portions of the shield down to and including the Dean River Volcanics.

The Far Mountain basalt is an extremely uniform, medium to dark grey, very fine grained, aphyric rock with cryptic, locally contorted flow banding.

The flows, commonly between 2 and 3 m thick, are separated by relatively thin layers of ropy flow-top breccia and, on Tundra Mountain, they have a cumulative thickness of at least 120 m. A 6 m thick lahar, interlayered with Far Mountain flows on the east side of Rich Creek valley, is the only intraflow deposit found in the otherwise monotonous succession of thin basalt flows. Thin sections confirm the uniform megascopic lithology of the Far Mountain basalt (Fig. 57). All of the sections examined have fine grained intergranular textures. Crudely aligned, subhedral plagioclase laths (labradorite) up to 0.5 mm long compose about 75% of the rock. Olivine, as intergranular crystals up to 0.2 mm, is the most abundant mafic mineral, forming about 15% of most sections. Grains of opaque oxide are about the same size as the olivine and occur in about the same abundance. Clinopyroxene, as tiny intergranular crystals, forms less than 5% of most specimens.

The Far Mountain basalt probably issued from a cluster of vents, now represented by necks and subvolcanic intrusions (map unit **MPT**fi) on the upper, north-facing slope of the shield (Fig. 58). One of the feeders, a 15 m dyke exposed on the north side of Far Mountain, cuts the underlying strata and extends up into Far Mountain pyroclastic deposits which form the summit ridge (Fig. 50). A large subvolcanic pluton of coarsely jointed, aphyric basalt is exposed near the head of

Figure 56. South side of Tundra Mountain where a thick succession of Far Mountain basalt flows forms the upper part of the Ilgachuz Range shield volcano. GSC 1993-184A

Table 2. K-Ar dates from rocks of the Ilgachuz Group and Tatla Lake Metamorphic Core Complex.

Sample No.	Unit Name	Unit Designator	Latitude	Longitude	Elevation	Laboratory	%K	$Ar^{40}x10^{-6}cm^3/gm$	% Ar^{40}	Ma
SE110583	Dean River	MDv	52° 46.6'	125° 16.7'	6600	U.B.C.	4.48 ± 0.01	0.9090	61.6	5.2 ± 0.2
SE310785	Dean River	MDv	52° 46.9'	125° 13.7'	5600	G.S.C.	4.51 ± 0.67	1.01	22.0	5.7 ± 0.1
DG213.85	Dean River	MDv	52° 44.8'	125° 25.4'	4200	G.S.C.	4.061 ± 0.01	0.8004	11.2	5.06 ± 0.09
SE2507A81	Mizzen Mtn.	MCm	52° 44.7'	125° 13.8'	6050	U.B.C.	4.12 ± 0.01	0.784	80.3	4.9 ± 0.2
DG135.85	Mizzen Mtn.	MCm	52° 46.1'	125° 14.3'	6700	U.B.C.	4.05 ± 0.01	0.8324	80.7	5.3 ± 0.2
SE040283	Rich Cr.	MCr	52° 47.8'	125° 19.3'	6750	U.B.C.	3.80 ± 0.00	0.7770	71.2	5.2 ± 0.2
SE040783	Rich Cr.	MCr	52° 48.2'	125° 19.3'	6450	U.B.C.	3.17 ± 0.01	0.7507	89.8	6.1 ± 0.2
CH190281	Pipe Organ	MCpov	52° 45.7'	125° 18.2'	7300	U.B.C.	4.65 ± 0.01	0.9089	50.6	5.0 ± 0.2
SE050883	Pipe Organ	MCpov	52° 46.4'	125° 18.2'	7000	U.B.C.	4.08 ± 0.01	0.7970	14.0	5.0 ± 0.3
SE071583	Pipe Organ	MCpov	52° 46.2'	125° 18.8'	6950	U.B.C.	2.98 ± 0.01	0.5614	30.1	4.8 ± 0.2
SE250581	Arnica L.	MAv	52° 44.9'	125° 14.0'	7100	U.B.C.	4.08 ± 0.00	0.791	77.4	5.0 ± 0.2
SE031583	Arnica L.	MAv	52° 47.4'	125° 20.4'	7100	U.B.C.	3.89 ± 0.02	0.7776	87.6	5.1 ± 0.2
SE0906B83	Arnica L.	MAv	52° 46.8'	125° 18.2'	7300	U.B.C.	3.95 ± 0.02	0.7845	20.3	5.1 ± 0.2
SE050183	Stonecrop	MPTsv	52° 46.4'	125° 17.1'	7500	U.B.C.	0.897 ± 0.006	0.1731	44.7	5.0 ± 0.2
SE2511A81	N. Rift	MPTnv	52° 47.2'	125° 19.9'	7500	U.B.C.	0.960 ± 0.006	0.2086	43.4	5.6 ± 0.2
SE010683	N. Rift	MPTnv	52° 47.8'	125° 20.7'	6950	U.B.C.	1.02 ± 0.01	0.2117	65.0	5.3 ± 0.2
SE250381	Hump Mtn.	MPTh	52° 45.1'	125° 14.2'	7500	U.B.C.	1.30 ± 0.01	0.272	55.8	5.4 ± 0.2
SE250481	Hump Mtn.	MPTh	52° 45.0'	125° 14.1'	7250	U.B.C.	0.840 ± 0.006	0.1815	60.3	5.5 ± 0.2
SE020783	Go-around	MPTgv	52° 47.2'	125° 19.8'	7650	U.B.C.	4.04 ± 0.03	0.6242	7.2	4.0 ± 0.6
SE251281	Far Mtn.	MPTfv	52° 52.6'	125° 25.4'	4300	U.B.C.	1.56 ± 0.00	0.3118	52.3	5.1 ± 0.2
SE021783	Far Mtn.	MPTfv	52° 47.7'	125° 18.0'	7450	U.B.C.	1.68 ± 0.01	0.3061	67.6	4.7 ± 0.2
SE100783	Far Mtn.	MPTfv	52° 46.7'	125° 16.8'	7100	U.B.C.	1.29 ± 0.01	0.2586	66.0	5.1 ± 0.2
SE4002B89	Tatla Lake	TT	52° 43.1'	125° 19.8'	5300	G.S.C.	3.63 ± 1.717	7.964	9.3	55.66 ± 2

Elevation is in feet above mean sea level.
U.B.C. = University of British Columbia
G.S.C. = Geological Survey of Canada

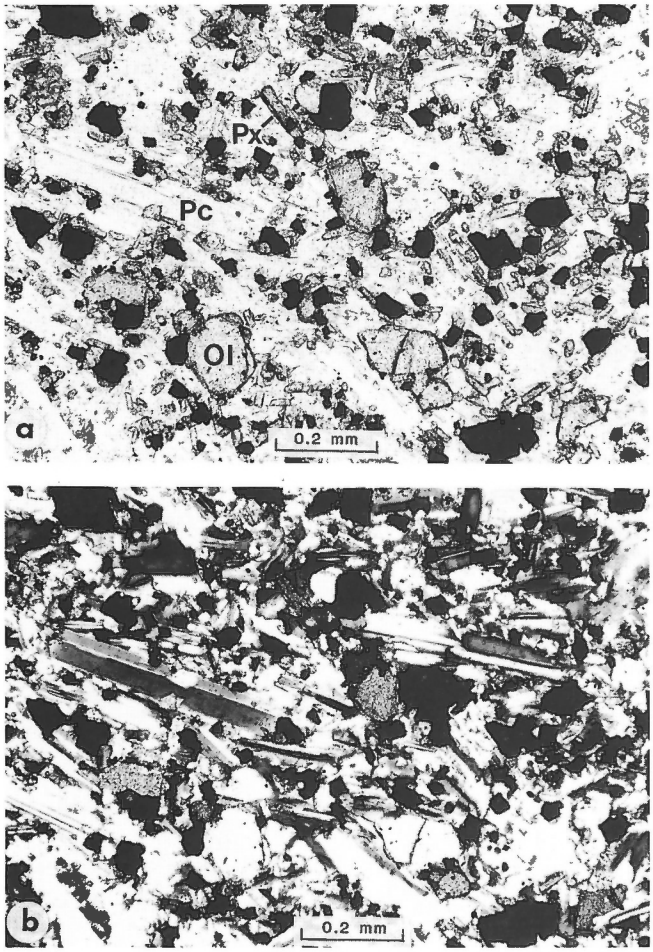

Figure 57. Photomicrographs of Far Mountain basalt. Fine grained, aphyric flow comprising intergranular labradorite laths (Pc), olivine grains (Ol), tiny prisms of clinopyroxene (Px), and opaque grains of titaniferous magnetite (a) plane-polarized light, (b) crossed polars. GSC 1993-154K

Blue Canyon Creek. It is close to a thick section of Far Mountain basalt on Tundra Mountain and probably represents part of a second major conduit system. Nana and Crepis peaks on the ridge east of Blue Canyon Creek may represent a third centre of Far Mountain activity (Fig. 59). These two circular, steep-sided knobs comprise fine grained aphyric basalt similar to the Far Mountain flows. Their contact relations are obscured by flanking talus slopes, but the shape of the peaks plus the presence of long, large-diameter columns suggest that they are necks rather than flow remnants.

Age of the Ilgachuz Group

Twenty-two K-Ar dates on lavas from the Ilgachuz Group (Table 2) range from 4.0 to 6.1 Ma. However, 20 of these, or 90%, are clustered in the short interval between 4.7 and 5.7 Ma (Fig. 60). This is consistent with field observations, which show little evidence of intraflow erosion. Disconformities within the Ilgachuz Group are limited to thin, discontinuous clastic deposits associated with shallowly incised drainage channels. From the initial eruption of Dean River comendite until the final effusion of Far Mountain basalt there appear to have been no significant periods of dormancy during which the volcanic pile was dissected. The K-Ar dates suggest that the entire edifice was built during an interval of less than two million years.

The short eruptive history of the Ilgachuz Range is of similar duration to that of the older Rainbow Range to the west (8.7-6.7 Ma) and the younger Itcha Range to the east (3.5-1.1 Ma) (Souther, 1986). Each of these central volcanoes appear to be the product of a complex but short-lived magmatic cycle in contrast to the Chilcotin Group lavas which issued from many widely separated vents during the period from 26 to 1.1 Ma (Mathews, 1989). The age relationships support the petrographic and chemical evidence for fundamental differences in the origin of the central volcanoes (Rainbow, Ilgachuz, and Itcha ranges) and the adjacent Chilcotin Group lavas. The Chilcotin Group was erupted

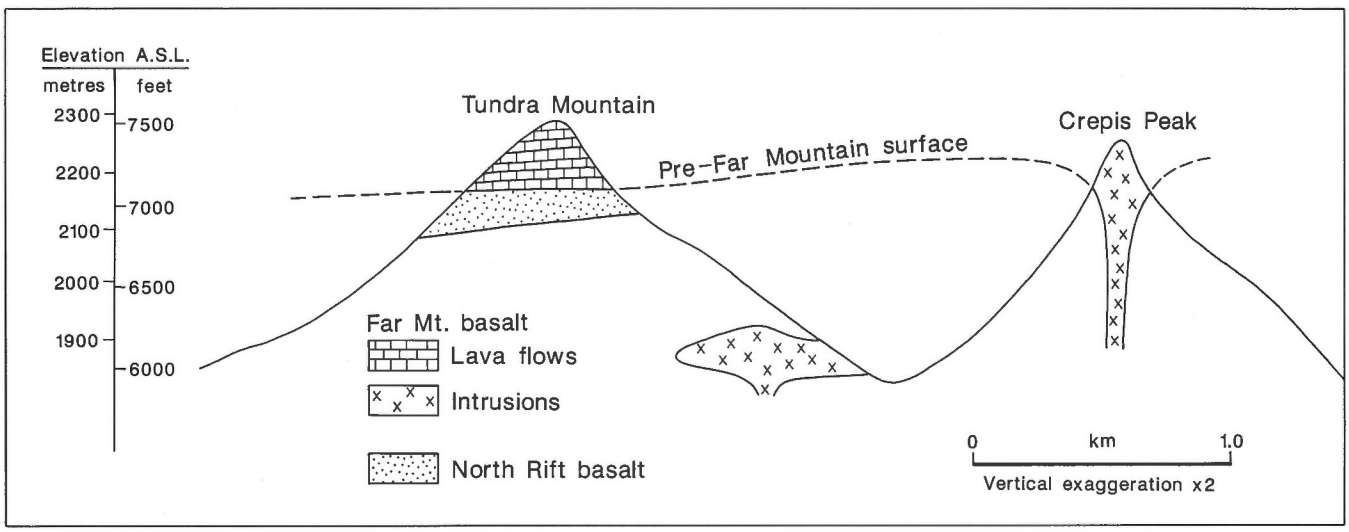

Figure 58. Schematic cross-section showing the relationship between Far Mountain flows and intrusions.

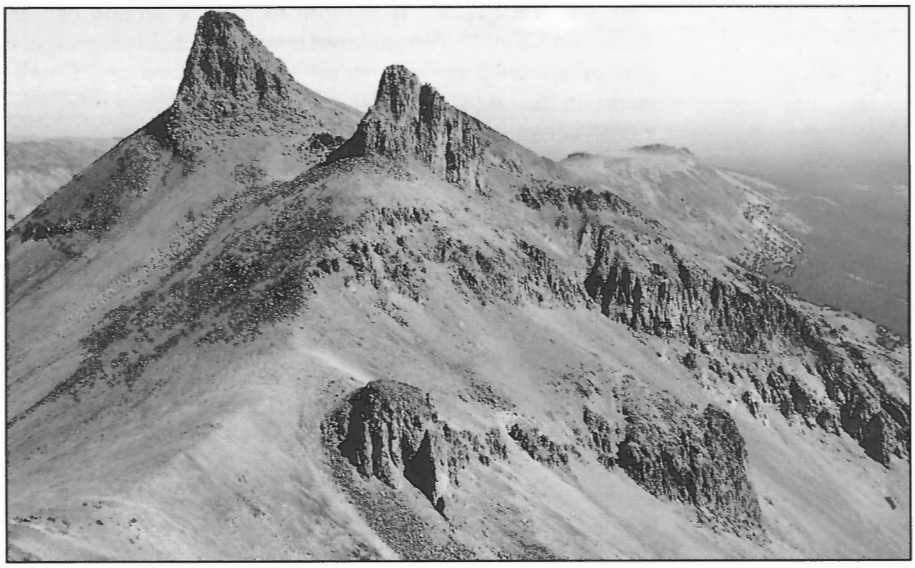

Figure 59.

Nana (left) and Crepis peaks as seen from Stonecrop Ridge. These are two of several possible sources of Far Mountain basalt. GSC 1993-184J

episodically in a relatively long-lived back-arc setting associated with the subduction of Juan de Fuca Plate (Souther, 1977; Bevier, 1983b; Souther and Yorath, 1991). In contrast, the central volcanoes were generated successively in relatively short bursts of activity. The age relationships support the concept of a genetic relationship between the Anahim Belt volcanoes and a mantle hotspot, which migrated from west to east across the Chilcotin back-arc (Bevier et al., 1979; Souther, 1986).

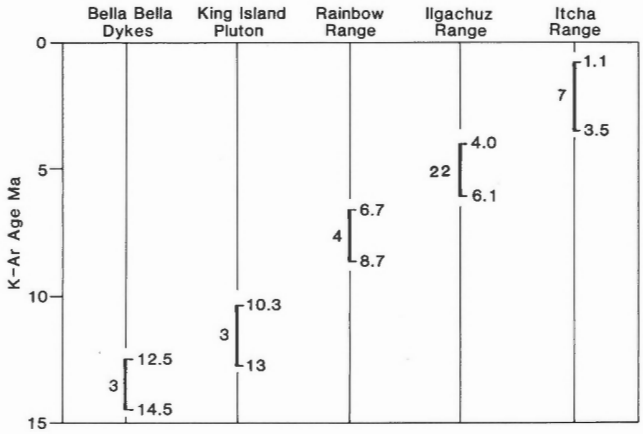

Figure 60. *Plot showing the range of K-Ar dates from the Ilgachuz Range and the progressive eastward decrease in K-Ar dates along the Anahim Belt (modified from Souther, 1986).*

Itcha Group

The western margin of the Itcha Range shield volcano (Charland et al., 1993) extends into Christensen Creek map area. Thick flows of flaggy-weathering, greenish-grey comenditic trachyte (map unit **PIc**) are exposed in west-facing bluffs east of Corkscrew Creek and isolated remnants of basalt (map unit **PIb**) outcrop along the creek banks. The basalt is a dark grey, fine grained, aphyric rock with small diameter, randomly oriented, and splayed columns that suggest quenching in a water- or ice-contact environment.

Flank basalt

Remnants of a Pliocene or younger pyroclastic cone are preserved near the treeline on the eastern flank of Mizzen Mountain. The rounded mound of red basaltic spatter and bombs is almost a kilometre across at the base and rises 200 ft. (60 m) above the gently eastward-sloping surface of the older shield. It occupies a deep valley and the present stream has eroded through the centre of the cone, dissecting it into two adjacent mounds.

Basalt erupted from this centre is exposed immediately northeast of the cone where at least 6 m of fresh, blocky-jointed basalt form the walls of small box canyons. The rock is medium grey and has open vesicles and abundant 1 to 2 mm phenocrysts of olivine and pyroxene. Two 10 m thick olivine-phyric flows of similar basalt that probably originated from this or other unrecognized Pliocene or younger centres, are exposed 8 km farther east in Pan Creek. There, two 10 m thick olivine-phyric flows are overlain by till containing mostly volcanic clasts.

Thin sections of the proximal and distal flows of Flank basalt are similar in texture and mineralogy (Fig. 61). Subhedral phenocrysts of olivine and strongly zoned clinopyroxene form about 20% of most sections. They are commonly less than 2 mm across, but megacrysts of clinopyroxene up to 5 mm across are present in some specimens. Partly resorbed euhedral magnetite crystals up to 2 mm across form rare phenocrysts. The groundmass contains about equal proportions of euhedral plagioclase laths, granular olivine and clinopyroxene, and finely disseminated opaques.

The Flank basalt is clearly much younger than the Ilgachuz Group but older than the last period of glaciation. The summit of the pyroclastic cone is scattered with locally-derived erratics, and associated flows are covered with a layer of till containing mostly volcanic clasts. Despite this evidence of glaciation, the pyroclastic cone consists entirely of subaerial deposits. It was probably erupted during a Pleistocene interstadial period and subsequently overridden by relatively thin ice flowing eastward off the Ilgachuz Range.

CHEMISTRY OF THE ILGACHUZ GROUP AND FLANK BASALT

Fifty-one samples from the Ilgachuz Group and two from the Pliocene or younger Flank basalt were analyzed for major and minor elements, and ten selected samples were analyzed for the rare earth elements (Table 4). A complete listing of whole rock analyses is given in Souther and Souther (1994), and 23 representative analyses are listed in Table 3. Whole rock analyses for major elements were done by Chemex Labs Limited of Vancouver using XRF for Si, Al, Fe, Mg, Ca, Na, K, Ti, P, Mn, Cr, and LOI, and titration for FeO. Minor element analyses were done by the Analytical Chemistry Section of the Geological Survey of Canada using ICP for Ba, Be, Co, Cr, Cu, La, Nb, Ni, Rb, Sr, V, Y, Yb, Zn, and Zr. The rare earth elements (Ce, Dy, Eu, Gd, La, Nd, Sm, Y, Yb) were also determined by the Geological Survey of Canada Laboratory using ICP on trace solutions after x10 preconcentration and separation of majors using ion exchange resin. Normative values were calculated using a program developed by G.J. Woodsworth.

Whole rock chemistry

Major elements

The whole rock chemistry of the Ilgachuz Group rocks is distinctly bimodal, comprising a mafic suite (45-52% SiO_2) and a felsic suite (59-76% SiO_2), which plot as distinct populations within the alkaline field of the Le Bas et al. (1986) and Irvine and Baragar (1971) total alkalis versus silica diagrams (Fig. 62). Harker variation diagrams (Fig. 63) show that the silica gap between the two suites corresponds to a distinct boundary zone across which there is a profound change in the proportions of CaO, MgO, K_2O, FeO, TiO_2 and P_2O_5; a moderate shift in the proportion of Na_2O; and considerable overlap in the Al_2O_3, and MnO, contents of the mafic and felsic suites.

The mafic suite is restricted to the Tundra Mountain Volcanics, which forms the outer part of the Ilgachuz shield. Normative olivine is present in all of the 13 analyzed samples, and about half of them are nepheline normative. Most of the analyses plot in the trachybasalt field of Le Bas et al. (1986) (Fig. 62) and in the Hawaiite field of Irvine and Baragar (1971) (Fig. 64). The Flank basalt is slightly more magnesian, but is otherwise similar in composition to the Tundra Mountain basalts. All of the Ilgachuz Group basalts are significantly more alkaline than Chilcotin Group lavas reported by Bevier (1983b) and Mathews (1989) (Fig. 62).

The felsic suite comprises 33 samples from the lower part of the Ilgachuz shield and dome complex (Arnica Lake, Carnlick Creek, and Dean River Volcanics), and two samples from the Go-around rhyolite. The latter is a thin, anomalous rhyolitic member interlayered with trachybasalt in the lower part of the Tundra Mountain Volcanics. With one exception – a trachyte from the Dean River Volcanics – the rocks of the felsic suite are quartz-normative. Six of the analyzed samples are trachytes (Fig. 64) and the remaining 27 samples are peralkaline (Fig. 65). Using the classification scheme of Macdonald and Bailey (1973), most of the oversaturated Ilgachuz Group rocks plot in the comendite and pantellerite fields (Fig. 66).

Minor elements

Discriminant plots, based on the minor element content of the Ilgachuz Group rocks, are in general agreement with the major element classifications. On the Log (Zr/TiO_2) versus

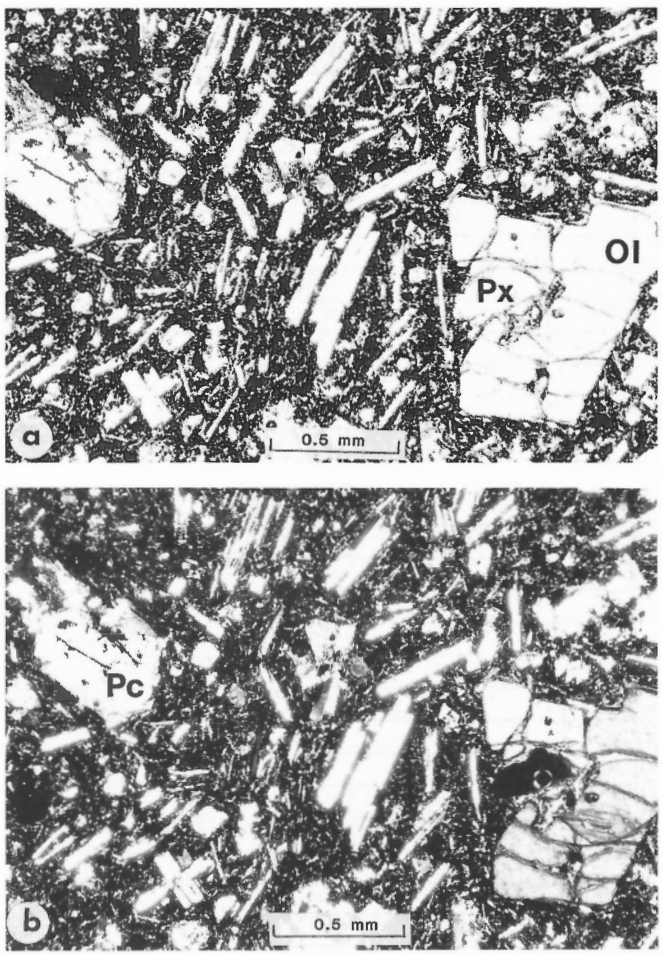

Figure 61. *Photomicrographs of Flank basalt. Medium grained flow. Phenocrysts of olivine (Ol), clinopyroxene (Px), and labradorite (Pc) in a groundmass of the same minerals plus granular opaque oxides (**a**) plane-polarized light, (**b**) crossed polars. GSC 1193-184B*

Table 3. Representative chemical analyses of rocks from the Ilgachuz Group and Flank basalt.

Map unit	MDv	MDv	MCmv2	MCmv1	MCmv2	MCcv	MCs	MCr	MCf	MCpov	MCpoi
Sample	SE0609A83	SE0609B83	DG8-135-2	SE361185	SE400788	SE360587	SE261385	SE040783	SE1103B83	SE050883	SE071583
SiO_2	68.37	67.18	66.80	73.30	68.00	61.10	63.70	75.66	67.48	64.06	63.62
Al_2O_3	14.96	15.13	12.80	11.60	11.70	16.70	16.40	10.92	14.15	16.77	16.93
Fe_2O_3	3.81	4.91	4.10	2.59	3.93	6.18	3.01	2.45	1.37	2.39	2.94
FeO	0.86	0.43	2.71	1.63	3.27	0.39	1.22	1.43	2.44	2.01	1.29
CaO	0.18	0.20	0.88	0.17	0.66	0.86	2.24	0.19	0.75	1.96	1.94
MgO	0.02	0.02	0.12	0.08	0.11	0.17	0.44	0.02	0.04	0.25	0.32
Na_2O	5.75	5.80	6.50	5.40	5.80	6.00	6.00	4.34	5.85	6.08	5.93
K_2O	5.44	5.36	4.95	4.70	4.90	5.57	4.49	4.62	5.51	4.75	4.69
TiO_2	0.51	0.52	0.48	0.22	0.45	0.64	0.77	0.23	0.35	0.58	0.55
P_2O_5	0.03	0.02	0.05	0.02	0.03	0.16	0.26	0.02	0.04	0.16	0.15
MnO	0.08	0.06	0.17	0.06	0.17	0.25	0.10	0.08	0.10	0.16	0.11
$+H_2O$	0.24	0.20	0.08	0.15	0.34	1.08	0.48	0.18	1.58	0.46	0.61
$-H_2O$	n.d.	n.d.	0.10	0.10	0.42	0.41	0.35	n.d.	n.d.	n.d.	n.d.
Total	100.25	99.83	99.74	100.02	99.78	99.51	99.46	100.14	99.66	99.63	99.08
LOI	0.67	0.56	0.08	0.18	0.65	1.86	1.23	0.43	2.51	1.06	1.57
Ba	140	140	30	30	90	760	890	0	50	1100	1100
Be	2.1	3.0	4.5	7.6	14	4.8	6.1	7.4	6.1	4.3	4.6
Co	0	0	1	0	2	2	6	0	0	6	4
Cr	19	12	86	98	71	85	69	34	24	23	25
Cu	3	2	3	4	8	4	4	5	4	3	3
La	70	54	67	29	130	41	54	32	73	49	58
Nb	110	110	140	180	250	75	80	260	110	72	73
Ni	0	0	3	1	4	0	0	2	2	0	0
Rb	80	67	92	180	140	70	81	210	110	65	64
Sr	0	0	0	0	0	140	290	0	0	250	260
V	0	0	0	0	0	0	5	0	0	0	0
Y	51	43	60	16	98	42	43	50	61	44	48
Yb	4.3	3.7	4.7	3.5	8.0	3.6	4.2	6.9	5.2	3.9	4.1
Zn	280	62	210	170	300	83	93	180	130	39	110
Zr	540	560	640	1300	1300	460	540	1500	730	530	490
Q	12.13	10.58	12.25	24.96	16.66	1.10	7.17	30.60	11.60	5.99	6.46
Or	32.01	31.70	29.40	27.94	29.38	33.36	26.61	27.70	32.89	27.97	27.82
Ab	49.38	50.97	40.84	35.77	35.44	54.61	54.05	32.79	45.15	54.41	53.46
An	0	0	0	0	0	2.22	4.57	0	0	4.42	5.75
Ne	0	0	0	0	0	0	0	0	0	0	0
CPx	0.56	0.69	3.25	0.57	2.50	0.84	3.29	0.66	2.80	3.38	2.34
OPx	2.04	2.60	4.66	3.48	6.64	4.36	0	2.80	2.20	0.53	0.94
Fo	0	0	0	0	0	0	0	0	0	0	0
Fa	0	0	0	0	0	0	0	0	0	0	0
Mt	1.48	1.77	0	0	0	2.27	2.38	0	0	2.17	2.15
Il	0.71	0.73	0.67	0.31	0.64	0.90	1.08	0.33	0.49	0.81	0.77
Al	1.0252	1.0141	1.254	1.2043	1.2688	0.952	0.8982	1.1117	1.1016	0.903	0.876
DI	93.52	93.25	85.29	90.57	84.14	89.07	87.83	91.27	90.48	88.36	87.73

n.d.=not determined

Map unit	MAv	MAv	MAv	MAi	MAi	MPTsv	MPTnv	MPTh	MPTgv	MPTfv	MPTfi	Pff
Sample	SE0906A83	SE0906B83	SE3005C84	SE071383	SE051083	SE050183	SE030783	SE241085	SE020783	SE021083	SE100783	SE430288
SiO_2	70.73	69.71	66.00	67.70	67.44	45.66	48.94	49.70	67.04	47.02	47.86	49.40
Al_2O_3	12.53	12.09	13.40	11.90	12.63	16.06	16.30	16.00	13.27	16.12	14.26	14.90
Fe_2O_3	3.01	3.30	5.16	5.06	5.13	5.14	5.56	4.20	3.16	4.93	4.88	5.29
FeO	2.29	2.72	1.78	2.01	2.29	9.03	7.02	8.60	3.73	8.89	9.46	6.11
CaO	0.47	0.54	0.87	0.50	0.62	8.43	7.48	6.43	0.81	7.05	7.94	7.80
MgO	0.02	0.05	0.17	0.11	0.02	5.61	3.73	3.87	0.12	4.35	3.99	6.73
Na_2O	5.52	5.26	6.50	6.50	6.68	3.15	4.43	5.00	5.78	4.27	3.91	4.20
K_2O	5.02	4.81	5.02	4.85	4.73	1.03	1.58	2.20	4.84	1.57	1.51	2.33
TiO_2	0.41	0.39	0.43	0.44	0.42	3.15	2.87	2.66	0.50	3.63	3.23	2.27
P_2O_5	0.02	0.03	0.04	0.03	0.02	0.56	1.12	1.05	0.04	0.81	1.59	0.56
MnO	0.13	0.21	0.17	0.18	0.17	0.20	0.22	0.19	0.16	0.22	0.27	0.17
$+H_2O$	0.14	0.38	0.15	0.17	0.14	1.17	0.27	0.24	0.65	0.12	0.75	0.25
$-H_2O$	n.d.	n.d.	0.10	0.14	n.d.	n.d.	n.d.	0.16	n.d.	n.d.	n.d.	0.25
Total	100.29	99.49	99.79	99.59	100.29	99.19	99.52	100.30	100.10	98.98	99.65	100.26
LOI	0.47	1.22	0.28	0.31	0.34	2.28	0.40	<0.01	1.53	0.25	1.70	<0.01
Ba	30	0	170	20	0	290	710	610	60	470	1100	530
Be	7.1	6.9	6.0	7.7	9.6	1.5	1.7	2.8	6.5	2.3	1.8	2.3
Co	0	0	1	0	1	43	16	29	2	35	27	40
Cr	43	60	87	130	32	34	2	41	37	23	13	220
Cu	4	4	4	3	5	15	4	8	4	10	3	29
La	71	71	84	56	100	8	18	42	92	24	18	28
Nb	140	130	140	150	210	28	32	54	130	37	24	52
Ni	11	3	2	2	5	44	4	7	3	8	0	100
Rb	110	110	91	100	86	16	21	33	91	33	23	33
Sr	0	0	14	0	0	660	720	840	1	850	690	610
V	0	0	0	0	0	220	98	66	0	120	86	140
Y	54	110	52	64	100	22	28	32	73	26	34	26
Yb	5.4	8.7	4.7	6.8	8.8	0.4	1.0	1.5	6.7	0.7	1.1	0.9
Zn	130	240	200	240	250	100	89	110	210	110	120	90
Zr	780	720	770	820	1200	180	260	340	720	260	200	290
Q	18.61	18.38	9.25	15.44	12.70	0	0	0	11.44	0	0	0
Or	29.71	29.03	29.69	28.85	27.87	6.33	9.54	13.10	28.81	9.53	9.24	13.78
Ab	38.81	38.39	43.52	36.55	40.88	29.41	40.64	39.90	44.17	38.49	36.37	29.50
An	0	0	0	0	0	27.70	20.36	14.84	0	20.74	17.51	14.94
Ne	0	0	0	0	0	0	0	3.21	0	0.54	0	4.94
CPx	1.76	2.03	3.25	1.84	2.35	9.59	8.06	8.32	3.03	7.81	10.03	16.11
OPx	3.90	5.22	5.78	6.57	6.56	7.68	3.68	0	5.82	0	12.00	0
Fo	0	0	0	0	0	5.74	4.20	6.20	0	7.26	0.96	9.39
Fa	0	0	0	0	0	2.72	2.38	4.10	0	3.40	0.66	3.06
Mt	0	0	0	0	0	5.05	4.67	4.38	0	5.30	5.12	3.94
Il	0.56	0.56	0.60	0.62	0.58	4.56	4.08	3.73	0.70	5.20	4.66	3.16
Al	1.1584	1.1463	1.2035	1.3397	1.2754	0.3921	0.552	0.6629	1.1113	0.5412	0.5657	0.633
DI	88.24	86.62	84.52	84.67	84.56	35.73	50.17	56.21	84.70	48.56	45.61	48.22

Table 4. Rare earth element analyses of a rocks from the Dean River Volcanics (**M**Dv), Mizzen Mountain rhyolite (**M**Cm), Arnica Lake Volcanics (**M**A), Stonecrop basalt (**MP**Ts), North Rift basalt (**MP**Tn), Hump Mountain basalt (**MP**Th), Far Mountain basalt (**MP**Tf), and Flank basalt (**P**ff).

Map unit Sample No.	**M**Dv SE400589	**M**Dv DG213-85	**M**Cm SE361185	**M**Cm DG8-135	**M**Av SE0906A	**MP**Ts SE050183	**MP**Tn SE030783	**MP**Th SE241085	**MP**Tf SE021783	**P**ff SE430688
Ce ppm :	95	110	190	140	140	47	77	88	81	74
Dy ppm :	5.9	9.5	5.0	13	12	5.2	7.7	7.2	7.0	5.7
Eu ppm :	1.5	1.9	0.3	2.2	1.4	2.3	3.7	3.3	3.2	2.7
Gd ppm :	7.5	12	4.9	15	13	6.5	10	9.5	9.3	7.4
La ppm :	39	61	33	72	71	26	39	46	42	36
Nd ppm :	46	62	34	74	71	32	53	54	50	40
Sm ppm :	10	11	5.3	17	11	5.3	8.2	8.3	7.6	8.5
Y ppm :	23	41	16	57	52	23	35	32	31	25
Yb ppm :	3.1	4.0	3.9	5.4	5.9	1.9	3.0	2.8	2.5	2.2

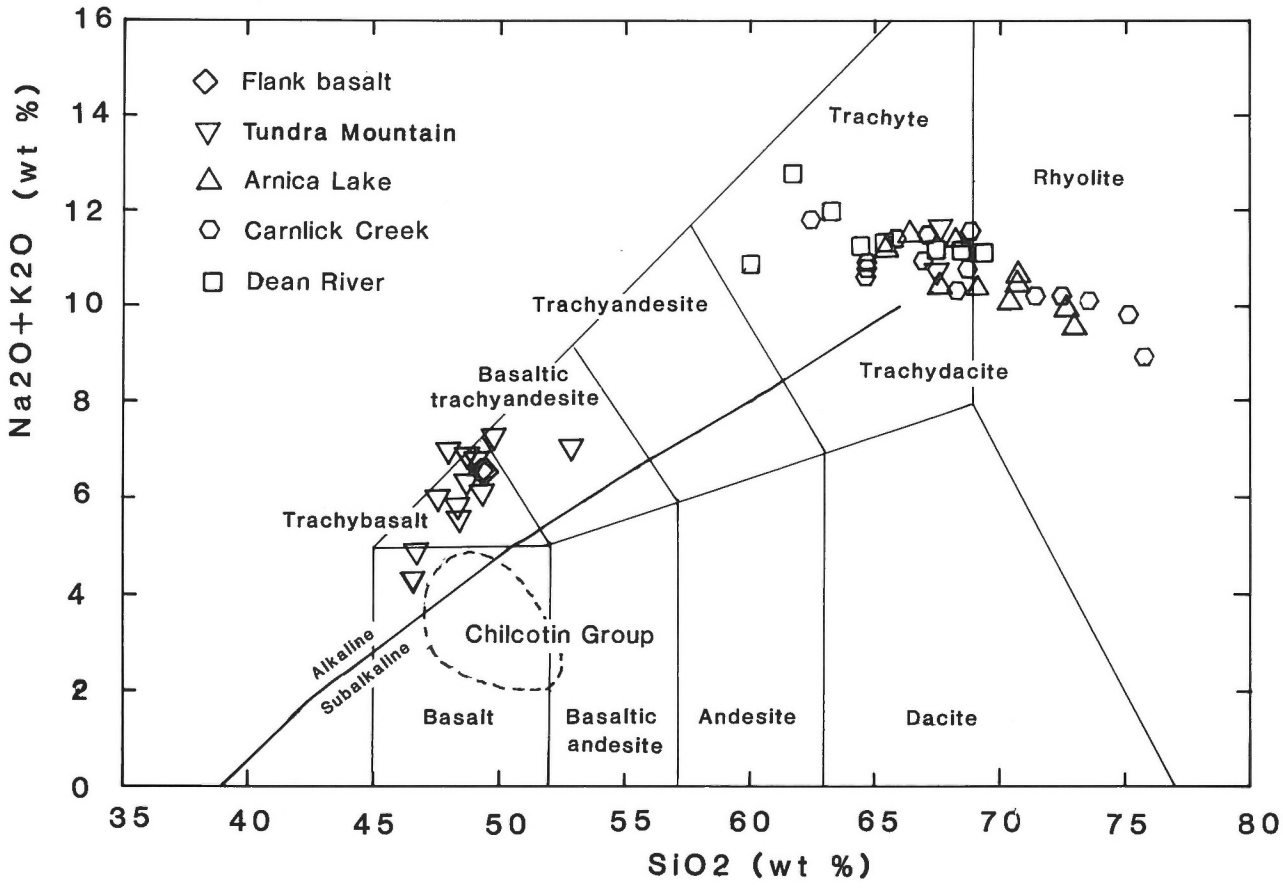

Figure 62. Plot of total alkalis versus silica showing the bimodal distribution of Ilgachuz Group rocks into distinct mafic and felsic suites. Field of Chilcotin Group basalt from Bevier (1983b). Species boundaries after Le Bas et al. (1986). Alkaline-subalkaline boundary from Irvine and Baragar (1971).

Log (Nb/Y) and SiO_2 versus Log (Zr/TiO_2) diagrams of Winchester and Floyd (1977) (Fig. 67, 68) the mafic suite plots within, or very near, the alkali basalt fields whereas the felsic suite displays more scatter and overlaps the fields of trachyte, comendite/pantellerite, and phonolite. All but one of the samples from the Ilgachuz Group mafic suite plot in the field of within-plate basalts on the Pearce and Cann (1973) Zr-Ti/100-Y*3 diagram (Fig. 69), and most of the samples from both the mafic and felsic suites plot in the field of within-plate alkali basalt on the Meschede (1986) Zr/4-Nb*2-Y diagram (Fig. 70).

The variation of 12 minor elements with increasing silica content (Fig. 71) show distinct differences in their distribution between the mafic and felsic suites. Zr, Y, Rb, Nb, and La are strongly enriched in the felsic suite although they display considerable scatter above about 65% SiO_2. Zn and Cr exhibit a similar trend but there is considerable overlap between the two suites. Sr, V, Co, and Ni decrease abruptly between 45 and 55% silica and approach the limits of detection in the felsic suite. Ba increases abruptly between 45 and 55% silica and then declines to very low values in most of the felsic suite.

The Flank basalt is significantly enriched in Ni and Cr compared to basalts of the Tundra Mountain Volcanics.

Rare earth elements

REE analyses were made on representative rocks from both the mafic and felsic suites of the Ilgachuz Group (Table 4). Samples from the mafic suite include four basalts from the Tundra Mountain Volcanics and one from the Flank basalt, whereas those from the felsic suite include two comendites from the Dean River Volcanics, two comendites from the Carnlick Creek, Volcanics and one comendite from the Arnica Lake Volcanics.

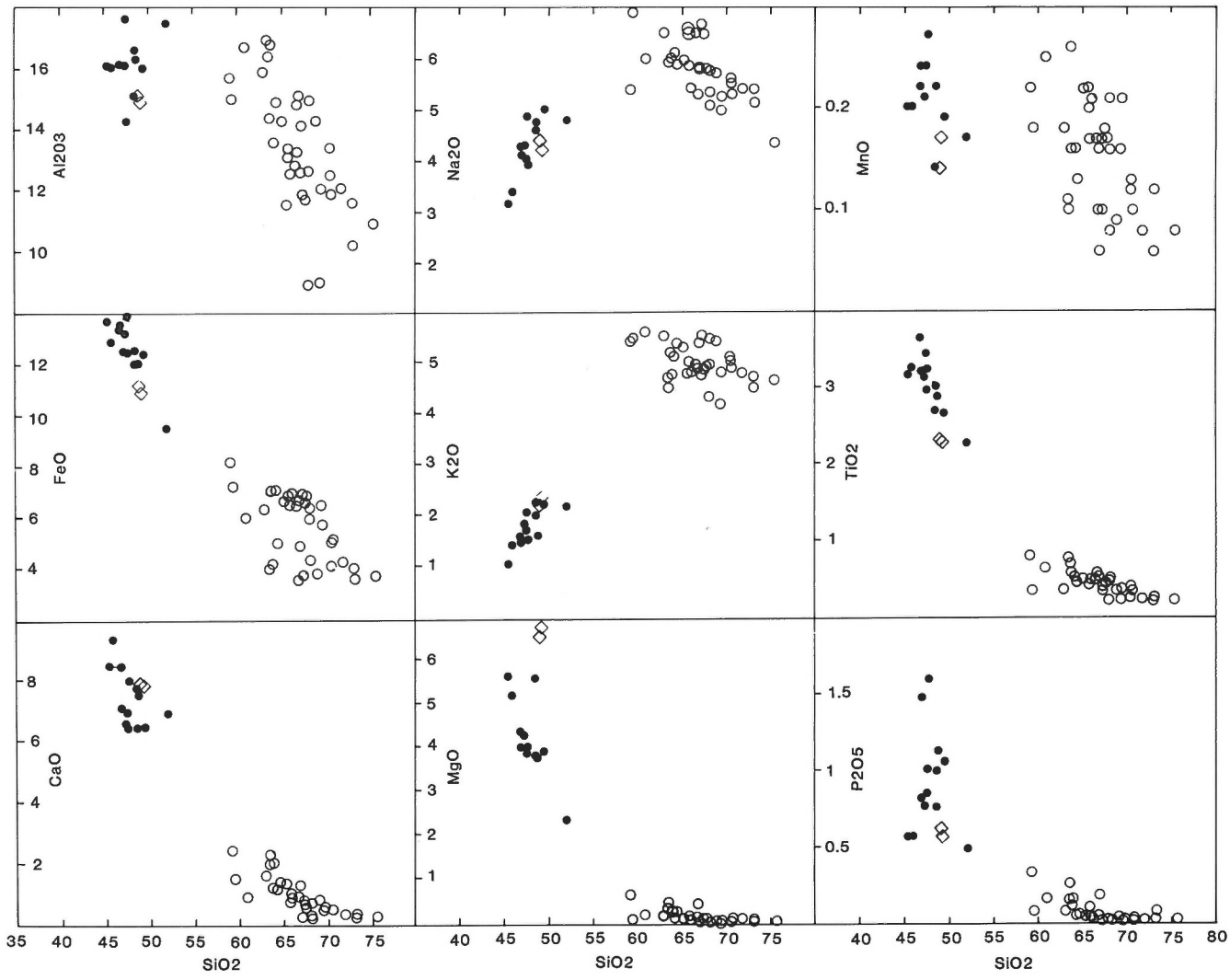

Figure 63. Harker diagram showing the variation in major-element abundances versus silica. (Ilgachuz Group felsic suite, open circles; Ilgachuz Group mafic suite, solid dots; Flank basalt, open diamonds).

Primitive mantle-normalized plots (Fig. 72) show moderate enrichment of light relative to heavy rare earths in both suites. The felsic suite is slightly more enriched in both heavy and light rare earths but, except for a pronounced negative europium anomaly, it is virtually parallel with the mafic suite plot.

Isotopes

Pb and Sr isotopic compositions of eight samples from the Ilgachuz Group (Table 5) were determined by M.L. Bevier as part of a broader study of isotopic variation along the entire Anahim Volcanic Belt (Bevier, 1989). Initial $^{87}Sr/^{86}Sr$ ratios of 0.7042-0.7031 for the Ilgachuz samples are consistent with low values for the belt as a whole. When plotted on a Rb-Sr isochron diagram, the Ilgachuz data give an initial ratio of 0.7032 and a date of 6.6 Ma which is slightly higher than the oldest K-Ar date (6.1 + 0.2 Ma) (Table 2). According to Bevier (1989), the initial Sr and Pb isotopic values (Table 5) for the Ilgachuz Range and adjacent Anahim Belt volcanoes are characteristic of depleted mantle, but the isotopic ratios are too radiogenic to represent a MORB source. Instead, Bevier (1989) argues that the ranges of values are most similar to those from oceanic islands and seamounts, specifically seamounts of the northeast Pacific Ocean.

Mineral chemistry

Microprobe analyses of the principal minerals in 19 selected samples from the Ilgachuz Group and one sample of Flank basalt were carried out by John Sterling of the Mineral Resources Division of the Geological Survey of Canada. A total of 586 analyses were done comprising 70 olivines,

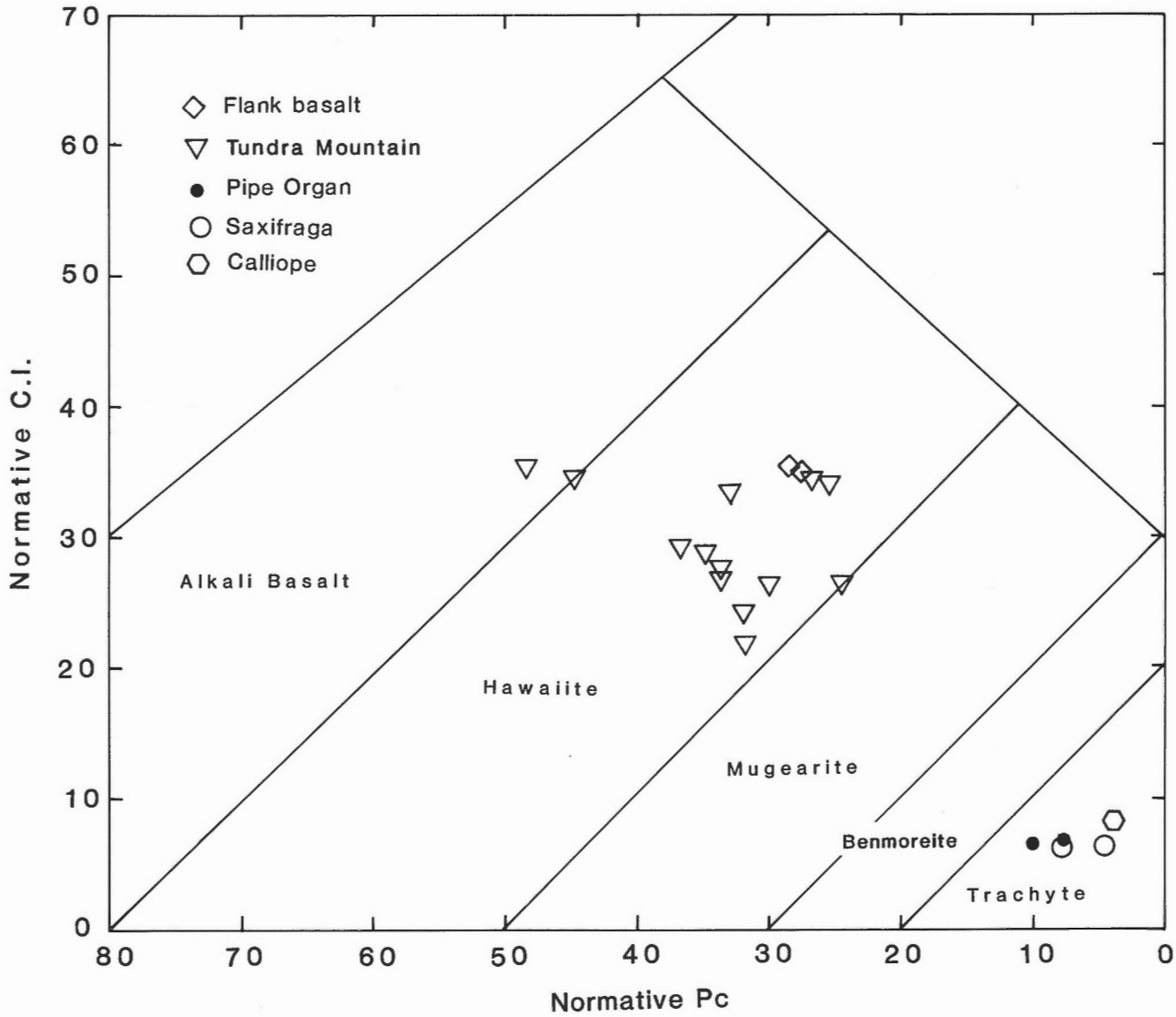

Figure 64. *Plot of normative colour index versus normative plagioclase composition showing the range of chemical variation among the Ilgachuz Group basalts and trachytes (normative An>0). Field boundaries after Irvine and Baragar (1971).*

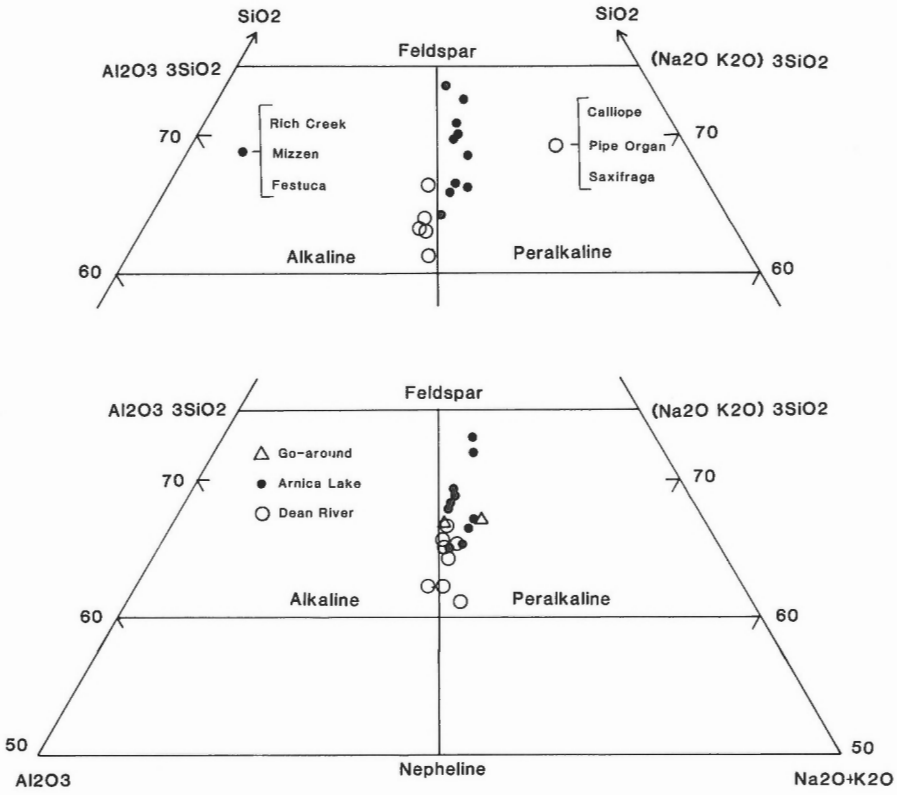

Figure 65. *Al_2O_3-SiO_2-(Na_2O+K_2O) plot showing the range of chemical variation among the Ilgachuz Group trachytes and rhyolites. Diagram adapted from Bailey and Macdonald (1969).*

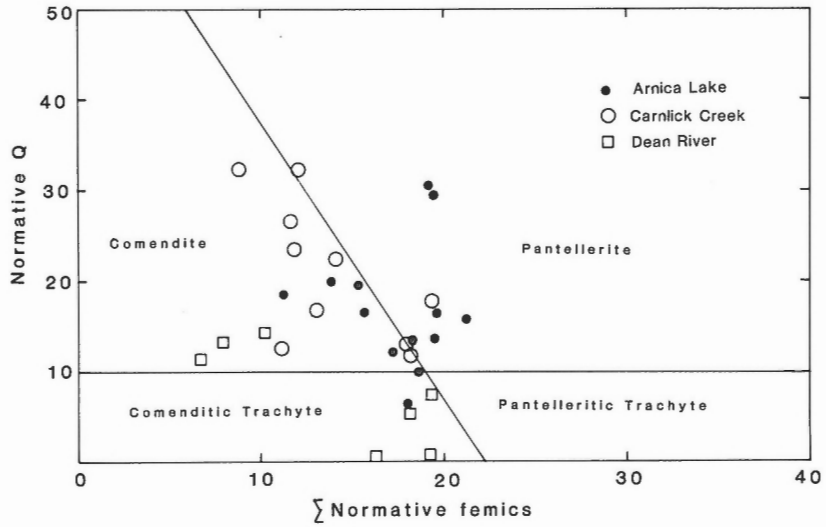

Figure 66. *Classification of the Ilgachuz Group peralkaline rocks using the normative quartz versus total femics diagram of Macdonald and Bailey (1973).*

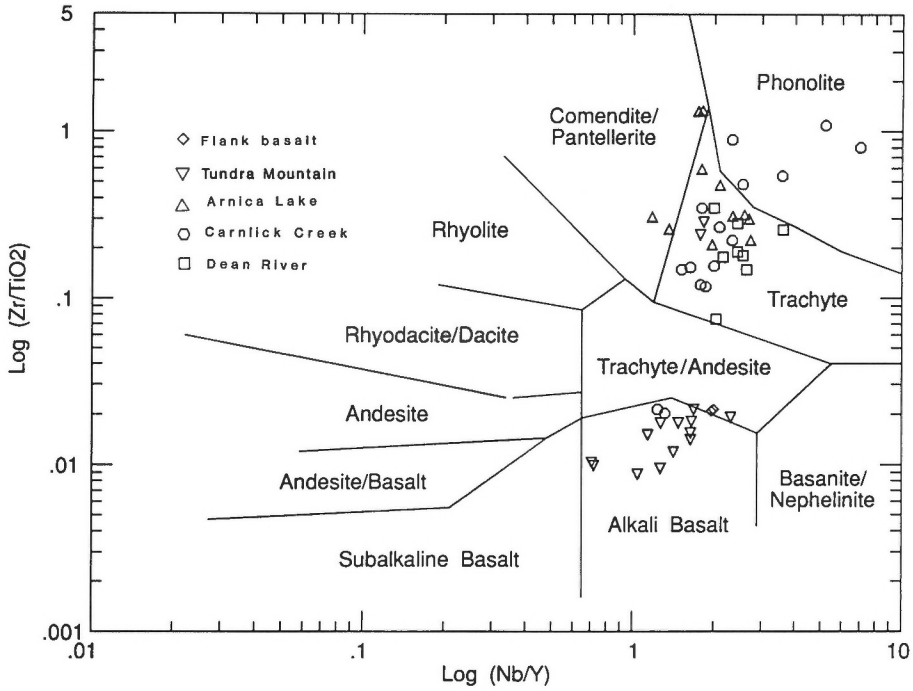

Figure 67. Plot showing the distribution of the Ilgachuz Group rocks on the Log (Zr/TiO_2) versus Log (Nb/Y) discriminant diagram of Winchester and Floyd (1977).

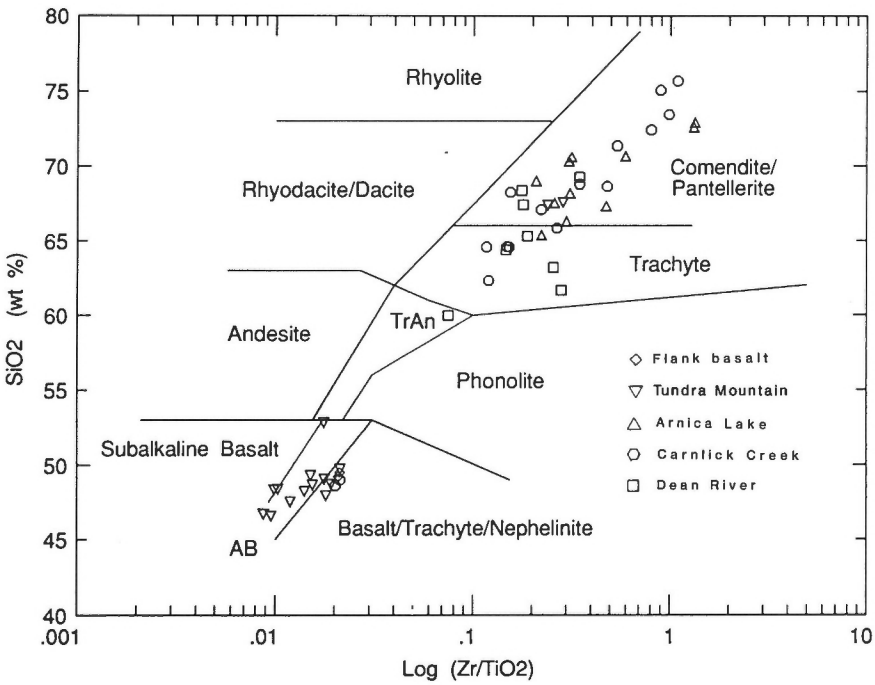

Figure 68. Plot showing the distribution of the Ilgachuz Group rocks on the SiO_2 versus Log (Zr/TiO_2) discriminant diagram of Winchester and Floyd (1977). TrAn = trachyendesite; AB = alkali basalt.

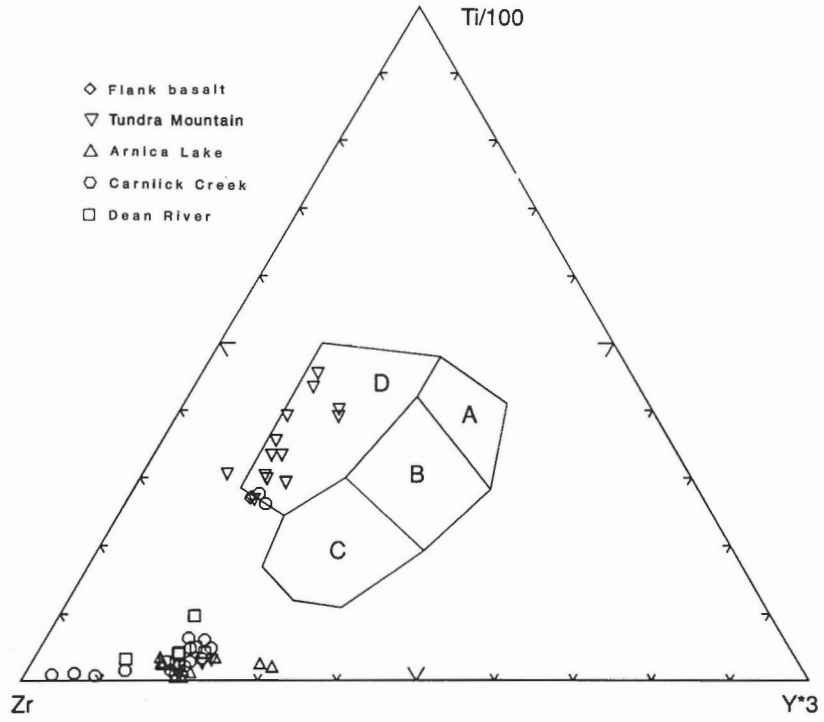

Figure 69. *Plot showing the distribution of the Ilgachuz Group rocks on the Zr-Ti/100-Y*3 discriminant diagram of Pearce and Cann (1973). Within-plate basalts (field D), ocean-floor basalts (field B), low-potassium tholeiites (fields A and B), calc-alkali basalts (fields C and B).*

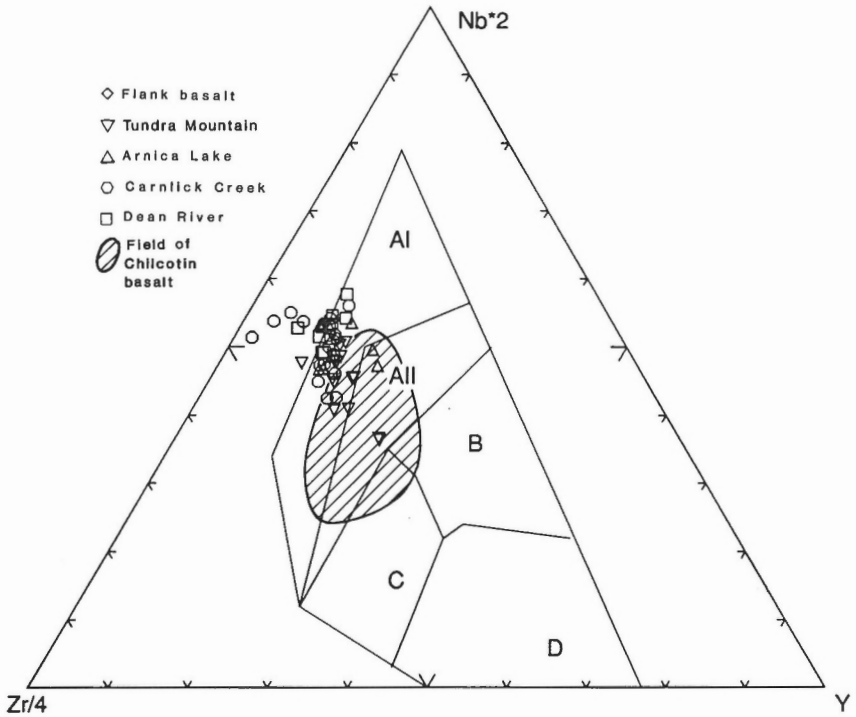

Figure 70. *Plot showing the distribution of the Ilgachuz Group rocks on the Zr/4-Nb*2-Y discriminant diagram of Meschede (1986). Within-plate alkali basalts (fields AI and AII), within-plate tholeiites (fields AII and C), P-type MORB (field B), N-type MORB (field D), volcanic arc basalts (fields C and D). Field of Chilcotin Group basalt from Bevier (1983b).*

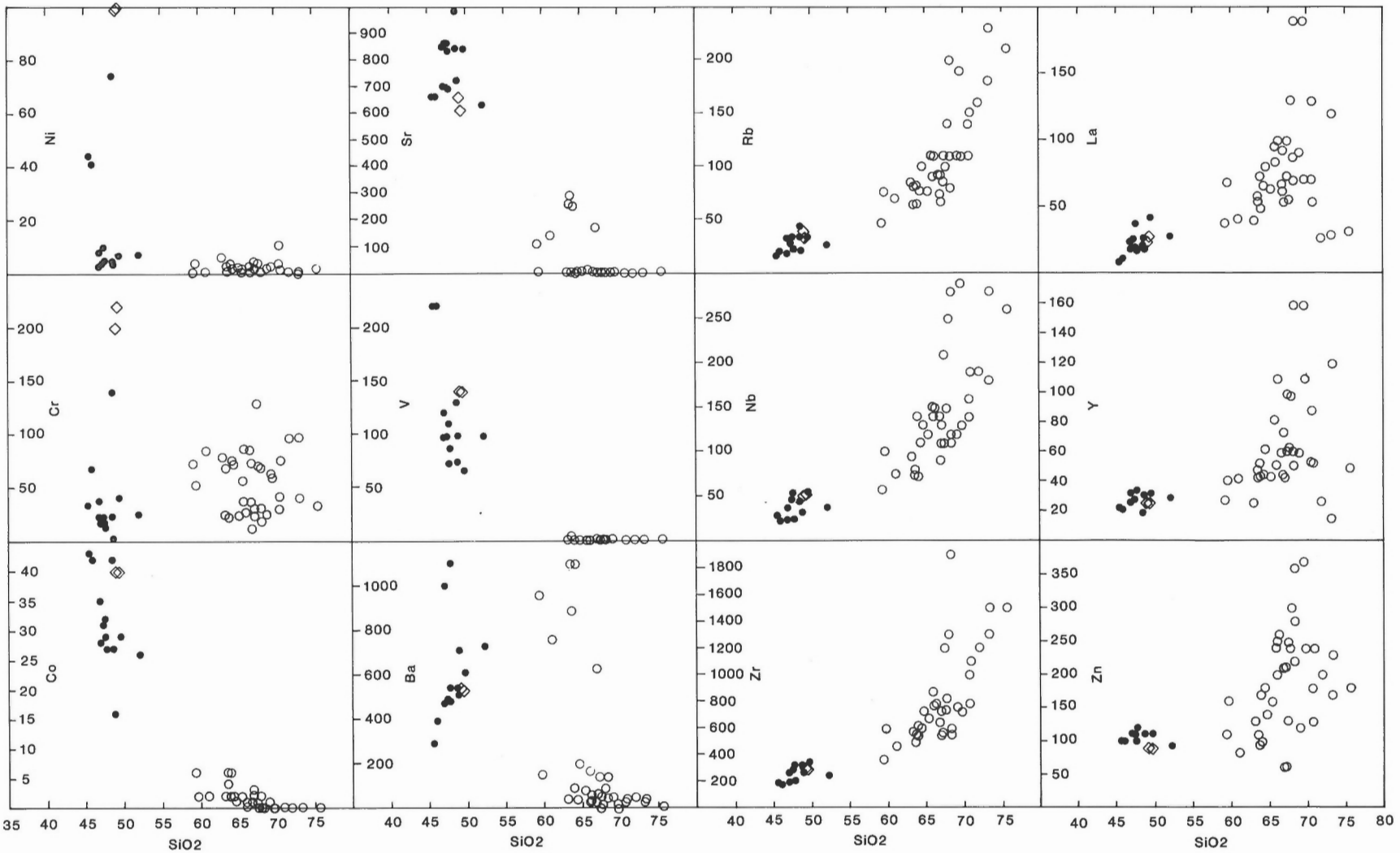

Figure 71. *Plot of minor elements versus silica of Ilgachuz Group rocks. Felsic suite, open circles; mafic suite, solid dots; Flank basalt, diamonds.*

Table 5. Isotope data (from Bevier, 1989).

Sample No.	Rock type	$^{208}Pb/^{204}Pb$	$^{207}Pb/^{204}Pb$	$^{208}Pb/^{204}Pb$	Rb (ppm)	Sr (ppm)	$^{87}Rb/^{86}Sr$	$^{87}Sr/^{86}Sr_m$	$^{87}Sr/^{86}Sr_i$
SE021383	haw	19.181	15.582	38.411	21.6	637	0.099	0.70331 = 3	0.70331
SE031083	com	18.957	15.582	38.425	100.7	9.3	31.39	0.70636 = 6	0.70369
SE101483	com	18.873	15.596	38.467	101.6	3.4	86.40	0.71161 = 3	0.70425
SE120383	com	18.962	15.578	38.411	69.8	12.3	16.37	0.70447 = 2	0.70308
SE120883	haw	18.984	15.571	38.345	31.5	751	0.021	0.70307 = 4	0.70307
SE120183	haw	18.990	15.604	38.436	27.0	789	0.099	0.70310 = 4	0.70310
SE030783	haw	18.916	15.585	38.396	19.6	694	0.081	0.70346 = 5	0.70346
SE070783	haw	18.929	15.589	38.415	29.5	527	0.161	0.70330 = 3	0.70330

Note: All errors are 2 S.E. ($2\alpha/\sqrt{n}$)
haw = hawaiite
com = comendite

187 pyroxenes, 104 plagioclases, 211 alkali feldspars, 8 sodic amphiboles, and 6 aenigmatites (Souther and Souther, 1994). End members from all of the olivine, pyroxene, and feldspar analyses are plotted on Figures 73-75, and representative analyses and structural formula data are listed in Table 6.

The mafic and felsic suites are characterized by distinct mineral assemblages, reflecting the same bimodal distribution as that defined by the whole rock chemistry.

Olivine

The olivine analyses fall into four groups (Fig. 73). The most magnesian olivines (Fo82-Fo85) occur in the Pliocene or younger Flank basalt. This is consistent with the whole rock analyses, which show the Flank basalt to have a higher content of MgO, Ni, and Cr than any of the Ilgachuz Group rocks.

A second group of slightly less magnesian olivines (Fo56-Fo78) is characteristic of the Tundra Mountain basalts. Olivines in this group are fairly uniformly distributed across the entire range of variation and show a slight increase in Ca content with decreasing Fo.

A third group of Fe-olivines (Fo0-Fo6) is confined to the felsic suite of Ilgachuz Group rocks. These olivines are relatively calcic and show a slight increase in Ca content with decreasing age – olivines in the Dean River being least calcic and those in the Go-around rhyolite being the most calcic.

A fourth group of olivines with intermediate compositions (Fo24-Fo37) are from the Pipe Organ trachyte and a highly porphyritic phase of the North Rift basalt. On the basis of their textures and mineralogy, both of these rocks were interpreted to be of cumulus origin.

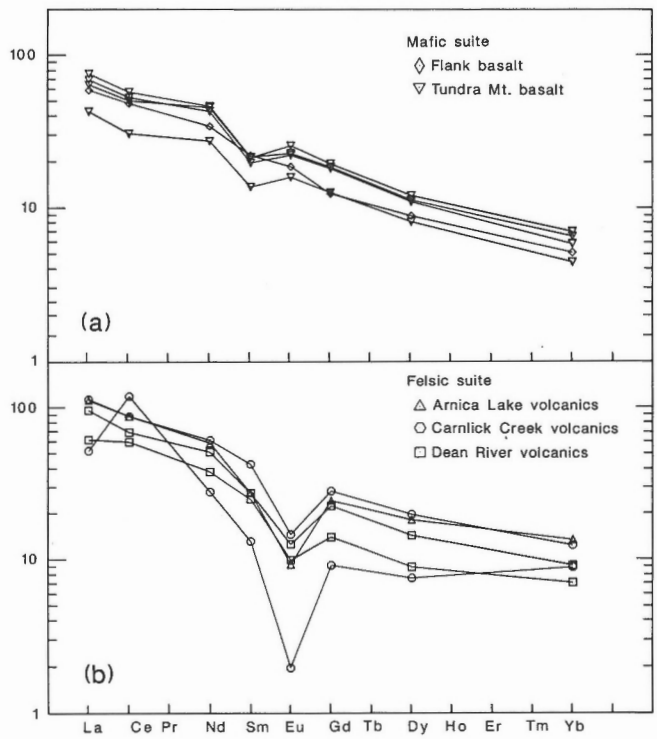

*Figure 72. Primitive mantle-normalized REE profiles of the Ilgachuz Group basalts (**a**), and felsic rocks (**b**). Normalization values from Taylor and McLennan (1985).*

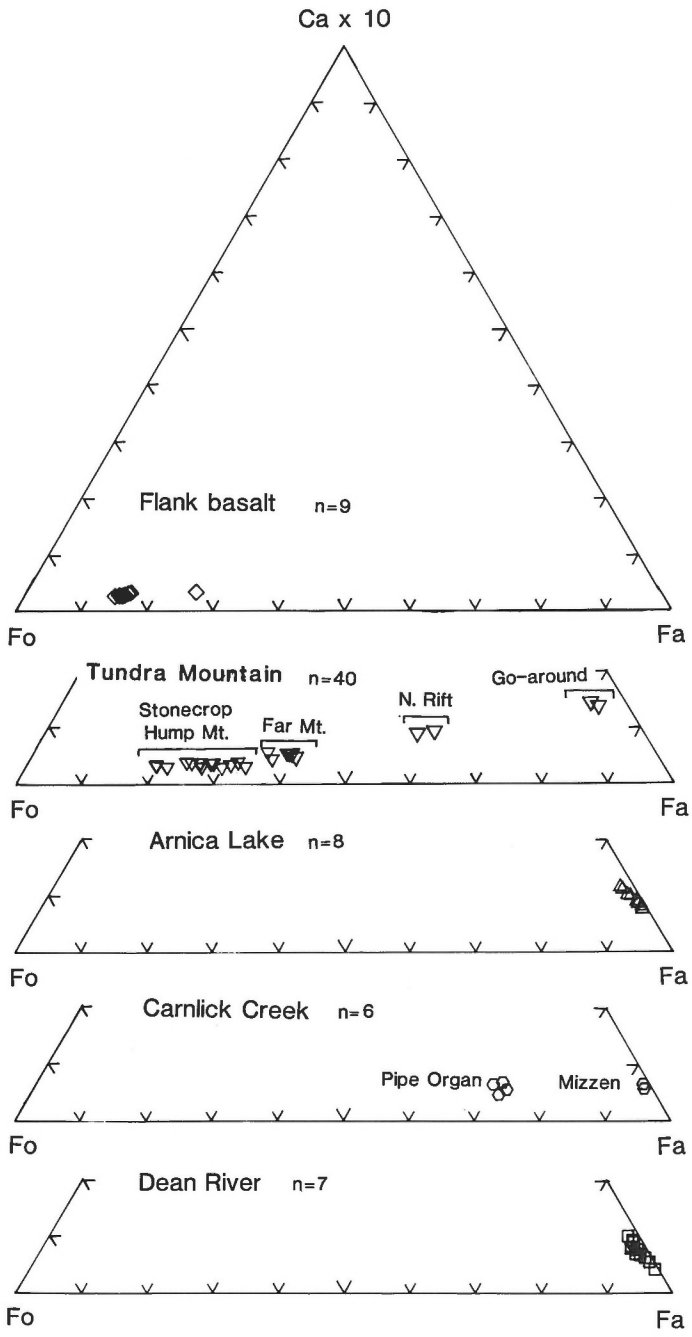

Figure 73. End-member plots showing variation in the composition of olivines from formations of the Ilgachuz Group.

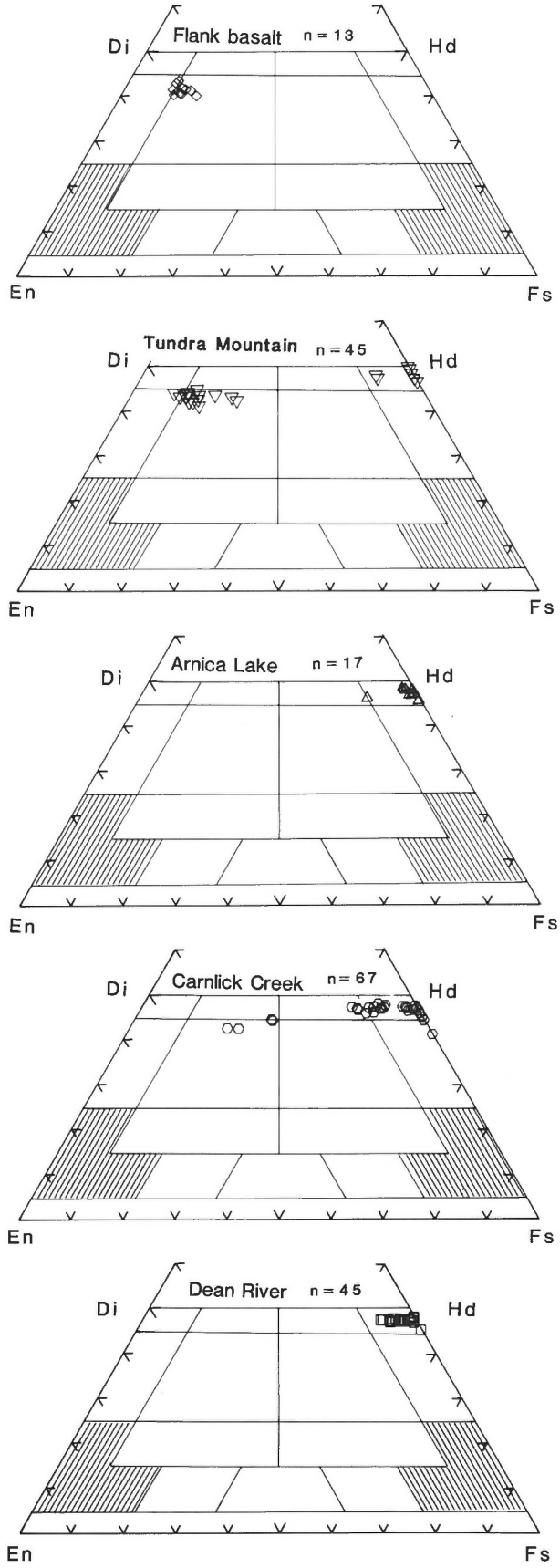

Figure 74. End-member plots showing variation in the composition of pyroxenes from formations of the Ilgachuz Group.

Pyroxene

Pyroxene analyses from the Ilgachuz Group form two distinct populations (Fig. 74). Those from the Tundra Mountain and Flank basalts are almost all calcic augites. Although their fields overlap, pyroxenes from the Flank basalt tend to be more magnesian than those from the Tundra Mountain basalt.

Pyroxenes from the felsic suite plot almost entirely within the hedenbergite field. Some of those on or near the Fs-Hd join (Fig. 74) contain significant Na and should be classified as aegirine. Pyroxenes with the highest NaFe content are most abundant in the older (Dean River) rocks. Those from the younger Carnlick Creek Volcanics have a wider range of compositions and include magnesian hedenbergites and a few augites. The latter are confined to the Pipe Organ trachyte.

Feldspar

A total of 102 feldspars from basalts in the Tundra Mountain Volcanics and two from the Flank basalt were analyzed (Fig. 75). All but four of the Tundra Mountain plagioclases are low-K_2O labradorite, indicating a very narrow range of feldspar compositions within the mafic suite of Ilgachuz Group rocks. However, the two analyzed feldspars from the Flank basalt are significantly more potassic. This difference is consistent with the whole rock analyses, which show the Flank basalt to be among the most potassic rocks of the mafic suite (Fig. 63).

Feldspars from the felsic suite of Ilgachuz Group rocks range from sodic sanidine through the complete range of anorthoclase compositions. There is a distinct trend from relatively high-K_2O feldspars (sanidine) in the Dean River and Arnica Lake volcanics to less potassic anorthoclases in the more highly fractionated Carnlick Creek Volcanics and Go-around rhyolite.

Amphibole and aenigmatite

End members were not calculated for the eight analyzed sodic amphiboles and six aenigmatites. The microprobe analyses and structural formula data are listed in Table 6.

ORIGIN OF THE ILGACHUZ RANGE PERALKALINE SHIELD AND FLANK BASALT

Discussion

Oversaturated peralkaline rocks are almost exclusively associated with intraplate volcanism in areas of crustal extension or hotspot activity. Petrogenesis of these rocks, however, is

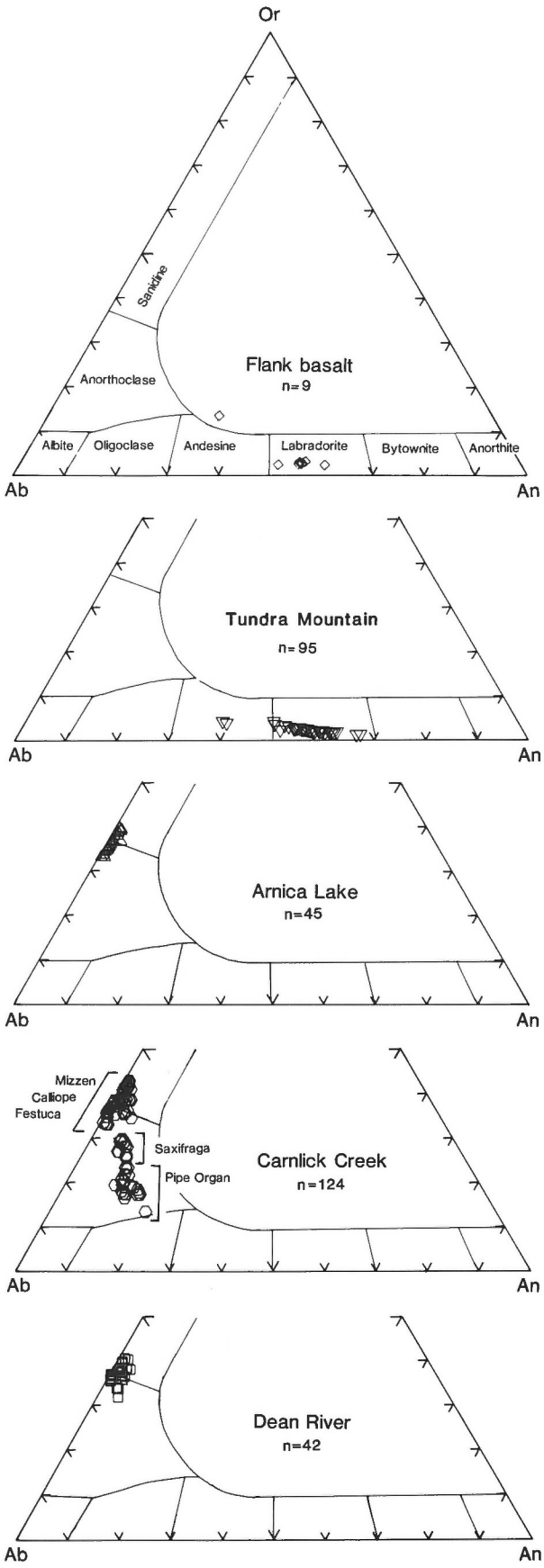

Figure 75. End-member plots showing variation in the composition of feldspars from formations of the Ilgachuz Group.

Table 6. Representative mineral analyses from rocks of the Ilgachuz Group and Flank basalt. Olivine (OL), clinopyroxene (CPX), plagioclase (PL), alkali feldspar (KF), amphibole (AF). Where possible the location of the area probed is given by C (core), R (rim), M (middle), or G (groundmass). Analyses of small grains are given without references to location of spot probed.

OLIVINE

	89-54 Dean R. OL-R	89-54 Dean R. OL-C	89-54 Dean R. OL-M	89-37 Pipe Org. OL-R	89-37 Pipe Org. OL-C	SE270385 Mizzen OL-R	SE270385 Mizzen OL-C	SE101483 Arnica OL-R	SE101483 Arnica OL-C	SE050183 Stonecrop OL	SE050183 Stonecrop OL
SiO_2	30.02	29.69	30.08	31.09	31.06	29.15	29.35	29.16	29.03	36.45	36.53
MgO	0.27	0.37	0.35	10.06	10.01	0.33	0.40	0.27	0.30	36.37	36.39
FeO	67.20	66.57	67.39	54.67	55.31	66.83	66.20	65.36	65.07	24.34	24.79
MnO	3.20	3.14	3.24	3.07	2.98	2.90	2.96	3.74	3.88	0.45	0.41
CaO	0.34	0.33	0.39	0.44	0.36	0.38	0.34	0.47	0.56	0.21	0.24
NiO	0.03	0.06	0.00	0.00	0.00	0.01	0.06	0.02	0.00	0.05	0.05
Total	101.06	100.16	101.45	99.33	99.72	99.60	99.31	99.02	98.84	97.87	98.41
Formula (Basis 4 Oxygens)											
Si	1.003	1.001	1.001	0.987	0.984	0.992	0.999	0.996	0.994	0.984	0.983
Mg	0.013	0.019	0.017	0.476	0.473	0.017	0.021	0.014	0.015	1.464	1.459
Fe	1.877	1.877	1.876	1.452	1.466	1.902	1.883	1.868	1.864	0.550	0.558
Mn	0.091	0.090	0.091	0.083	0.080	0.084	0.085	0.108	0.113	0.010	0.009
Ca	0.012	0.012	0.014	0.015	0.012	0.014	0.012	0.017	0.020	0.006	0.007
Ni	0.001	0.002	0.000	0.000	0.000	0.000	0.002	0.000	0.000	0.001	0.001
Z	1.003	1.001	1.001	0.987	0.984	0.992	0.999	0.996	0.994	0.984	0.983
X	1.994	2.000	1.998	2.026	2.031	2.017	2.003	2.007	2.012	2.031	2.034
Fo	0.66	0.96	0.86	23.67	23.43	0.85	1.05	0.70	0.75	72.30	71.98
Fa	94.70	94.42	94.56	72.20	72.61	94.96	94.58	93.87	93.57	27.16	27.53
Ni-Ol	0.05	0.10	0.00	0.00	0.00	0.00	0.10	0.00	0.00	0.05	0.05
Mn-Ol	4.59	4.53	4.59	4.13	3.96	4.19	4.27	5.43	5.67	0.49	0.44

CLINOPYROXENE

	89-53 Dean R. CPX-C	89-54 Dean R. CPX-R	89-37 Pipe Org. CPX-R	89-37 Pipe Org. CPX-C	89-67 Calliope CPX-R	89-67 Calliope CPX-C	SE270385 Mizzen CPX-R	SE270385 Mizzen CPX-C	89-8 Festuca CPX-R	89-8 Festuca CPX-C	SE101483 Arnica CPX-R
SiO_2	48.78	48.62	49.52	49.42	47.40	47.53	48.16	48.41	46.94	46.98	47.70
Al_2O_3	0.56	0.57	0.80	0.95	0.20	0.17	0.20	0.22	0.51	0.56	0.25
Fe_2O_3	0.05	0.98	3.29	3.39	5.69	5.33	2.94	3.01	2.86	3.22	2.83
TiO_2	0.71	0.72	0.47	0.52	0.33	0.30	0.40	0.44	0.55	0.58	0.45
Cr_2O_3	0.01	0.03	0.01	0.08	0.01	0.05	0.01	0.00	0.00	0.07	0.00
MgO	2.13	1.98	9.42	9.32	0.06	0.06	0.79	0.79	2.66	3.25	0.56
FeO	26.56	25.97	14.33	14.39	24.66	25.20	26.79	26.58	23.12	22.62	26.62
MnO	1.05	1.17	0.97	0.79	1.04	1.15	1.02	1.13	1.19	1.10	1.35
CaO	20.08	20.37	19.84	20.11	16.82	16.97	18.84	19.15	19.77	19.65	19.37
Na_2O	0.39	0.42	0.47	0.43	2.05	1.92	0.98	0.99	0.48	0.44	0.79
Total	100.32	100.83	99.12	99.40	98.26	98.68	100.13	100.72	98.08	98.47	99.92
Formula (Basis 12 Oxygens)											
Si	3.958	3.932	3.873	3.856	3.959	3.959	3.953	3.949	3.890	3.868	3.935
Al	0.042	0.055	0.074	0.087	0.019	0.017	0.020	0.022	0.049	0.055	0.024
Fe^{+3}	0.000	0.013	0.053	0.057	0.022	0.024	0.027	0.029	0.061	0.077	0.041
	4.000	4.000	4.000	4.000	4.000	4.000	4.000	4.000	4.000	4.000	4.000
Al	0.012	0.000	0.000	0.000	0.000	0.000	0.000	0.000	0.000	0.000	0.000
Fe^{+3}	0.003	0.047	0.140	0.142	0.336	0.310	0.155	0.156	0.118	0.122	0.135
Ti	0.043	0.044	0.028	0.031	0.021	0.019	0.025	0.027	0.034	0.036	0.028
Cr	0.001	0.002	0.000	0.005	0.001	0.003	0.001	0.000	0.000	0.005	0.000
Mg	0.258	0.239	1.098	1.084	0.007	0.008	0.096	0.096	0.329	0.400	0.069
Fe^{+2}	1.683	1.668	0.734	0.738	1.635	1.660	1.723	1.721	1.519	1.437	1.768
Mn	0.000	0.000	0.000	0.000	0.000	0.000	0.000	0.000	0.000	0.000	0.000
	2.000	2.000	2.000	2.000	2.000	2.000	2.000	2.000	2.000	2.000	2.000
Mg	0.000	0.000	0.000	0.000	0.000	0.000	0.000	0.000	0.000	0.000	0.000
Fe^{+2}	0.120	0.088	0.203	0.201	0.088	0.095	0.116	0.092	0.083	0.121	0.068
Mn	0.073	0.080	0.065	0.052	0.074	0.081	0.071	0.078	0.083	0.077	0.094
Ca	1.746	1.765	1.662	1.681	1.505	1.514	1.657	1.674	1.756	1.734	1.712
Na	0.061	0.066	0.071	0.065	0.332	0.310	0.156	0.157	0.077	0.070	0.127
	2.000	1.999	2.001	1.999	1.999	2.000	2.000	2.001	1.999	2.002	2.001
Wo	41.83	42.55	37.41	37.50	35.55	35.82	39.69	39.95	40.49	38.73	40.10
En	4.39	3.79	24.79	24.73	0.00	0.00	0.59	0.41	5.78	7.61	0.00
Fs	43.16	42.29	22.51	22.52	41.40	42.17	44.78	44.02	37.85	36.88	44.03
Jd	2.27	0.00	0.00	0.00	0.00	0.00	0.00	0.00	0.00	0.00	0.00
Ae	0.57	3.09	3.35	3.05	15.78	14.75	7.48	7.51	3.57	3.24	5.99
Ka	3.57	3.94	3.17	2.53	3.60	3.94	3.50	3.84	3.99	3.71	4.58
Jo	0.00	0.00	0.00	0.00	0.00	0.00	0.00	0.00	0.00	0.00	0.00
S3-Al	0.00	0.00	0.00	0.00	0.00	0.00	0.00	0.00	0.00	0.00	0.00
S3-Fe	0.00	0.00	6.05	6.64	1.63	1.48	1.49	1.61	5.04	6.36	2.57
S4-Fe	3.55	3.68	1.20	1.35	1.67	1.53	2.14	2.31	2.60	2.66	2.45
S4-Mg	0.51	0.50	1.41	1.56	0.01	0.01	0.11	0.12	0.53	0.68	0.09
S2-Fe	0.12	0.14	0.05	0.05	0.37	0.31	0.20	0.22	0.11	0.11	0.18
S2-Mg	0.02	0.02	0.06	0.06	0.00	0.00	0.01	0.01	0.02	0.03	0.01

OLIVINE

	SE021383 N. Rift OL-R	SE021383 N. Rift OL-C	89-48 Hump Mt. OL-R	89-48 Hump Mt. OL-C	SE020783 Go-around OL-R	SE020783 Go-around OL-C	SE021083 Far Mt. OL-C	SE021083 Far Mt. OL-C	89-4 Flank Bt. OL-R	89-4 Flank Bt. OL-C
SiO_2	32.78	32.76	37.04	38.07	29.40	29.45	35.23	35.26	38.46	38.97
MgO	16.70	15.23	33.36	37.99	2.03	2.34	27.83	28.66	44.65	45.67
FeO	47.55	49.16	29.25	23.83	63.41	63.55	35.43	35.14	15.00	14.14
MnO	1.56	1.88	0.46	0.34	3.35	3.27	0.95	0.81	0.22	0.19
CaO	0.59	0.63	0.28	0.28	0.85	0.91	0.35	0.39	0.24	0.21
NiO	0.00	0.08	0.05	0.09	0.04	0.19	0.00	0.00	0.23	0.36
Total	99.18	99.74	100.44	100.60	99.08	99.71	99.79	100.26	98.80	99.54
Formula (Basis 4 Oxygens)										
Si	0.992	0.995	0.994	0.993	0.991	0.986	0.987	0.981	0.982	0.983
Mg	0.753	0.690	1.335	1.477	0.102	0.117	1.162	1.189	1.700	1.718
Fe	1.203	1.249	0.657	0.520	1.788	1.780	0.830	0.818	0.320	0.298
Mn	0.040	0.048	0.010	0.008	0.096	0.093	0.023	0.019	0.005	0.004
Ca	0.019	0.020	0.008	0.008	0.031	0.033	0.010	0.012	0.007	0.006
Ni	0.000	0.002	0.001	0.002	0.001	0.005	0.000	0.000	0.005	0.007
Z	0.992	0.995	0.994	0.993	0.991	0.986	0.987	0.981	0.982	0.983
X	2.015	2.009	2.011	2.015	2.018	2.028	2.025	2.038	2.037	2.033
Fo	37.73	34.69	66.65	73.59	5.13	5.86	57.67	58.69	83.74	84.76
Fa	60.27	62.80	32.80	25.91	89.98	89.22	41.19	40.38	15.76	14.70
Ni-Ol	0.00	0.10	0.05	0.10	0.05	0.25	0.00	0.00	0.25	0.35
Mn-Ol	2.00	2.41	0.50	0.40	4.83	4.66	1.14	0.94	0.25	0.20

CLINOPYROCENE

	SE101483 Arnica CPX-C	SE050183 Stonecrop CPX-R	SE050183 Stonecrop CPX-C	SE021383 N. Rift CPX-R	SE021383 N. Rift CPX-C	89-48 Hump Mt. CPX-R	89-48 Hump Mt. CPX-C	SE020783 Go-around CPX-C	SE020783 Go-around CPX-R	89-4 Flank Bt. CPX-C	89-4 Flank Bt. CPX-R
SiO_2	47.55	49.64	47.46	49.76	50.79	47.65	50.98	46.71	47.22	45.50	44.52
Al_2O_3	0.27	2.40	3.82	3.40	2.74	5.23	2.30	0.58	0.28	7.38	7.75
Fe_2O_3	2.16	2.57	3.74	2.17	1.97	3.11	2.13	2.91	2.55	4.34	4.57
TiO_2	0.56	1.77	2.62	1.69	1.37	2.45	1.11	0.67	0.46	2.11	3.10
Cr_2O_3	0.06	0.01	0.04	0.00	0.00	0.04	0.00	0.04	0.01	0.05	0.22
MgO	0.82	13.88	12.90	14.18	14.33	13.17	15.06	2.81	0.35	12.96	12.17
FeO	26.71	7.44	6.33	6.79	7.55	5.61	7.10	22.96	26.53	4.59	4.89
MnO	1.54	0.28	0.21	0.22	0.38	0.16	0.15	1.25	1.26	0.15	0.15
CaO	19.28	20.76	21.38	20.88	20.70	21.27	20.35	19.59	18.58	19.78	20.85
Na_2O	0.62	0.41	0.47	0.42	0.43	0.57	0.39	0.46	0.99	0.66	0.56
Total	99.57	99.16	98.97	99.51	100.26	99.26	99.57	97.98	98.23	97.52	98.78
Formula (Basis 12 Oxygens)											
Si	3.934	3.749	3.606	3.725	3.779	3.583	3.805	3.875	3.958	3.471	3.380
Al	0.027	0.214	0.342	0.275	0.221	0.417	0.195	0.056	0.028	0.529	0.620
Fe^{+3}	0.039	0.037	0.052	0.000	0.000	0.000	0.000	0.069	0.014	0.000	0.000
	4.000	4.000	4.000	4.000	4.000	4.000	4.000	4.000	4.000	4.000	4.000
Al	0.000	0.000	0.000	0.025	0.019	0.047	0.007	0.000	0.000	0.134	0.073
Fe^{+3}	0.095	0.109	0.162	0.122	0.110	0.176	0.119	0.113	0.147	0.249	0.261
Ti	0.035	0.101	0.150	0.095	0.077	0.139	0.062	0.042	0.029	0.121	0.177
Cr	0.004	0.001	0.002	0.000	0.000	0.003	0.000	0.002	0.001	0.003	0.013
Mg	0.102	1.562	1.461	1.582	1.589	1.476	1.675	0.347	0.044	1.474	1.377
Fe^{+2}	1.764	0.227	0.225	0.176	0.205	0.159	0.137	1.496	1.779	0.019	0.099
Mn	0.000	0.000	0.000	0.000	0.000	0.000	0.000	0.000	0.000	0.000	0.000
	2.000	2.000	2.000	2.000	2.000	2.000	2.000	2.000	2.000	2.000	2.000
Mg	0.000	0.000	0.000	0.000	0.000	0.000	0.000	0.000	0.000	0.000	0.000
Fe^{+2}	0.084	0.243	0.177	0.249	0.265	0.194	0.306	0.097	0.081	0.274	0.211
Mn	0.108	0.018	0.013	0.014	0.024	0.010	0.010	0.088	0.089	0.010	0.010
Ca	1.709	1.680	1.740	1.675	1.650	1.713	1.627	1.741	1.669	1.617	1.696
Na	0.100	0.060	0.070	0.061	0.062	0.083	0.057	0.073	0.161	0.098	0.082
	2.001	2.001	2.000	1.999	2.001	2.000	2.000	1.999	2.000	1.999	1.999
Wo	40.95	35.08	32.85	35.00	35.72	32.42	36.21	39.10	39.91	27.25	27.12
En	0.00	35.99	32.44	37.34	37.63	33.88	40.14	6.08	0.00	34.10	30.62
Fs	43.94	10.96	9.01	10.13	11.31	8.16	10.68	37.70	44.96	6.83	6.95
Jd	0.00	0.00	0.00	0.46	0.42	0.74	0.15	0.00	0.00	1.47	0.72
Ae	4.65	2.60	2.85	2.26	2.41	2.77	2.48	3.37	7.65	2.74	2.57
Ka	5.23	0.88	0.63	0.70	1.20	0.50	0.50	4.26	4.37	0.50	0.50
Jo	0.00	0.00	0.00	0.00	0.00	0.00	0.00	0.00	0.00	0.00	0.00
S3-Al	0.00	0.00	0.00	0.76	0.53	1.59	0.25	0.00	0.00	5.28	3.29
S3-Fe	1.83	4.56	7.59	3.85	3.09	6.04	3.43	5.44	0.25	9.72	10.50
S4-Fe	3.03	2.21	3.03	1.94	1.69	2.56	1.24	3.20	2.54	1.89	3.11
S4-Mg	0.17	7.36	11.03	7.23	5.73	10.71	4.71	0.70	0.06	9.52	13.81
S2-Fe	0.18	0.08	0.12	0.07	0.06	0.12	0.04	0.13	0.24	0.11	0.15
S2-Mg	0.01	0.26	0.44	0.26	0.22	0.52	0.16	0.03	0.01	0.58	0.67

Table 6. (cont.)

PLAGIOCLASE	89-23 Festuca PL-R	89-23 Festuca PL-C	89-23 Festuca PL-R	89-23 Festuca PL-C	SE050183 Stonecrop PL	SE050183 Stonecrop PL	SE050183 Stonecrop PL-R	SE050183 Stonecrop PL-C	SE021383 N. Rift PL-R	SE021383 N. Rift PL-C
SiO_2	54.43	54.21	65.10	64.49	53.06	53.51	52.53	51.92	57.26	52.37
Al_2O_3	27.99	27.86	20.07	20.09	27.89	27.55	27.71	28.03	25.27	28.50
Na_2O	5.31	5.27	7.25	7.09	4.88	5.20	4.86	4.68	6.58	4.46
CaO	10.63	10.53	1.09	1.29	11.32	10.96	11.25	11.72	7.87	11.90
K_2O	0.43	0.43	6.01	5.88	0.33	0.38	0.36	0.32	0.73	0.32
BaO	0.05	0.00	0.29	0.54	0.04	0.10	0.03	0.01	0.00	0.00
SrO	0.16	0.31	0.04	0.00	0.10	0.15	0.12	0.30	0.26	0.20
FeO	0.41	0.47	0.30	0.23	0.51	0.48	0.58	0.46	0.58	0.54
Total	99.41	99.08	100.15	99.61	98.13	98.33	97.44	97.44	98.55	98.29
Formula (Basis 32 Oxygens)										
Si	9.917	9.917	11.697	11.665	9.816	9.882	9.796	9.701	10.463	9.688
Al	6.012	6.008	4.250	4.283	6.080	5.996	6.090	6.174	5.444	6.214
	15.929	15.925	15.947	15.948	15.896	15.878	15.886	15.875	15.907	15.902
Na	1.876	1.870	2.526	2.488	1.749	1.860	1.757	1.697	2.333	1.601
Ca	2.076	2.064	0.209	0.250	2.243	2.169	2.247	2.346	1.541	2.359
K	0.099	0.101	1.377	1.358	0.077	0.089	0.086	0.076	0.170	0.076
Ba	0.004	0.000	0.021	0.038	0.003	0.007	0.002	0.001	0.000	0.000
Sr	0.017	0.033	0.004	0.000	0.010	0.016	0.013	0.033	0.027	0.021
	4.072	4.068	4.137	4.134	4.082	4.141	4.105	4.153	4.071	4.057
Fe	0.063	0.071	0.045	0.034	0.079	0.074	0.090	0.073	0.088	0.084
Ab	46.07	45.97	61.06	60.18	42.85	44.92	42.80	40.86	57.31	39.46
An	50.98	50.74	5.05	6.05	54.95	52.38	54.74	56.49	37.85	58.15
Or	2.43	2.48	33.28	32.85	1.89	2.15	2.10	1.83	4.18	1.87
Ba	0.10	0.00	0.51	0.92	0.07	0.17	0.05	0.02	0.00	0.00
Sr	0.42	0.81	0.10	0.00	0.24	0.39	0.32	0.79	0.66	0.52

ALKALI FELDSPAR	89-12 Dean R. KF-R	89-12 Dean R. KF-C	89-37 Pipe Org. KF	89-37 Pipe Org. KF	89-67 Calliope KF-R	89-67 Calliope KF-C	SE270385 Mizzen KF	SE270385 Mizzen KF	89-39 Saxifraga KF	89-39 Saxifraga KF
SiO_2	66.29	65.82	64.02	62.72	65.43	65.62	66.65	66.48	63.35	63.58
Al_2O_3	18.71	18.20	20.92	21.58	17.82	17.97	18.23	18.20	21.05	20.75
Na_2O	7.36	7.24	7.96	7.97	7.53	7.57	7.58	7.62	8.02	8.01
CaO	0.03	0.04	2.19	2.90	0.00	0.01	0.04	0.04	2.60	2.42
K_2O	6.64	6.62	3.85	3.17	6.24	6.15	6.33	6.41	2.95	3.17
BaO	0.05	0.00	0.21	0.33	0.00	0.00	0.04	0.02	0.36	0.14
SrO	0.00	0.00	0.16	0.22	0.00	0.18	0.00	0.02	0.15	0.16
FeO	0.42	0.64	0.26	0.29	0.63	0.42	0.49	0.38	0.15	0.23
Total	99.50	98.56	99.57	99.18	97.65	97.92	99.36	99.17	98.63	98.46
Formula (Basis 32 Oxygens)										
Si	11.955	11.992	11.513	11.342	12.020	12.017	12.024	12.019	11.472	11.523
Al	3.978	3.908	4.436	4.601	3.859	3.879	3.877	3.878	4.493	4.434
	15.933	15.900	15.949	15.943	15.879	15.896	15.901	15.897	15.965	15.957
Na	2.575	2.559	2.776	2.794	2.683	2.688	2.650	2.672	2.817	2.813
Ca	0.006	0.008	0.421	0.562	0.000	0.002	0.008	0.008	0.504	0.469
K	1.527	1.539	0.882	0.731	1.463	1.437	1.457	1.479	0.680	0.732
Ba	0.004	0.000	0.015	0.024	0.000	0.000	0.003	0.002	0.025	0.010
Sr	0.000	0.000	0.017	0.023	0.000	0.019	0.000	0.002	0.016	0.017
	4.112	4.106	4.111	4.134	4.146	4.146	4.118	4.163	4.042	4.041
Fe	0.063	0.097	0.039	0.044	0.097	0.064	0.074	0.057	0.023	0.035
Ab	62.62	62.32	67.53	67.59	64.71	64.83	64.35	64.18	69.69	69.61
An	0.15	0.19	10.24	13.59	0.00	0.05	0.19	0.19	12.47	11.61
Or	37.14	37.48	21.45	17.68	35.29	34.66	35.38	35.53	16.82	18.11
Ba	0.10	0.00	0.36	0.58	0.00	0.00	0.07	0.05	0.62	0.25
Sr	0.00	0.00	0.41	0.56	0.00	0.46	0.00	0.05	0.40	0.42

PLAGIOCLASE

	SE021383 N. Rift PL-R	SE021383 N. Rift PL-C	SE021083 Far Mt. PL-G	SE021083 Far Mt. PL-R	SE021083 Far Mt. PL-C	SE021083 Far Mt. PL-G	89-4 Flank Bt. PL-G	89-4 Flank Bt. PL-R	89-4 Flank Bt. PL-M	89-4 Flank Bt. PL-C
SiO_2	52.86	53.72	53.74	52.90	52.99	53.41	53.41	54.93	53.71	53.37
Al_2O_3	28.39	27.83	27.46	28.57	28.40	28.13	27.42	26.75	28.31	28.28
Na_2O	4.69	5.11	5.39	4.89	4.79	5.07	5.35	6.58	4.85	4.93
CaO	11.51	10.85	10.59	11.50	11.67	11.25	10.21	7.47	11.10	11.27
K_2O	0.31	0.33	0.31	0.28	0.30	0.28	0.40	2.54	0.51	0.44
BaO	0.00	0.12	0.04	0.00	0.00	0.14	0.04	0.11	0.09	0.00
SrO	0.09	0.16	0.16	0.23	0.23	0.20	0.32	0.08	0.13	0.20
FeO	0.67	0.47	0.42	0.48	0.40	0.40	0.82	0.59	0.44	0.45
Total	98.52	98.59	98.11	98.85	98.78	98.88	97.97	99.05	99.14	98.94
Formula (Basis 32 Oxygens)										
Si	9.744	9.881	9.925	9.723	9.745	9.811	9.904	10.118	9.828	9.794
Al	6.168	6.035	5.979	6.191	6.157	6.090	5.992	5.806	6.106	6.118
	15.912	15.916	15.904	15.914	15.902	15.901	15.896	15.924	15.934	15.912
Na	1.675	1.823	1.929	1.744	1.707	1.807	1.924	2.352	1.722	1.754
Ca	2.273	2.138	2.096	2.265	2.299	2.213	2.029	1.473	2.176	2.216
K	0.073	0.077	0.073	0.066	0.070	0.066	0.096	0.596	0.120	0.103
Ba	0.000	0.008	0.003	0.000	0.000	0.010	0.003	0.008	0.007	0.000
Sr	0.009	0.018	0.017	0.024	0.025	0.021	0.034	0.009	0.014	0.022
	4.030	4.064	4.118	4.099	4.101	4.117	4.086	4.438	4.039	4.095
Fe	0.103	0.073	0.065	0.074	0.062	0.062	0.128	0.091	0.068	0.069
Ab	41.56	44.86	46.84	42.55	41.62	43.89	47.09	53.00	42.63	42.83
An	56.40	52.61	50.90	55.26	56.06	53.75	49.66	33.19	53.87	54.11
Or	1.81	1.89	1.77	1.61	1.71	1.60	2.35	13.43	2.97	2.52
Ba	0.00	0.20	0.07	0.00	0.00	0.24	0.07	0.18	0.17	0.00
Sr	0.22	0.44	0.41	0.59	0.61	0.51	0.83	0.20	0.35	0.54

ALKALI FELDSPAR

	89-8 Festuca KF-R	89-8 Festuca KF-M	SE230985 Arnica KF-C	SE230985 Arnica KF-G	SE021383 N. Rift KF-R	SE021383 N. Rift KF-M	SE020783 Go-around KF-R	SE020783 Go-around KF-C
SiO_2	64.96	64.89	67.11	66.62	65.36	63.43	65.87	65.55
Al_2O_3	19.53	19.46	18.72	18.37	19.51	20.80	18.04	18.30
Na_2O	7.02	6.93	7.11	7.69	7.46	7.75	7.83	7.37
CaO	0.84	0.84	0.16	0.08	0.94	2.46	0.03	0.04
K_2O	6.29	6.37	7.12	6.40	5.68	3.62	5.93	6.22
BaO	0.21	0.26	0.07	0.13	0.12	0.38	0.02	0.00
SrO	0.11	0.00	0.00	0.00	0.00	0.00	0.00	0.03
FeO	0.23	0.21	0.21	0.55	0.17	0.22	0.43	0.42
Total	99.19	98.96	100.50	99.84	99.24	98.66	98.15	97.93
Formula (Basis 32 Oxygens)								
Si	11.777	11.789	11.989	11.986	11.799	11.505	12.017	11.987
Al	4.173	4.167	3.941	3.896	4.151	4.446	3.879	3.945
	15.950	15.956	15.930	15.882	15.950	15.951	15.896	15.932
Na	2.466	2.442	2.461	2.683	2.612	2.727	2.770	2.613
Ca	0.163	0.164	0.030	0.016	0.182	0.478	0.005	0.008
K	1.456	1.476	1.624	1.468	1.307	0.838	1.381	1.452
Ba	0.015	0.019	0.005	0.009	0.009	0.027	0.002	0.000
Sr	0.012	0.000	0.000	0.000	0.000	0.000	0.000	0.004
	4.112	4.101	4.120	4.176	4.110	4.070	4.158	4.077
Fe	0.036	0.031	0.032	0.083	0.026	0.034	0.065	0.064
Ab	59.97	59.55	59.73	64.25	63.55	67.00	66.62	64.09
An	3.96	4.00	0.73	0.38	4.43	11.74	0.12	0.20
Or	35.41	35.99	39.42	35.15	31.80	20.59	33.21	35.61
Ba	0.36	0.46	0.12	0.22	0.22	0.66	0.05	0.00
Sr	0.29	0.00	0.00	0.00	0.00	0.00	0.00	0.10

still a matter of debate. Fractional crystallization of a mantle-derived mafic magma is seen as the primary process in the evolution of peralkaline magmas at Volcano Fantale (Gibson, 1974) and the Afar Depression (Barberi et al., 1974) in the African rift system, and for peralkaline silicic volcanic rocks of the western United States (Noble and Parker, 1975). Conversely, Bailey and Macdonald (1970), who conducted an extensive study of peralkaline obsidians from different environments, concluded that the oceanic comendite could be derived from the fractionation of an alkali basalt parent magma, but that continental comendites were generated by partial melting of the lower continental crust. A further study of trachytic to pantelleritic obsidians from the East African rift (Macdonald et al., 1970) concluded that fractionation and crystal-liquid equilibria could not, in themselves, account for the peralkaline compositions without the participation of an alkali-bearing vapour phase. The possible role of volatile transfer to explain the disproportionate volume of silicic rocks in many peralkaline suites has been invoked by other volcanologists including Bowden (1974, p. 122) who states that volatile transfer and concentration "may be the mechanism responsible for the variation seen over the whole peralkaline spectrum".

In British Columbia, peralkaline silicic rocks occur in the principal shield volcanoes and subvolcanic plutons of the Anahim Volcanic Belt (Fig. 9) and in the larger central volcanic complexes of the Stikine Volcanic Belt (Souther and Yorath, 1991; Souther, 1992). Both of these belts are linear zones of intraplate continental volcanism, but they exhibit some important tectonic differences. At Mount Edziza, in the Stikine Volcanic Belt, volcanism began at least 10 million

Table 6. (cont.)

AMPHIBOLE	89-63 Mizzen AF-R	89-63 Mizzen AF-C	89-63 Mizzen AF-R	89-63 Mizzen AF-C	SE270385 Mizzen AF-R	SE270385 Mizzen AF-C	SE020783 Go-around AF-R	SE020783 Go-around AF-C
SiO_2	47.98	47.75	48.10	47.87	49.00	47.38	47.32	47.53
Al_2O_3	0.17	0.20	0.22	0.36	0.27	0.24	0.24	0.21
TiO_2	0.30	0.38	0.24	0.37	0.48	0.12	0.30	0.52
Cr_2O_3	0.00	0.00	0.00	0.00	0.00	0.03	0.00	0.00
Fe_2O_3	2.70	4.74	4.69	5.37	0.62	7.75	5.25	5.35
FeO	31.63	30.87	30.93	30.80	31.52	29.20	28.04	26.78
MnO	1.13	1.28	1.14	1.06	1.14	1.21	1.05	1.26
MgO	0.36	0.21	0.10	0.24	0.06	0.14	2.02	2.49
CaO	2.35	2.31	1.74	2.48	0.52	2.33	3.43	3.26
Na_2O	7.62	7.77	8.04	7.46	8.66	7.39	6.72	6.82
K_2O	1.65	1.35	1.54	1.53	1.51	1.21	1.60	1.41
F	2.79	2.93	2.80	2.82	2.98	2.85	2.71	2.71
Cl	0.02	0.01	0.04	0.05	0.03	0.05	0.03	0.02
Total	98.70	99.80	99.58	100.41	96.79	99.90	98.71	98.36
Formula (Basis 23 Oxygens)								
Si	7.959	7.852	7.909	7.815	8.213	7.771	7.773	7.785
Al	0.033	0.039	0.043	0.069	0.000	0.046	0.047	0.041
	7.992	7.891	7.952	7.884	8.213	7.817	7.820	7.826
Al	0.000	0.000	0.000	0.000	0.053	0.000	0.000	0.000
Ti	0.038	0.047	0.030	0.046	0.060	0.015	0.038	0.064
Cr	0.000	0.000	0.000	0.000	0.000	0.005	0.000	0.000
Fe^{+3}	0.337	0.587	0.580	0.659	0.078	0.956	0.649	0.659
Fe^{+2}	4.388	4.246	4.253	4.205	4.419	4.005	3.852	3.668
Mn	0.158	0.178	0.159	0.147	0.162	0.168	0.146	0.175
Mg	0.089	0.052	0.025	0.059	0.014	0.033	0.495	0.608
	5.010	5.110	5.047	5.116	4.786	5.182	5.180	5.174
Ca	0.417	0.407	0.307	0.433	0.093	0.410	0.603	0.572
Na	1.583	1.593	1.693	1.567	1.907	1.590	1.397	1.428
	2.000	2.000	2.000	2.000	2.000	2.000	2.000	2.000
Na	0.868	0.886	0.870	0.795	0.908	0.759	0.743	0.737
K	0.349	0.282	0.323	0.319	0.324	0.254	0.336	0.294
	1.217	1.168	1.193	1.114	1.232	1.013	1.079	1.031
F	1.461	1.524	1.455	1.454	1.579	1.478	1.406	1.402
Cl	0.006	0.004	0.010	0.012	0.008	0.014	0.008	0.006
	1.467	1.528	1.465	1.466	1.587	1.492	1.414	1.408

AENIGMATITE	89-67 Calliope AEN-R	89-67 Calliope AEN-C	89-67 Calliope AEN-R	89-67 Calliope AEN-C	89-67 Calliope AEN-R	89-67 Calliope AEN-C
SiO_2	38.81	38.95	38.30	38.62	38.96	39.24
Al_2O_3	0.86	1.00	0.80	1.01	0.87	0.80
Fe_2O_3	21.92	20.86	21.94	21.23	21.03	20.76
TiO_2	8.74	8.80	8.84	8.94	8.94	8.97
Cr_2O_3	0.01	0.00	0.00	0.00	0.00	0.00
MgO	0.04	0.05	0.06	0.04	0.03	0.05
FeO	22.28	22.65	21.73	22.37	22.52	23.49
MnO	1.02	0.94	0.93	0.91	0.92	0.92
CaO	0.81	0.93	0.76	0.88	0.82	0.70
Na_2O	6.44	6.38	6.49	6.41	6.48	6.37
Total	100.93	100.56	99.85	100.41	100.57	101.30
Formula (Basis 12 Oxygens)						
Si	3.241	3.258	3.231	3.238	3.259	3.264
Al	0.085	0.099	0.079	0.100	0.085	0.079
Fe^{+3}	0.674	0.643	0.690	0.662	0.656	0.657
	4.000	4.000	4.000	4.000	4.000	4.000
Al	0.000	0.000	0.000	0.000	0.000	0.000
Fe^{+3}	0.703	0.670	0.703	0.678	0.668	0.643
Ti	0.549	0.554	0.561	0.564	0.562	0.561
Cr	0.000	0.000	0.000	0.000	0.000	0.000
Mg	0.006	0.006	0.008	0.006	0.004	0.007
Fe^{+2}	0.742	0.770	0.728	0.752	0.766	0.789
Mn	0.000	0.000	0.000	0.000	0.000	0.000
	2.000	2.000	2.000	2.000	2.000	2.000
Mg	0.000	0.000	0.000	0.000	0.000	0.000
Fe^{+2}	0.814	0.815	0.805	0.816	0.810	0.845
Mn	0.072	0.067	0.066	0.064	0.065	0.065
Ca	0.073	0.083	0.069	0.079	0.074	0.062
Na	1.043	1.036	1.061	1.042	1.051	1.028
	2.002	2.001	2.001	2.001	2.000	2.000
Wo	0.00	0.00	0.00	0.00	0.00	0.00
En	0.00	0.00	0.00	0.00	0.00	0.00
Fs	16.53	17.19	15.89	16.54	16.81	17.60
Jd	0.00	0.00	0.00	0.00	0.00	0.00
Ae	0.55	0.34	0.24	0.00	0.03	0.00
Ka	2.36	2.23	2.15	2.10	2.15	2.13
Jo	0.00	0.00	0.00	0.00	0.00	0.00
S3-Al	0.00	0.00	0.00	0.00	0.00	0.00
S3-Fe	44.57	43.36	45.15	44.27	43.80	43.54
S4-Fe	2.34	2.73	2.22	2.60	2.44	2.08
S4-Mg	0.01	0.01	0.01	0.01	0.01	0.01
S2-Fe	33.50	34.01	34.15	34.34	34.67	34.49
S2-Mg	0.13	0.13	0.18	0.13	0.09	0.15

years ago and continued episodically into Quaternary time (Souther, 1992). The activity was characterized by several distinct eruptive cycles, each beginning with the effusion of a relatively large volume of alkali basalt and culminating with the eruption of a lesser volume of peralkaline silicic rocks. The volcanic succession and structural setting are consistent with episodic injection of primitive alkali basalt into an extensional zone where crystal fractionation in shallow crustal reservoirs produced the silicic end members (Souther and Hickson, 1984). In contrast, the peralkaline shield volcanoes of the Anahim Volcanic Belt comprise relatively large initial volumes of silicic lavas overlain by smaller volumes of basalt. Moreover, the age of volcanism decreases systematically from west to east along the belt and its duration at any given centre is relatively short (ca. 2 Ma) (Souther, 1986). The latter is powerful evidence against a rifting origin for the Anahim Belt volcanoes and suggests instead that they are the product of an easterly migrating hotspot (Bevier et al., 1979). The difference in tectonic setting between volcanoes of the Stikine and Anahim belts may explain the observed differences in eruptive style and provide some general guidelines for differentiating between rift-related and hotspot-related peralkaline volcanoes.

The eruption of a relatively large volume of silicic peralkaline lavas from the Ilgachuz Range and other Anahim Belt volcanoes during the initial stages of their activity is difficult to reconcile with a fractionation model. Bevier (1981) speculated that Chilcotin Group basalt may have been the primary, mantle-derived magma from which the diverse alkaline and peralkaline rocks of the Rainbow Range were produced by crystal fractionation in crustal reservoirs. Effusion of the Chilcotin Group basalts (26-1.1 Ma) was roughly coeval with eruption of the Anahim Belt volcanoes, but there are important differences that mitigate against a cogenetic relationship. The Chilcotin Group lavas are the product of back-arc volcanism along a northwesterly trending zone that parallels the continental margin. Although the area flooded by Chilcotin Group basalt extends throughout the Interior Plateau of British Columbia, the highly alkaline silicic rocks that characterize the Rainbow, Ilgachuz, and Itcha ranges are unique to the narrow east-trending zone of Anahim Belt volcanism. Moreover, the basal felsic lavas of the Rainbow and Ilgachuz ranges rest in part directly on pre-Tertiary basement rocks near the western limit of Chilcotin Group flows. Still farther west, where the King Island syenite and Bella Bella alkaline dyke swarms comprise the western, subvolcanic extension of the Anahim Belt (Souther, 1986), there is no evidence that Chilcotin Group basalt was ever present. Indeed all of the field evidence suggests that the Chilcotin Group and Anahim Belt volcanoes are the products of distinct tectonic environments and very different mechanisms of petrogenesis.

Further evidence of different origins of the two groups is provided by the chemistry. The Chilcotin Group lavas are defined as transitional "plains" basalts (Bevier, 1983b) and, although lava from different centres may exhibit minor chemical and isotopic variations, the total range of compositions is small. On the alkali versus silica diagram (Fig. 62), the Chilcotin Group basalts and the more alkaline basalts from the upper part of the Ilgachuz Group plot in distinct, relatively small fields. Either of these basaltic suites could, theoretically, fractionate to produce the peralkaline felsic rocks of the Ilgachuz Range. However, the trace element distribution shows a strong genetic linkage between the mafic and felsic suites of Ilgachuz Range rocks and little correlation with the Chilcotin Group basalts. This is particularly evident in the ratios of the excluded (LIL) elements. Y, Zr, and Nb for example do not enter readily into any of the common rock-forming minerals. Thus their total abundance may increase in the more differentiated species of a genetically related rock series but their ratios remain more or less constant, unaffected by processes of fractionation or partial melting (Meschede, 1986). This phenomenon is clearly illustrated by the Ilgachuz Range rocks. Despite their extreme bimodality, the mafic and felsic suites plot in the same small area of the Zr/4-Nb*2-Y ternary diagram (Fig. 70). In contrast the field of Chilcotin Group rocks is significantly displaced toward lower Nb values. In terms of the statistically defined discriminant fields of Meschede (1986), the Ilgachuz Group rocks plot mainly in the field of "within-plate alkali basalt" while the plot of Chilcotin Group rocks is displaced toward the field of "p-type MORB".

In addition to their extreme bimodality, rocks of the Ilgachuz Range exhibit several less obvious trends within the end-member suites. The basaltic suite, which ranges from 45 to 53% SiO_2, comprises three distinct groups. The first of these includes the Stonecrop, Hump Mountain, and Far Mountain basalts, which show no consistent bias in the distribution of major or minor elements across their range of variation. Olivines in this group range from about Fo80 to Fo60 with the most iron-rich olivines occurring in the youngest, Far Mountain, basalt. The second group comprises the highly porphyritic North Rift basalts. These rocks are distinctly more calcic than basalts of the first group and are interpreted to be of cumulous origin. They contain phenocrysts of relatively iron-rich olivine (Fo35-Fo60) and relatively calcic plagioclase (>An60). The third group comprises the Pliocene or younger Flank basalt. These rocks are relatively high in MgO, K_2O, Cr, and Ni, and their olivines (Fo83-Fo86) are more magnesian than those in any of the other basalts. The Ni content of the Flank basalt is an order of magnitude higher than that in the Ilgachuz Group basalts.

These relationships suggest that the Ilgachuz Group basalts are not primary mantle melts. The extremely low Ni content of these rocks and the relatively high iron content of their olivines suggest that olivine was crystallizing and being removed from the rising basalt magma. The North Rift basalt may be a cumulate rock whereas the Far Mountain basalt, with its iron-rich olivines, is the most highly fractionated of the Ilgachuz Group basalts. The Quaternary Flank basalt, with its relatively magnesian olivines and high Ni content appears to be the product of a different, primitive batch of magma that could have been in equilibrium with mantle peridotite. It is enriched in the LIL elements and may be the product of partial melting in a deeper, less depleted, source than that of the Ilgachuz Group basalts.

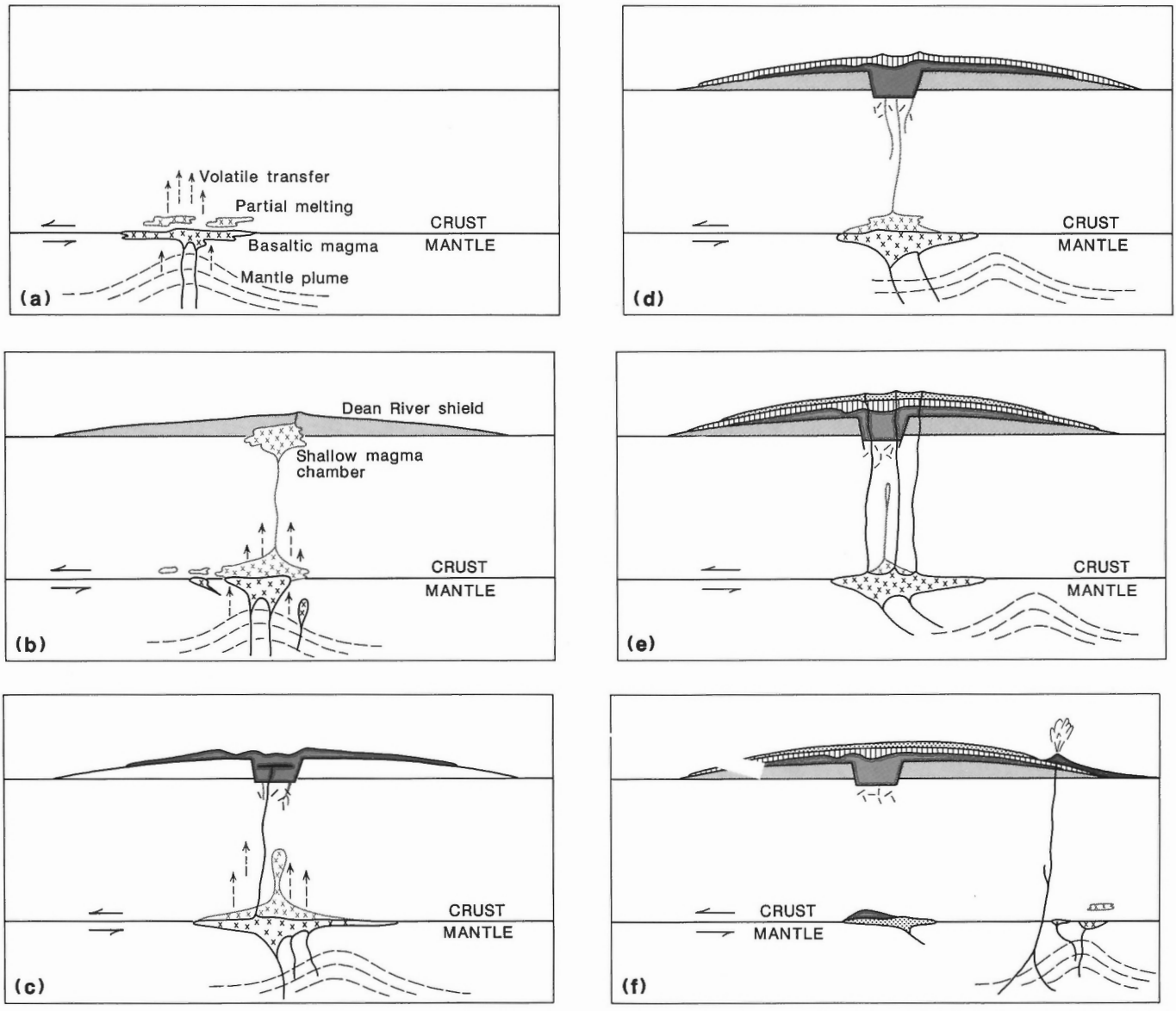

a – Generation and rise of basaltic magma and partial melting of lower crustal rocks above a mantle hotspot. Crustal plate is moving west relative to the mantle.

b – Eruption of Dean River comenditic lavas and formation of a shallow magma reservoir where the Carnlick Creek magmas evolved through crystal fractionation.

c – Caldera collapse followed by eruption of the Carnlick Creek highly fractionated rhyolites and trachytes. Arnica Lake comendite starting to ascend from the zone of melting while underplating basaltic magma continues to be modified by olivine fractionation. Small precursor eruption of basalt produces the intracaldera Phacelia tuff.

d – Eruption of Arnica Lake comendite and continued fractionation of underplating basaltic magma.

e – Widespread eruption of Tundra Mountain basalt from the underplating reservoir accompanied by the rise of a small volume of residual (Go-around) silicic magma. During its long residence time in the underplating reservoir the primary basaltic magma was modified by olivine fractionation.

f – Eruption of a small volume of primary mantle-derived (Flank) basalt near the eastern edge of the Ilgachuz Range shield.

Figure 76. *Schematic sketches showing possible origin and evolution of the Ilgachuz Group magmas.*

Chemical and mineralogical variations within the felsic suite of Ilgachuz Group rocks show a distinct correlation with age. The Dean River Volcanics, the oldest and most voluminous part of the felsic pile, have a narrow range of variation. These rocks are the least silicic and the most alkaline of the felsic units, and plots of their principal mineral species (Fig. 73-75) show remarkably little scatter. The younger Carnlick Creek Volcanics include two distinct phases. A coarse grained cumulate and intrusive phase (Pipe Organ and Saxifraga trachytes) is slightly less alkaline but otherwise similar to the Dean River Volcanics, whereas a fine grained phase (Mizzen Mountain, Calliope, Festuca, and Rich Creek rhyolites) includes rocks that are significantly more silicic than either the Pipe Organ-Saxifraga phase or the Dean River flows. Feldspars from the Pipe Organ and Saxifraga rocks are significantly less potassic than those from the fine grained Mizzen Mountain, Festuca, and Calliope rhyolites (Fig. 75). The Arnica Lake Volcanics, which comprise the youngest volumetrically significant felsic suite in the Ilgachuz Group, are mineralogically similar to the Dean River but their bulk chemistry shows a slight shift toward less alkaline and more silicic compositions (Fig. 62). Like the Dean River Volcanics, the Arnica Lake Volcanics display remarkably little chemical or mineralogical variation.

The foregoing chemical and field relationships suggest that the Dean River comenditic trachyte represents the initial batch of Ilgachuz Group magma. Part of this was erupted to form the basal shield of the volcano and part resided in a crustal reservoir where fractionation of fayalitic olivine and alkali feldspar produced a cumulate phase represented by the coarse grained Pipe Organ and Saxifraga trachytes, and a siliceous residual liquid that gave rise to the fine grained Mizzen Mountain, Calliope, Festuca, and Rich Creek rhyolites. Eruption of this fractionated suite lead to caldera collapse and was followed by effusion of the Arnica Lake flows. The latter are slightly more siliceous than the Dean River Volcanics but they exhibit the same narrow range of chemical and mineralogical variation suggesting that they too are part of a large undifferentiated batch of magma the origin of which was similar to but later than that of the initial Dean River comenditic trachyte.

CONCLUSIONS

Field relationships, ages, and chemistry provide some broad constraints on the origin of the Ilgachuz Range rocks and suggest the general conclusions outlined below and in Figure 76:

1. The Ilgachuz Range shield volcano is one of the principal centres of peralkaline igneous activity that constitute the Anahim Volcanic Belt. The belt trends easterly, across the Coast Ranges and Interior Plateau of British Columbia, and the age of activity decreases progressively from about 14 Ma on the Coast to a few thousand years at Nazko Cone in the east (Souther et al., 1987). The Ilgachuz activity was confined to a relatively short interval of time between 6.1 and 4.0 Ma, approximately the same duration of activity that built the older Rainbow Range farther west and the younger Itcha Range farther east. The distribution and timing of these events suggested to Bevier et al. (1979) that the peralkaline volcanoes and subvolcanic intrusions of the Anahim Belt are related to the westward movement of North America over a mantle plume or hotspot. The data collected during this study support that interpretation.

2. Volcanic activity along the Anahim Belt as a whole is approximately coeval with eruption of the Chilcotin Group transitional basalts. These extensive flood basalts erupted from numerous separate centres that trend northwesterly through central British Columbia and are interpreted to be the product of back-arc extension related to subduction of Juan de Fuca plate (Bevier, 1983b). The Chilcotin Group and Ilgachuz Group basalts are chemically distinct, both in their major and trace element compositions. This and the fact that highly fractionated, silicic rocks such as those in the Ilgachuz Range are confined to the narrow zone of Anahim Belt volcanism argues against a genetic relationship between the Chilcotin Group basalts and the volcanoes of the Anahim Belt.

3. The initial magma (Dean River Volcanics) that issued to form the voluminous basal shield of the Ilgachuz Range varies in composition from trachyte to basic comendite. The absence of any visible basaltic parent for these rocks argues against their origin by crystal fractionation and supports petrogenetic models that generate the continental silicic peralkaline volcanic rocks by crustal melting (Bailey and Macdonald, 1970) combined with volatile transfer of alkalis (Macdonald et al., 1970). In the case of the Ilgachuz Range, this process was probably accompanied by underplating with mantle-derived basalt which was modified by olivine fractionation during the early stages of silicic volcanism and later erupted to form the outer (Tundra Mountain) part of the Ilgachuz shield (Fig. 76).

4. Part of the initial batch of comenditic trachyte magma was trapped in a shallow reservoir where fractionation of fayalitic olivine and alkali feldspar produced a zoned chamber. Crystal accumulation in the lower part of the chamber gave rise to a coarse grained cumulous phase (Pipe Organ and Saxifraga) and a silica-rich liquid phase (Pan Creek, Mizzen Mountain, Calliope, Festuca, Rich Creek). Eruption of magma from this reservoir was accompanied by collapse of a small central caldera.

5. Caldera collapse was followed by the eruption of a small volume of basalt from a vent in the water- or ice-filled caldera, producing the Phacelia tuff. This material, a precursor of later, more extensive basaltic volcanism, probably originated from the zone of basaltic underplating beneath the zone of crustal melting that produced the initial silicic magma.

6. A second, postcaldera phase of silicic volcanism produced the voluminous Arnica Lake comendite and pantellerite flows and lava domes. This material is slightly more silicic and less alkaline but otherwise similar to the initial Dean River rocks. It was probably either part of the initial batch of siliceous magma or genetically equivalent magma produced by continued crustal melting. The slight compositional differences between the Dean River and Arnica Lake lavas could be due either to modification of the original magma batch by fractionation of olivine and alkali feldspar or to melting at higher crustal levels. The Arnica Lake Volcanics represent the last major effusion of silicic magma

in the Ilgachuz Range. Their eruption was followed by a period of widespread basaltic volcanism during which only one small eruption of residual silicic magma (Go-around rhyolite) occurred.

7. The shift from silicic to basaltic volcanism occurred when basaltic magma beneath the zone of crustal melting was tapped. The relatively high-iron olivines in these basalts and their extremely low Ni content suggest that they are not primary mantle-derived melts. Instead they appear to have been modified by olivine fractionation, possibly during residence in an underplating reservoir below the zone of crustal melting that produced the initial Dean River and subsequent Arnica Lake batches of comenditic trachyte and related magmas.

8. The Flank basalt is clearly distinct from the voluminous basalts that form the upper part of the Ilgachuz Range shield volcano. Its Ni content is an order of magnitude greater than that of the Ilgachuz Group basalts and its olivines (Fo_{82}-Fo_{85}) are more magnesian. Unlike the Ilgachuz Group basalts, which appear to have been modified by fractionation, the Flank basalt represents a more primitive magma that could have been in equilibrium with mantle peridotite and risen to the surface without undergoing significant change in composition. Although the volume of Flank basalt associated with the Ilgachuz Range is extremely small, it is chemically, lithologically, and morphologically similar to part of a much more extensive Pliocene and younger basalt succession that issued from fissures and cinder cones on the east flank of the Itcha Range where Charland et al. (1993) have postulated a mantle origin. It is reasonable to speculate that the Flank basalt of the Ilgachuz Range had a similar origin and that it was derived by partial melting in a deeper, less depleted mantle source area than that of the older Chilcotin Group and Ilgachuz Group basalts.

REFERENCES

Armstrong, R.L.
1988: Mesozoic and early Cenozoic magmatic evolution of the Canadian Cordillera; Geological Society of America, Special Paper 218, p. 55-91.

Bailey, D.K. and Macdonald, R.
1969: Alkali feldspar fractionation trends and derivation of peralkaline liquids; American Journal of Science, v. 276, p. 242-248.
1970: Petrochemical variations among mildly peralkaline (comendite) obsidians from the oceans and continents; Contributions to Mineralogy and Petrology, v. 28, p. 340-351.

Barberi, F., Santacroce, R., and Varet, J.
1974: Silicic peralkaline rocks of the Afar Depression (Ethiopia); Bulletin Volcanologique, v. 38, p. 755-790.

Bevier, M.L.
1981: The Rainbow Range, British Columbia: a Miocene peralkaline shield volcano; Journal of Volcanology and Geothermal Research, v. 11, p. 225-251.
1983a: Regional stratigraphy and age of Chilcotin Group basalts, south-central British Columbia; Canadian Journal of Earth Sciences, v. 20, p. 515-524.
1983b: Implications of chemical and isotopic composition for petrogenesis of Chilcotin Group basalts, British Columbia; Journal of Petrology, v. 24, p. 207-226.
1989: A lead and strontium isotopic study of the Anahim volcanic belt, British Columbia: additional evidence for widespread suboceanic mantle beneath western North America; Geological Society of America Bulletin, v. 101, p. 973-981.

Bevier, M.L., Armstrong, R.L., and Souther, J.G.
1979: Miocene peralkaline volcanism in west-central British Columbia – its temporal and plate-tectonics setting; Geology, v. 7, p. 389-392.

Bowden, P.
1974: Oversaturated alkaline rocks: granites, pantellerites and comendite; in The Alkaline Rocks, (ed.) H. Sorensen; John Wiley and Sons, New York, N.Y., p. 109-123.

Charland, A., Francis, D., Ludden, J.
1993: Stratigraphy and geochemistry of the Itcha Volcanic Complex, central British Columbia; Canadian Journal of Earth Sciences, v. 30, no. 1, p. 132-144.

Dawson, G.M.
1878: Report on explorations in British Columbia, chiefly in the basins of the Blackwater, Salmon, and Nechako rivers, and on Francois Lake; in Geological Survey of Canada, Report of Progress for 1876-77.

Ewing, T.E.
1981: Regional stratigraphy and structural setting of the Kamloops Group, south-central British Columbia; Canadian Journal of Earth Sciences, v. 18, p. 1464-1477.

Friedman, R.M. and Armstrong, R.L.
1988: Tatla Lake metamorphic complex: an Eocene metamorphic core complex on the southwestern edge of the Intermontane Belt of British Columbia; Tectonics, v. 7, no. 6, p. 1141-1166.

Gabrielse, H., Monger, J.W.H., Wheeler, J.O., and Yorath, C.J.
1991: Part A. Morphogeological belts, tectonic assemblages, and terranes; in Chapter 2 of Geology of the Cordilleran Orogen in Canada, (ed.) H. Gabrielse and C.J. Yorath; Geological Survey of Canada, Geology of Canada, no. 4, p. 15-28 (also Geological Society of America, The Geology of North America, v. G-2).

Gibson, I.L.
1974: A review of the geology, petrology and geochemistry of the volcano fantale; Bulletin Volcanologique, v. 38, p. 791-802.

Greeley, R.
1982: The Snake River Plain, Idaho: representative of a new category of volcanism; Journal of Geophysical Research, v. 87, p. 2705-2712.

Irvine, T.N. and Baragar, W.R.A.
1971: A guide to the chemical classification of the common volcanic rocks; Canadian Journal of Earth Sciences, v. 8, p. 523-548.

Le Bas, M.J., Le Maitre, R.W., Streckeisen, A., and Zanettin, B.
1986: Chemical classification of volcanic rocks; Journal of Petrology, v. 27, p. 746-750.

Macdonald, R. and Bailey, D.K.
1973: The chemistry of the peralkaline oversaturated obsidians; United States Geological Survey, Professional Paper 440-N-1, p. 1-37.

Macdonald, R., Bailey, D.K., and Sutherland, D.S.
1970: Oversaturated peralkaline glassy trachytes from Kenya; Journal of Petrology, v. 11, p. 507-517.

Mackenzie, A.
1802: Voyages from Montreal on the River St. Lawrence, through the Continent of North America, to the Frozen and Pacific Oceans; London, 1802.

Mathews, W.H.
1989: Neogene Chilcotin basalts in south-central British Columbia: geology, ages, and geomorphic history; Canadian Journal of Earth Sciences, v. 26, p. 969-982.

McBirney, A.R.
1984: Igneous Petrology; Freeman Cooper and Company, San Francisco, p. 137-138.

Meschede, M.
1986: A method of discriminating between different types of mid-ocean ridge basalts and continental tholeiites with the Nb-Zr-Y diagram; Chemical Geology, v. 56, p. 207-218.

Noble, D.C. and Parker, D.F.
1975: Peralkaline silicic volcanic rocks of the western United States; Bulletin Volcanologique, v. 38, p. 803-827.

Pearce, J.A. and Cann, J.R.
1973: Tectonic setting of basic volcanic rocks determined using trace element analyses; Earth and Planetary Science Letters, v. 19, p. 290-300.

Sibson, R.H.
1983: Continental fault structure and the shallow earthquake source; Journal of Geological Society of London, v. 140, p. 741-767.

Souther, J.G.
1976: Geothermal power, the Canadian potential; Geoscience Canada, v. 3, p. 14-20.

1977: Volcanism and tectonic environments in the Canadian Cordillera – a second look; in Geological Association of Canada, Special Paper 16, (ed.) W.R.A. Baragar, L.C. Coleman and J.M. Hall, p. 3-24.
1984: The Ilgachuz Range, a peralkaline shield volcano in central British Columbia; in Current Research, Part A; Geological Survey of Canada, Paper 84-1A, p. 1-10.
1986: The western Anahim Belt: root zone of a peralkaline magma system; Canadian Journal of Earth Sciences, v. 23, no. 6, p. 895-908.
1992: The late Cenozoic Mount Edziza Volcanic Complex, British Columbia; Geological Survey of Canada, Memoir 420.

Souther, J.G. and Hickson, C.J.
1984: Crystal fractionation of the basalt comendite series of the Mount Edziza Volcanic Complex, British Columbia: major and trace elements; Journal of Volcanology and Geothermal Research, v. 21, p. 79-106.

Souther, J.G. and Souther, M.E.K.
1994: Chemical analyses of rocks and minerals from the Ilgachuz Range, a late Tertiary shield volcano in central British Columbia; Geological Survey of Canada, Open File No. 2838.

Souther, J.G. and Yorath, C.J.
1991: Neogene assemblages, Chapter 10 in Geology of the Cordilleran Orogen in Canada, (ed.) H. Gabrielse and C.J. Yorath; Geological Survey of Canada, Geology of Canada, no. 4, p. 373-401 (also Geological Society of America, The Geology of North America, v. G-2).

Souther, J.G., Clague, J.J., and Mathewes, R.W.
1987: Nazko Cone: a Quaternary volcano in the eastern Anahim Belt; Canadian Journal of Earth Sciences, v. 24, p. 2477-2485.

Taylor, S.R. and McLennan, S.M.
1985: The Continental Crust: Its Composition and Evolution; Blackwell, Oxford, 312 p.

Tipper, H.W.
1963: Nechako River map-area, British Columbia; Geological Survey of Canada, Memoir 324.
1969: Anahim Lake, British Columbia; Geological Survey of Canada, Map 1202A.
1971: Glacial geomorphology and Pleistocene history of central British Columbia; Geological Survey of Canada, Bulletin 196.
1978: Taseko Lakes, British Columbia; Geological Survey of Canada, Open File Map 534.

Tullis, J. and Yund, R.A.
1977: Experimental deformation of dry Westerly Granite; Journal of Geophysical Research, v. 82, p. 5705-5718.

Wheeler, J.O., Brookfield, A.J., Gabrielse, H., Monger, J.W.H., Tipper, H.W., and Woodsworth, G.J.
1988: Terrane Map of the Canadian Cordillera; Geological Survey of Canada, Open File 1894.

Winchester, J.A. and Floyd, P.A.
1977: Geochemical discrimination of different magma series and their differentiation products using immobile elements; Chemical Geology, v. 20, p. 325-343.